THE ELECTROLYTIC PRODUCTION OF PARA-ANISIDINE

by

Jonathan M.T. Clark

Thesis submitted in partial fulfilment of the requirement for the degree of Doctor of Philosophy in the Faculty of Engineering of the University of Newcastle upon Tyne

NEWCASTLE UNIVERSITY LIBRARY
088 22909 3
Thesis L3411

Department of Chemical and Process Engineering
University of Newcastle upon Tyne
August 1988

To my Mother

ABSTRACT

In this thesis the electrochemical reduction of nitrobenzene in a methanol / sulphuric acid electrolyte is studied. Major products are shown to be para-anisidine, ortho-anisidine, para-aminophenol and aniline.

A simple reaction model is derived, based on the well accepted mechanism for nitrobenzene reduction. Kinetic constants are determined from experimental results using a laboratory scale glass cell. Predictions as to potential - current behaviour and product formation as a function of mass transport and current density are made. It is shown that the rate of mass transport and the current density are crucial parameters in determining the chemical yields of the products formed. High rates of mass transfer and low current densities favour para-anisidine formation, whilst aniline is preferred under poor mass transfer conditions and high current densities. Results from a bench scale parallel plate cell fit the model predictions for the conditions used.

The use of packed and fluidised bed electrodes is also investigated for the production of para-anisidine. Using copper particles, serious dissolution is shown to occur which leads to an increased yield of aniline. The copper dissolution is shown to have an electro-catalytic effect for the reduction of nitrobenzene to aniline. Results using Monel as an electrode material showed an improvement over copper, but preferential dissolution of nickel occurred. On the basis of the work in this thesis, copper or Monel packed and fluidised bed electrodes are not suitable for the production of para-anisidine.

ACKNOWLEDGEMENTS

I would firstly like to thank Professor F. Goodridge for his help, guidance and patience throughout this work. Particular thanks are also due to Dr. R.E. Plimley for his invaluable insight and thoughtful discussions. For help with the rotating disk work, I would like to thank Dr. J.A. Harrison of the Department of Chemistry, University of Newcastle upon Tyne. Mention must be made, too, of Drs. S. Harrison and B. Swanson for their ever useful comments and help in solving day-to-day problems.

My special thanks go to the technical staff under the leadership of Mr. E. Horsley and, in particular, Ian and Stuart. Without this skilled team none of the experimental work would have been possible.

I would also like to thank BASF AG, Ludwigshafen, FRG for their generous financial support and Dr. D. Degner of BASF for his useful comments and continuing interest in the work.

Finally, I wish to thank Shell Research BV, Amsterdam for great patience during the writing up and for the use of their computing facilities.

CONTENTS

CHAPTER ONE

INTRODUCTION AND LITERATURE SURVEY

Organic electrochemistry can sometimes offer a cleaner, more selective synthetic route than conventional catalytic technology. The production of para-aminophenol is a good example. The current commercial process involves several synthesis and purification steps, but high selectivity at good yields can be obtained in the one step electrochemical reduction of nitrobenzene in aqueous sulphuric acid[1]. Much attention has, therefore, been focused on this reaction and many patents have been published.

Para-aminophenol is just one of the many products that can be produced by the reduction of nitrobenzene. Chloroanilines, azo- and azoxybenzenes are further examples that have received the attention of industry. Some novel work claimed by BASF[2] the sponsors of this work, in a 1977 patent, concerned the reduction of nitrobenzene in acidic methanol. The major product was reported to be para-anisidine (4-methoxyaniline) or substituted anisidines if a substituted nitrobenzene was used. This family of amines are intermediates useful in the dyestuff industry. It is interesting to note that this is the only reference to the electrochemical production of para-anisidine from nitrobenzene to be found in the literature. The combined electrochemical and chemical reactions are shown in the scheme below:

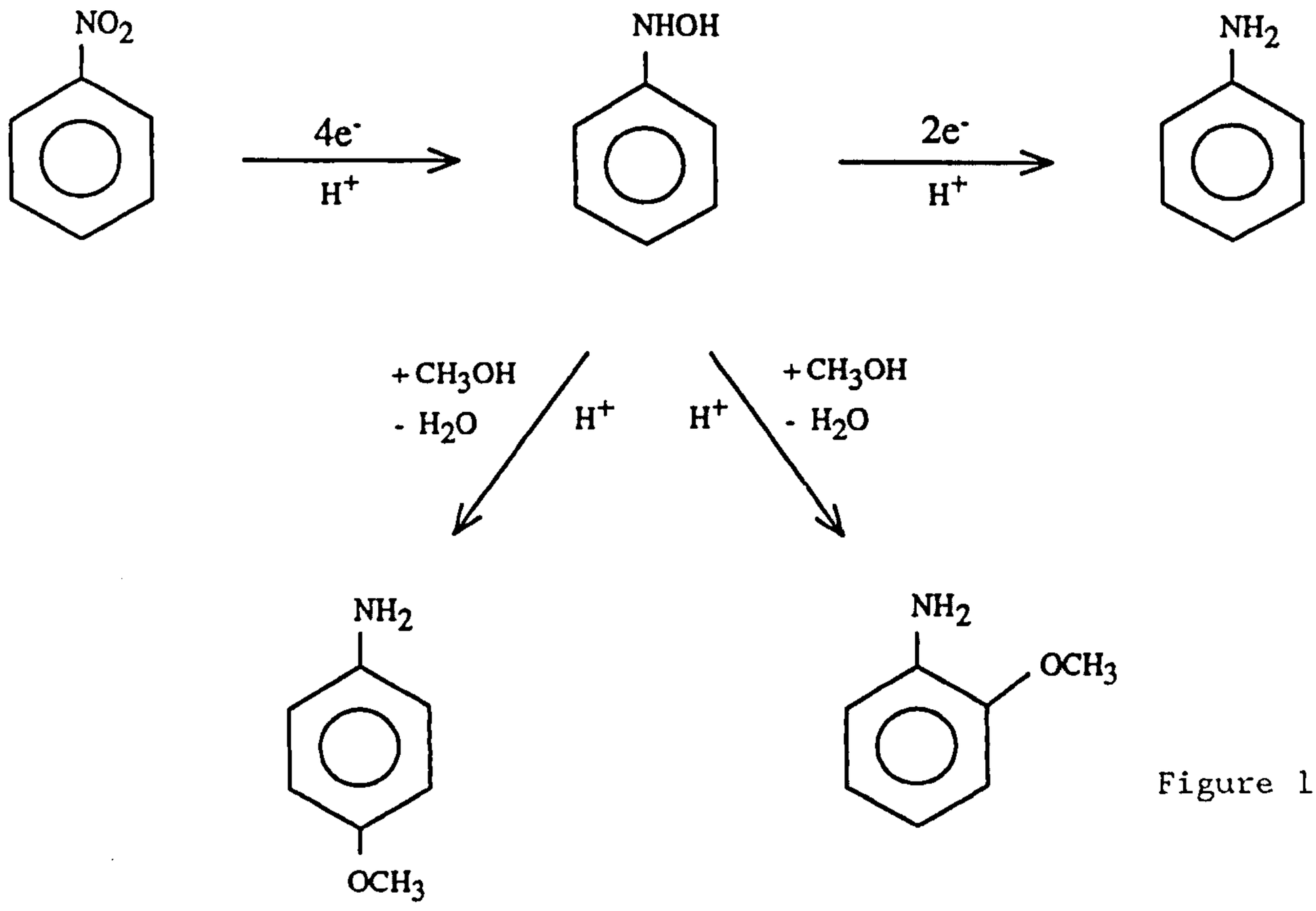

Figure 1.1

The initial aims of this study were to investigate the effect of different electrochemical cell configurations on the reduction of nitrobenzene in acidified methanol, with particular attention to current efficiency and chemical yield. A reaction model was to be developed, which could, where feasible, be incorporated into the appropriate reactor models. The models would then be validated and, if necessary, modified using experimental observations. Once established, these models were to be used as an aid to process optimisation, from which recommendations on reactor type and process conditions could be made. This logical progression of work could not be pursued in its entirety, however, for reasons which will become plain as this thesis is developed.

As an introduction to the work, the published literature concerning the reduction of nitrobenzene will be briefly reviewed in this chapter. No attempt will be made to exhaustively review the enormous amount of work done on this subject, only the more relevant and important material will be included. Some relevant aspects of cell design will then be introduced, in particular the concept of three dimensional electrodes and their applications. Finally, the arrangement of this thesis will be outlined.

1.1 The Production of Para-anisidine

Para-anisidine, or 4-methoxyaniline, and its related compounds are mainly in use as intermediates for all major classes of dyestuffs. The halogen substituted anisidines are particularly useful, 2-chloro-4-methoxyaniline for example being used for the production of Fast Red R. Base.

Anisidines are usually manufactured by the reduction of nitroanisoles (para-methoxynitrobenzenes), which are produced by alkylation of the appropriate phenol followed by nitration. The reduction can be carried out in either liquid or vapour phases, generally the vapour phase is preferred, the anisole being hydrogenated over a Ni-Magnesia catalyst. Many other methods are available of which the ones in current use have been described by **Kirk and Othmer**[1]. The liquid phase reduction of nitroanisole has also been performed electrochemically. **Anantharaman et al.**[3,4,5,6] in a large number of papers and patents described extensive pilot plant work on the

electrochemical reduction of many nitrophenols and anisoles to their respective amines. They reported the use of a copper cathode and the addition of $Ti(SO_4)_2$ for the production of para-anisidine from nitroanisole. In a Japanese patent, **Hirajima and Nishiguchi**[7] disclosed a similar process using a graphite or copper electrode. Recent work in this direction has concentrated on the electrocatalytic reduction of nitrobenzene. **Chiba, Okimoto et al.**[8], for example, used Raney nickel and showed that hydrogen was generated electrochemically, absorbed and then activated on the surface of the catalyst. Hydrogenation of nitrobenzenes by the activated hydrogen gave high yields of products.

Developments in the direction of process simplification have concentrated on the one step conversion of nitrobenzene to para-anisidine. **Tsenyuga et al.**[9] reported the reduction of nitrobenzene by hydrogen in methanol / sulphuric acid solution, using PtO_2 or platinised carbon catalysts at 75-125 ^oC and 6-10 atm. pressure. The product was para-anisidine or para-phenetidine if an ethanol / sulphuric acid solution was used. The work formed the basis of two patent applications for the production of para-anisidine. **Sone et al.**[10] and more recently, **Mitsui Toatsu Chemicals Inc.**[11] substantially confirmed this work, although with somewhat lower yields of para-anisidine. This process is essentially the catalytic equivalent of the electrochemical process claimed by BASF[2], which forms the basis of the present work.

Clearly a process where para-anisidines could be produced directly from the corresponding nitrobenzene, either catalytically or electrochemically, removes the need for the alkylation and nitration steps, greatly simplifying the product purification. Such a process could well be an economically attractive alternative to the more conventional methods.

1.2 The Electrochemical Reduction of Nitrobenzene.

The reduction of nitrobenzene was one of the first reactions ever to be studied electrochemically. Work by **Gatterman**[12], **Haussermann**[13] and **Noyes**[14] in the 1890's was followed by the extensive investigations of **Haber**[15]. He reported the main products in the reduction in aqueous acid to be aniline and para-aminophenol. **Bamberger**[16] studied the formation of

para-aminophenol and concluded that it arose from the rearrangement of phenylhydroxylamine, an intermediate in the reduction from nitrobenzene to aniline. Reactions of phenylhydroxylamines to substituted amines are now eponymously called "Bamberger rearrangements".

Many reaction mechanisms for the electrochemical reduction of nitrobenzene have been proposed[17,18,19,20,21,22,23]. The most generally accepted one at present is that of Heyrovsky[17], shown in figure 1.2. Doubt, however, still exists over the formation of nitrosobenzene. Either, as Heyrovsky stated, it is an intermediate in the first reduction step or, as favoured by Marquez and Pletcher[19] and earlier by Fleischmann et al[22], it is formed through oxidation of phenylhydroxylamine by dissolved oxygen in the electrolyte.

Despite the differing views on the precise mechanism, there is no doubt that the reaction can be represented by the simplified scheme shown in figure 1.1. The large number and diversity of reaction products can be explained by the reactivity of the intermediate phenylhydroxylamine. Depending upon the pH, the nature of the media and the electrode potential, possible reactions of the intermediate are: substitution (the Bamberger rearrangement); condensation; or further reduction. Possible products include aniline, substituted amines, azo- and azoxybenzenes.

The present work is concerned only with the reduction of nitrobenzene in acidic media and the Bamberger type rearrangements occurring under these conditions, which lead to substituted amines. The reader is referred to Lund[25] and several other good reviews[26] and handbooks[27] for a survey of the other possible reaction conditions and the products they yield.

1.2.1 The Preparation of para-Aminophenol

In strongly acidic solutions, that is at pH less than 3, the protonated intermediate, phenylhydroxylamine, can undergo nucleophillic attack resulting in para- or ortho- substitution into the aromatic ring. Thus in hydrochloric acid solution a mixture of the para- and ortho-chloroaniline is formed, together with para-aminophenol [25]. If sulphuric acid is used, only para-aminophenol is formed [16]. This is due

HEYROVSKY REACTION SCHEME

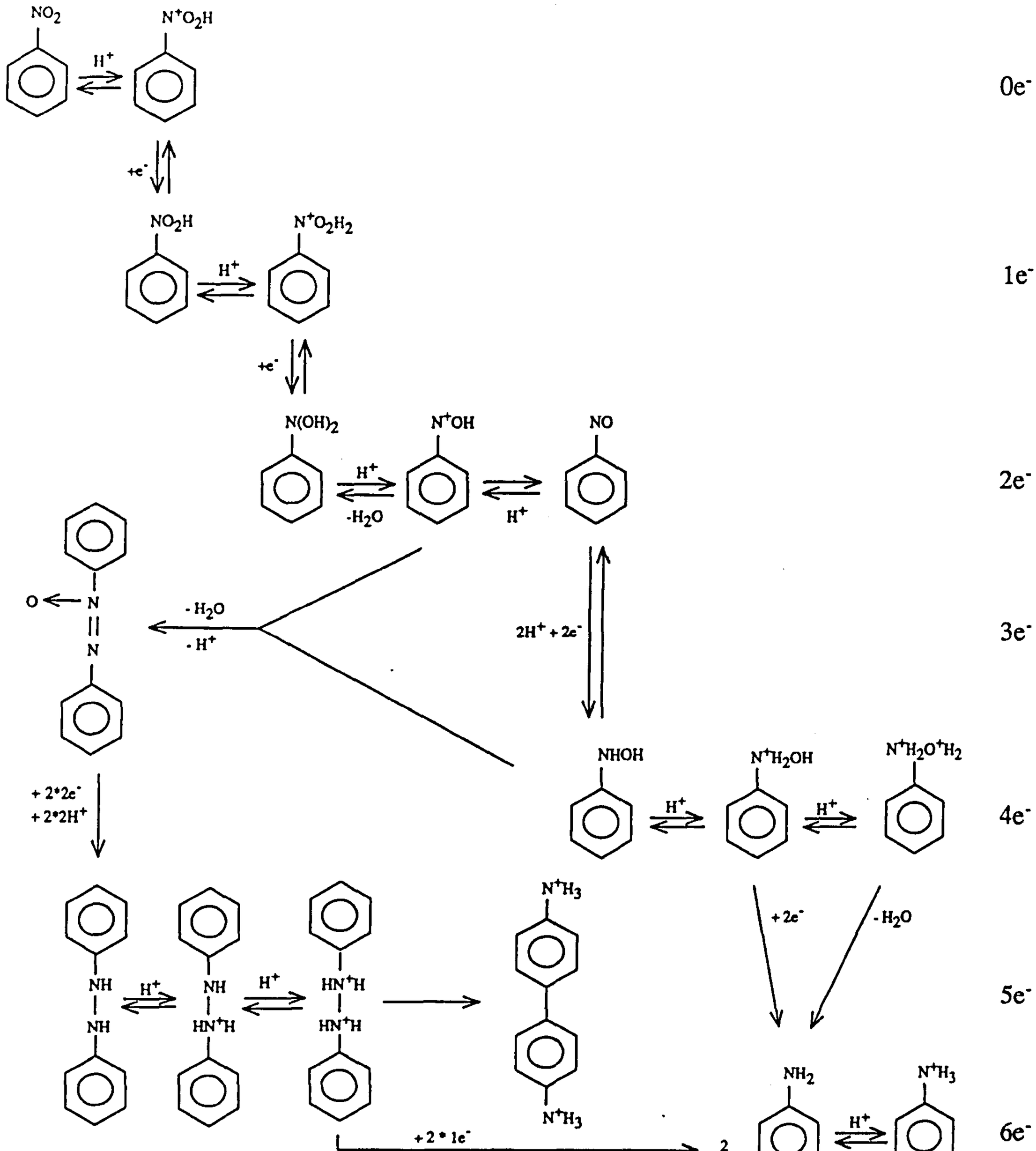

Figure 1.2

to the much greater nucleophillic strength of water compared to the hydrogen sulphate ion. In addition, of course, the intermediate can be further reduced resulting in aniline formation.

Para-aminophenol was an important chemical in the photographic industry early in the 20th century and thus received much attention. Important parameters identified by these early studies were temperature, acid concentration and agitation of the electrolyte. Experiments showed that electrodes such as copper, nickel or graphite were preferred. A good review of this early work, which concentrated mainly on optimising the chemical yield of product, can be found in **Fichter**[28]. One particularly interesting paper from **Dey et al.**[29] reported a pilot plant for para-aminophenol production, using a Monel cathode, with a selectivity of over 70% with respect to aniline.

Since 1950 much has been published on the reduction of nitrobenzene, partly due to the continued commercial interest in para-aminophenol and partly because of the suitability of the reaction to modern electrochemical studies. The reader is referred to the reviews and standard texts mentioned above for a wider and more complete survey than can be attempted here.

In the early 1950's **Udupa et al.**[30] studied the electrochemical preparation of para-aminophenol on amalgamated copper or Monel electrodes. They found that the conditions for an optimum yield of the phenol were 30% sulphuric acid and 80-90^{o}C. Using rotating electrodes to agitate the electrolyte the yield was further increased up to a maximum of 60%.

The first thorough potentiometric and preparative study of this reaction was reported by **Harwood, Hurd and Jackson**[18]. Using a mercury pool electrode, they investigated the effect of electrode potential on the products formed during the reduction of nitrobenzene in a catholyte containing 2N H_2SO_4 in a 40% ethanol-60% water mixture. They confirmed that the reduction was a two-step process with phenylhydroxylamine as the intermediate product after the first 4e- transfer. A further 2e- reduction gave aniline but rearrangement of the hydroxylamine with water or ethanol gave para-aminophenol or para-phenetidine respectively. At low electrode potentials (-0.4 Volt vs. S.C.E) para-aminophenol was the major product formed (over 70% of the total current passed) with aniline completely absent. As the potential was increased, however, aniline became the

preferred product (at -0.8 Volt vs. S.C.E only 20% of the current was used to form the phenol). They concluded that for an complex organic electrochemical reaction, such as the nitrobenzene reduction, control of electrode potential was crucial.

Udupa et al. followed up their earlier work with a detailed study of the depolarization characteristics of nitrobenzene at amalgamated electrodes published in 1966[31]. Much work by this group has since followed leading to the development of a pilot plant where the electrochemical reductions of many aromatic nitro compounds have been performed[32,4,33]. Their efforts have concentrated on the complete reduction to the aniline for which a number of patents have appeared [5,6], although a process for production of para-aminophenol has also been reported by them[34].

Rance and Coulson[35] concluded that the rate and product spectrum of the electrochemical nitrobenzene reduction depended primarily on cathode potential. By use of copper or nickel cathodes, electrolyte agitation and the addition of stannous ions they improved, but could not fundamentally alter, this basic dependance. The use of stannous ions and other redox compounds to enhance yield had been previously reported by **Dey and coworkers**[36] among others[37], and has since been confirmed by **Benkesser et al.**[38], **Gigi and Paucescu**[39] and the group of **Udupa**[3,4,6,40]. Recent work by **Pletcher and Gunawardena**[41] also used metal redox catalysts to improve the yield of amines in the complete six electron reduction of various nitrobenzenes.

1.2.2 The Addition of Organic Solvents to the Electrolyte.

Nitrobenzene has a very low solubility in aqueous solutions (about 2 g/l in 5 molar aqueous sulphuric acid). Whilst this is no problem for studies of basic electrode kinetics, it is a major limitation to any industrial application of the electrochemical reduction. One possibility would be to add an amount of an organic solvent to the electrolyte and hence increase the solubility of nitrobenzene. This section reviews the work done in this direction leading to the complete replacement of water by

an organic solvent, which results in different product spectrum and forms the basis of the present work.

It is worth mentioning some recent work aimed at increasing the concentration of the nitrobenzene. Pletcher[41] or H.V.K Udupa et al[40], for example, where an emulsion of dispersed nitrobenzene in an aqueous electrolyte has successfully been used for the reduction. A further possibility might be the use of recently developed phase-transfer catalysts, indeed a US patent for the production of para-aminophenol using this technique was disclosed by PPG Industries Inc.[42] in 1986. They used tri-alkylamine N-oxide surfactants to emulsify the nitrobenzene in an aqueous sulphuric acid electrolyte. Nitrobenzene concentrations of between 5 and 20 g/l were claimed, considerably higher solubility than in aqueous sulphuric acid alone (2 g/l).

Harwood, Hurd and Jordan[18] used a 40% ethanol / 60% water catholyte in their 1963 work. They could then prepare a homogeneous electrolyte solution of as much as 0.1M nitrobenzene (= 12 g/l). For the reduction at all electrode potentials chosen they reported the formation of para-phenetidine (para-ethoxyaniline). The authors suggested that this was due to the reaction of p-aminophenol with ethanol. It is now accepted that this product is formed from the competing nucleophillic attack by an ethoxy- group on the intermediate, phenylhydroxylamine ie. the Bamberger rearrangement with ethanol. The ratio of p-phenetidine to p-aminophenol was always around 1:6, indicating that the alcohol was a poorer nucleophile when compared to the water.

A study on the depolarisation of nitrobenzene at an amalgamated copper cathode by Subbiah, Subramanian and Udupa[31] concluded that addition of ethanol had a detrimental effect on the reduction. They found that the depolarisation decreased as a result of ethanol addition and that the range of current densities where reduction could occur was lowered. Their explanation was that the ethanol formed a layer on the cathode surface which hindered the electron transfer to the polar nitro- group more than to hydrogen ions.

Pecheva et al.[43] reported the preparation of both para-aminophenol and para-phenetidine during the reduction of nitrobenzene in aqueous acidic ethanol at 80^{o}C using an amalgamated copper cathode.

Marquez and Pletcher[19], in their 1980 paper, investigated the production of para-aminophenol with a view to maximising the yield of product. Using a mixture of acetone and water containing sulphuric acid as catholyte, they showed that using a copper electrode at elevated temperatures with stirring of the electrolyte gave the best production of the phenol. Interestingly, they also investigated the effect of trace amounts of oxygen in the catholyte. They found a very large increase in azoxybenzene formation when oxygen was present, this could be greatly reduced by thoroughly deoxygenating the electrolyte before use. They explained that the azoxybenzene was formed by the coupling of nitrosobenzene and the reduction intermediate, phenylhydroxylamine. The nitrosobenzene being formed by oxidation of phenylhydroxylbenzene by the dissolved oxygen. Previous workers have explained this formation by considering nitrosobenzene as a stable intermediate in the reduction of nitrobenzene to phenylhydroxylbenzene. Marquez and Pletcher and also earlier Fleischmann[22] have rejected this possibility arguing that the nitrosobenzene was more easily reduced than nitrobenzene and that hence could not be present in quantities sufficient for side reactions.

In further experiments they found that the yield of para-aminophenol was dependant on the organic co-solvent that was used. They determined that acetone or 1-propanol gave the best results (up to 85% yield of the phenol). Surprisingly, they reported that no para-propoxyaniline was found amongst the products. In a later paper Marquez and Pletcher[44] used the same acidic 50% 1-propanol/ 50% water electrolyte to investigate the reduction of o-halonitrobenzenes. Again no para-propoxy was reported in the product.

1.2.3 The Non-Aqueous Reduction.

In the previous section it was shown that the addition of organic solvents to the electrolyte not only allowed a higher concentration of nitrobenzene to be used, but also resulted in a new product spectrum. As aromatic amine compounds have become more important commercially, research into the electrochemical reduction of nitrobenzene has broadened. The Bamberger rearrangements using nucleophiles other than water have begun to

be investigated as possible routes for the future manufacture of speciality chemicals such as pesticides or pharmaceuticals.

Subbiah, Subramanian and Udupa[33] have extensively studied the production of p-phenetidine by the electrochemical reduction of nitrobenzene in an electrolyte containing ethanol. Using amalgamated copper or Monel electrodes they achieved current efficiencies for p-phenetidine of 50%. They reported that at increased current density (and hence electrode potential) the current efficiency for p-phenetidine formation decreased. Since most of the experiments were carried out in electrolytes of water, ethanol and sulphuric acid, an increase in the proportion of ethanol in the mixture led somewhat unsurprisingly to an increase in p-phenetidine production. If the reduction was carried out in only an ethanol / sulphuric acid electrolyte, however, the amalgamated copper electrodes were found to corrode seriously. Amalgamated Monel proved excellent giving current efficiencies of between 50 and 60%, with a negligible formation of aniline. The authors did not account for the remaining 40 to 50% of the current.

In a later paper[32] **Subbiah et al.** explored the possibility of other cathode materials for the reduction in a non-aqueous electrolyte. Considering nickel, zinc, tin, graphite and platinised titanium, they concluded that only amalgamated copper or Monel cathodes gave a current efficiency for p-phenetidine production of over 45%. It is unclear why they did not try natural copper or Monel as cathode materials. The results in this paper show a surprisingly large amount of the aminophenol being formed, considering the catholyte was water free. The authors explained this by diffusion of water through the membrane from the anode compartment.

As already mentioned **BASF**[2] disclosed a patent in 1977 concerning the preparation of aminomethoxybenzenes from nitrobenzenes. The nitrobenzene was electrochemically reduced in a methanol-sulphuric acid solution. Preferred conditions included using a copper cathode, a catholyte containing 30 wt% sulphuric acid, a temperature of 55°C, agitation of the catholyte and a current density of between 50 and 200 mA / cm^2. The first example quoted gave a yield of para-anisidine (para-methoxyaniline) of 54%. Further examples showed the application of the technique to the preparation of 2-methyl-3-chloro-4-methoxyaniline and 3-methyl-4-methoxyaniline although a large number of other methoxyanilines were also claimed. This

patent and the work that was behind it's publication[45,46] form the basis for the present work.

1.2.4 Reaction Mechanism and Kinetics

A very large number of papers have been published concerning the mechanism and kinetics of the nitrobenzene reduction. As will become apparent from the discussion in chapter two, the purpose of the first part of this work is to produce a reaction model, not a reaction mechanism. For this reason only papers which are relevant to this aim are discussed.

The reaction scheme of Heyrovsky[17] shown in figure 1.2 illustrates the "mixed mechanism" of the nitrobenzene reduction proposed formally by Martinyuk and Shlygin[23] in 1958. The mechanism proceeds stepwise; protonation by absorbed hydrogen is then followed by transfer of an electron, a further protonation and so on. This type of mechanism gives rise to many intermediates and explains the diversity of products obtained during the reduction process.

Pezzatini and Guidelli[21] confirmed the findings of Fleischmann[22], Heyrovsky[17] and others[47] that the rate determining step depended on the pH of the electrolyte medium. They all agreed that in solutions of pH less than four, the rate determining step was the first electron transfer and that this process was first order with respect to nitrobenzene.

In this thesis the simplified reaction scheme presented at the start of this chapter will be used. Considering the highly acidic conditions and the electrode potentials that will be employed, this seemed a valid assumption.

Since Bamberger[16] first reported the rearrangement of phenylhydroxylamine, the reaction has been much used but kinetically poorly understood. Several authors have postulated a mechanism[48,49,50], but it was not until some elegant work, first by Oae and Kitao[51] and later by Kukhtenko[51], that proved that the reaction occurs through intramolecular rearrangement (see figure 1.3 below). They used ^{18}O labelled water to investigate the rearrangement of phenylhydroxylamine with water in

sulphuric acid to form para-aminophenol. The incorporation of the ^{18}O into the para-aminophenol proved that the mechanism involved the nucleophillic attack at the para- position by the solvent water. They could not, however, determine whether this occurred simultaneously with the elimination of water from the $-NHOH_2^+$ group or shortly afterwards.

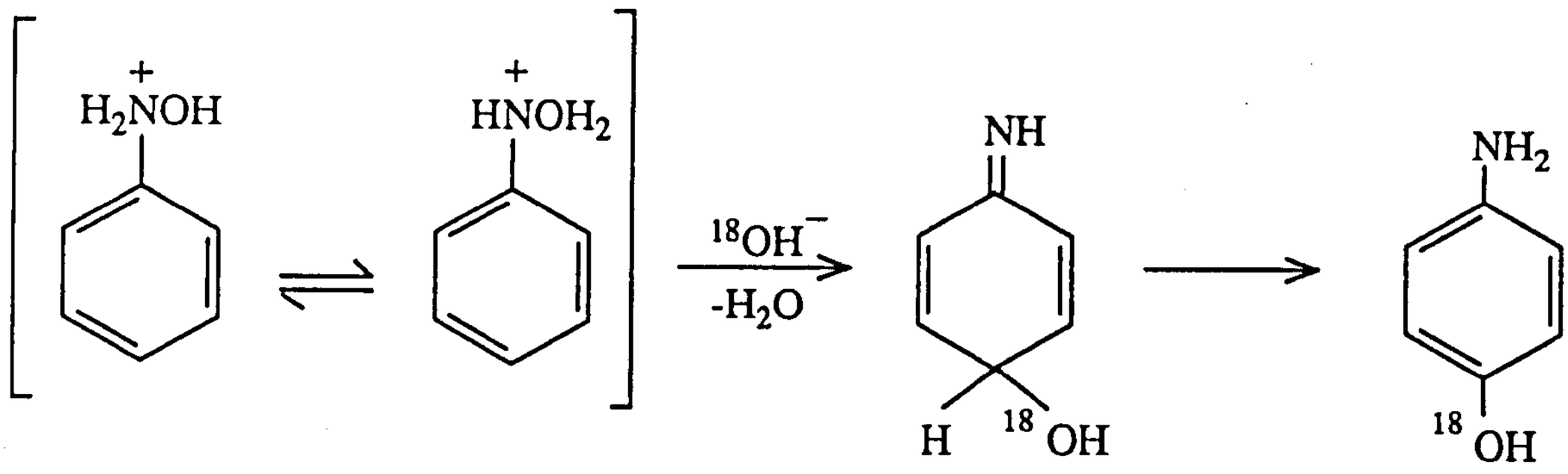

Figure 1.3

Recently, an extremely thorough investigation into the kinetics and mechanism of the Bamberger rearrangement has been attempted by Sone, Manabe et al.[52,10]. They demonstrated that nucleophillic attack by the solvent molecule occurred after the elimination of water from the hydroxylamine. Furthermore they showed that this water elimination was rate determining and that it was pseudo-first-order for pH less than one.

1.3 Electrochemical Cell Design.

The preparation of para-aminophenol or para-anisidine according to the simplified reaction scheme (figure 1.1) is a competitive process between the Bamberger rearrangement or the further reduction of the intermediate. Several important factors can be considered when attempting to maximise the yield of the rearrangement product. An increase of reaction temperature, for instance, has been shown to preferentially increase the rate of rearrangement. However, two factors stand out, namely current density and mass transfer. It has been conclusively shown that a low current density and a high rate of mass transport favour the production of p-aminophenol, p-phenetidine or p-anisidine. To assess the impact of these factors upon cell design and cost, the concept of space-time yield is often used.

Space-time yield provides a means of quantifying the rate of production for a given volume of cell. It is defined as the quantity of product obtained per unit volume of cell in unit time and is given by:

$$Y_{ST} = ajQ_E C_E$$

where **a** is the superficial geometrical electrode area per unit volume of cell, **j** the current density, Q_E the amount of product per unit charge if the current efficiency, C_E, is 100%[53]. This parameter is of importance since it gives a direct guide to cell costs. A high space-time yield implies a high rate of production for a given cell volume and, since cell costs are directly related to the volume, a more economic use of the cell volume and thus lower cell costs.

It has been shown that a high current density results in more aniline formation. However, a low current density would make the process economically unfavourable due to the low space-time yields that would result. For a given set of reaction conditions, it has also been shown that an increase in the rate of mass transfer favours the production of the phenol. This can easily be understood, since if the phenylhydroxylamine is removed from the electrode surface it cannot be further reduced to aniline, but can rearrange in the bulk to form para-aminophenol.

If, therefore, a electrochemical cell could be designed to combine a high rate of mass transfer with a low current density and yet maintain a good space-time yield, it would be extremely useful for this type of reaction. An example of such a cell is one that employs a three dimensional electrode ie. an electrode where current can flow in three dimensions. Such an electrode has a very high specific area increasing the space-time yield without having to increase the current density. Furthermore, mass transfer to and from the electrode surface is also enhanced.

1.3.1 Three Dimensional Electrodes

Three dimensional electrodes can be classified as porous flow-through electrodes (PFTE) and particulate electrodes. PFTE's can either be a porous electron-conducting material through which the electrolyte flows or a fixed

bed of individual electron-conducting particles where the electrolyte flows in the free volume between the particles (a packed bed electrode, PBE). Particulate electrodes can be a packed bed or a bed of electron-conducting particles fluidised by the flow of electrolyte (a fluidised bed electrode, FBE) or a circulated slurry of particles in the electrolyte[53].

To date the commercial uses of such electrode have generally been rather limited. Metal deposition in effluent treatment is one area, however, where fluidised bed electrodes have been extensively investigated[54]. John Brown (Developments) Ltd.[56,59] have been active in this field with several patented fluidised bed designs. The NALCO process for tetra-alkyl lead manufacture used a packed bed electrode[55]. For further information the reader is referred to several good reviews[53,57] and, in particular to the literature survey in the thesis of Hamilton[58].

Despite the possible advantages outlined above, organic electrochemical systems using three dimensional electrodes have received relatively little attention. The most relevant to this thesis is the work by Yoshizawa et al. and Goodridge and Hamilton. They both studied the reduction of nitrobenzene using packed bed electrodes. John Brown Ltd.[59] have patented a particulate electrode cell for the production of para-aminophenol, but gave no examples.

In their first design Yoshizawa et al.[60] used copper plated resin particles in a packed bed through which current and electrolyte flowed parallel to each other. They found that at a constant current with a flowing electrolyte almost 100% current efficiency for the reduction to aniline. If the electrolyte was stationary, build up of products on the electrode surface resulted in a much lower efficiency. By measuring the potential profiles in the bed during the reduction, they showed that the effective depth of the electrode, that is the area in which significant reaction took place, was only 3 mm. This low value was explained by the low conductivity of the electrolyte compared to the relatively high value for the copper coated particles.

In a second paper[61] a more uniform potential distribution was obtained by using carbon particles and an increased electrolyte conductivity. Unfortunately, due to the reduced hydrogen overvoltage at carbon the current efficiency for aniline production was greatly reduced.

Goodridge and Hamilton[58,62] used the reduction of nitrobenzene as a model reaction to study the performance of a packed bed electrode. Although the thrust of his work was towards the modelling of the packed bed, the results he obtained do show the potential use of a packed bed electrode in the production of para-aminophenol. Using a packed bed of Monel particles with a geometric current density of 65 mA / cm^2 , he obtained typically 70% current efficiency for para-aminophenol production. At 12 mA / cm^2 this could be increased to over 90%. Taking his results for a planar Monel electrode, current efficiencies of around 90% could only be achieved at current densities as low as 1 mA / cm^2, and at 5 mA / cm^2 current efficiency for para-aminophenol was already under 60%, the rest being aniline.

Despite the problems Hamilton experienced with the analysis of his reaction products (he was forced to assume that aniline and para-aminophenol were the only products), it is clear that the use of a packed bed electrode allowed a much higher geometric current density to be used for the reduction and yet maintain a very high selectivity to the para-aminophenol product. Hence, a substantial increase in space-time yield for this reaction could be achieved by the use of a packed bed electrode (from Hamilton's figures more than a hundred fold increase).

1.4 Arrangement of Thesis

From the foregoing study of the existing literature it seemed that the production of para-anisidine by the reduction of nitrobenzene in acidic methanol could form the basis for some useful research. The reduction, involving a Bamberger type rearrangement, had been well demonstrated for other similar systems and there was clearly commercial incentive in the production of para-methoxy anilines. As measured earlier, to the author's and BASF's knowledge there had been no previous attempt to prepare para-anisidine by the electrochemical reduction of nitrobenzene in methanol and sulphuric acid. Furthermore, there had been little work done to date in exploiting the advantages demonstrated by Goodridge and Hamilton[58,62] of using a three dimensional electrode for the nitrobenzene reduction.

The aims, therefore, of this study were to extend the initial work done by BASF[46] on the preparation of para-anisidine. In particular to investigate the possibility of using different cell configurations and the effect of this on the current efficiency and chemical yield of para-anisidine. Inherent in such a study would be an attempt to model the reaction and incorporate it into existing reactor models along similar lines to the approach taken by Hamilton. These models could then, after testing, be used to design further process studies.

The initial study by BASF for the preparation of their patent considered the effect of cathode material, nitrobenzene concentration, temperature and current density on the current efficiency, yield and selectivity of para-anisidine production. These results were used as the starting point for the present work, indeed the first experiments used identical conditions. Thereafter only the effect of current density, electrode potential and cell configuration were considered, although an alternative cathode material was later used. As will be seen this provided ample scope for investigation.

After some early experiments with a packed bed electrode it became apparent that there were two major problem areas. Firstly, analysis of the products proved to be difficult and inaccurate using the methods then available and secondly the reduction seemed to be rather more complex than had been anticipated. For these reasons it was decided to attempt a more detailed study of the basic electrode reaction than was originally planned and at the same time develop a new and better analysis technique.

Returning to the comparison between planar and three dimensional electrode configurations, further work showed that the three dimensional electrodes were not suitable for this particular reaction under the conditions used. Indeed it proved futile to attempt the modelling of these reactor types. Reasons for this failure and some possible solutions were investigated, but with only partial success. Subsequently, the basic electrode kinetics were more deeply investigated and a model of the reaction developed. The scale-up of this model was tested using the results from the planar electrode cell.

For the sake of clarity, this thesis does not strictly adhere to this chronological series of events. Firstly, the reaction model is considered

together with the work leading to its derivation and validation – this is chapter two. The work using a bench scale cell is then described in chapter three and the reaction model predictions are compared to the parallel plate results. A comparison between the parallel plate electrode and the three dimensional electrodes is also described. The last chapters draw final conclusions and suggest some future work. Throughout this thesis all detailed results and derivations, together with descriptions of the analysis techniques used are to be found in the appendices.

CHAPTER TWO

REACTION MODEL

The first step in the investigation of a reaction must always be the elucidation of the reaction scheme or mechanism. It must be pointed out, however, that in reaction modelling the term reaction scheme must not be confused with that of reaction mechanism. All a model attempts to do is to obtain a relationship describing performance (current density) as a function of various parameters such as electrode potential, mass transfer and temperature. The reaction scheme will obviously be based on a mechanism but is by no means synonymous with it. The discussion in section 1.2.4 highlighted only a small part of the large volume of work published on the mechanism of the electrochemical reduction of nitrobenzene. Although there is still some uncertainty over the exact reaction mechanism, it is widely accepted that the process can be represented by the simplified scheme shown below in figure 2.1. By assuming that the two consecutive electrochemical steps are first order, irreversible, and have kinetics that can be described by Tafel equations, a reaction model is proposed to describe the reduction of nitrobenzene. A similar method has also been used by Scott[63], taking data from Marquez and Pletcher[19] for the production of para-aminophenol, to demonstrate techniques of electrochemical reactor engineering.

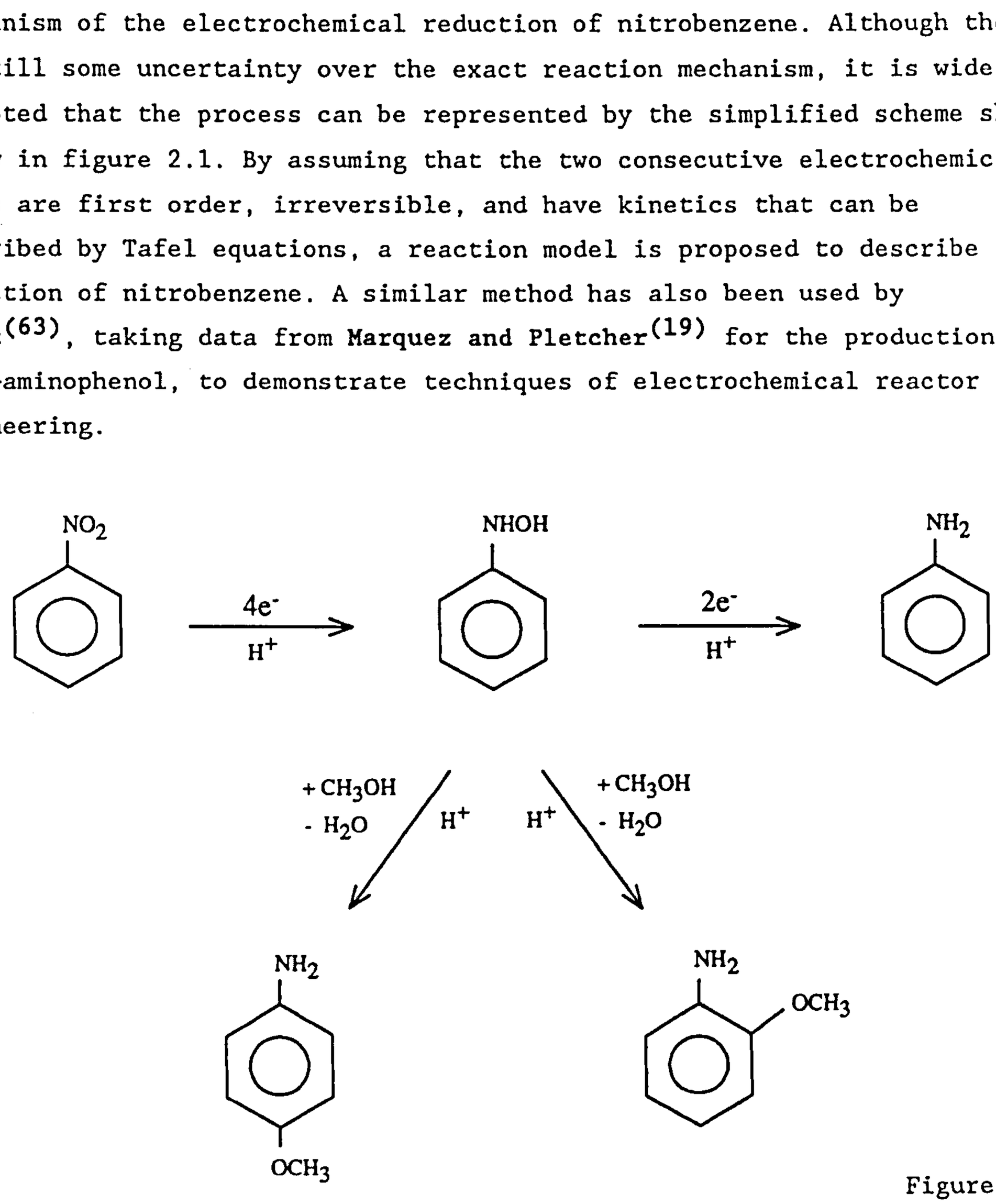

Figure 2.1

The derivation of such a reaction model requires the knowledge of the kinetics of the competing mass transfer and electrochemical reaction steps. This chapter describes the techniques used to obtain that necessary data. The first part of the chapter describes the equipment and methods that were used in the investigation. The model is then introduced and the results obtained for the kinetic constants presented and discussed. Finally the validity and scope of the model is discussed.

2.1 Experimental

2.1.1 Rotating Disk Electrode

Some initial work using a rotating copper disk was carried out in a glass cell (figure 2.2) using custom built precision stirrer, manufactured by Sycopel, Station Rd., East Bolden, Tyne and Wear. The electrode was a copper rod sealed in a PTFE holder so that one end formed the disk electrode and the other allowed electrical contact to be made (see figure 2.2).

For later work a rotating disk system developed by Dr. J.A. Harrison, of the chemistry department at the University of Newcastle-upon-Tyne, was used. This sophisticated computer-based system was designed to automate the study of electrode kinetics. A very flexible hardware system combined with a large library of reaction schemes and models, enabled the measured data to be fitted to an appropriate electrochemical model. Real time software both controlled the process and collected the data from experiments. The rotating copper disk electrode and cell were of the same type described above and shown in figure 2.2. The equipment and the data manipulation techniques have been extensively described by Harrison and co-workers[64] and the reader is referred to these publications for further information.

DIAGRAM OF ROTATING DISK APPARATUS

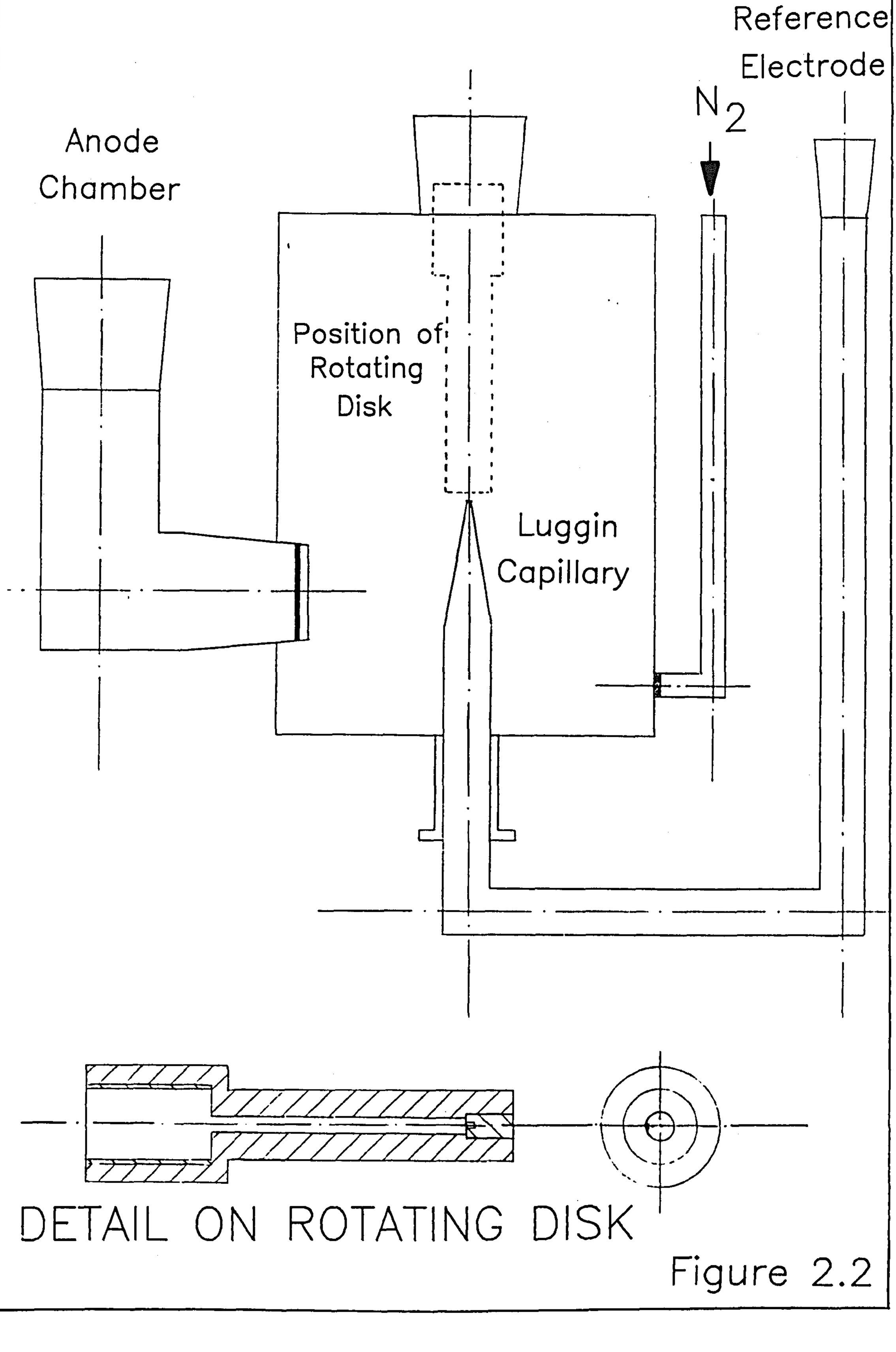

DETAIL ON ROTATING DISK

Figure 2.2

2.1.2 H-Cell Equipment

The H-cell used in this work was designed to allow bulk electrolysis as well as basic electrode studies. The design gave provision for maximum electrode area with minimum electrolyte volume.

Short experiments yielding significant product concentrations were thus possible. The cell was constructed from "Quickfit" glass components in our own University. Diagrams of the cell and its attachments are shown in figures 2.4 and 2.5.

The cell was made in two flanged sections with a membrane sandwiched between them. A good seal was achieved by using Dow Corning "Silicoset" and flange clamps. The cells were checked regularly for any signs of leakage around the membrane and flanges. Initially a Nafion 423 membrane from Du Pont[65] was used, but later Ionac MC-3470 from Sybron Corp.[66] was found to be superior for this work.

Fittings were provided on the cell for a Luggin capillary, a thermometer and a sample port. The Luggin was made from modified "Quickfit" glass components. Connection to a calomel reference electrode was made via a loose fitting 3-way tap and a salt bridge. The working and counter electrodes were introduced through the lids of the two compartments. The lid of the catholyte section was later modified to allow stirring of the electrolyte from above.

The cathode was a copper, later Monel, disc 4 cm in diameter. The reverse side of the electrode was insulated using a stopping-off medium, Lacromite. The same medium was used to reduce the electrode area for polarisation studies and to insulate the electrode supporting rods. The anode was a graphite rod with a surface area somewhat greater than the cathode area, to avoid possible current distribution problems. For the same reason, the cell was designed to ensure the membrane surface area was always greater than that of the cathode.

Catholyte agitation was first achieved by the use of a magnetically stirred bar, however, this was found to be unsatisfactory. Instead an

DIAGRAM OF H–CELL

Showing Position of Electrodes and Stirrer

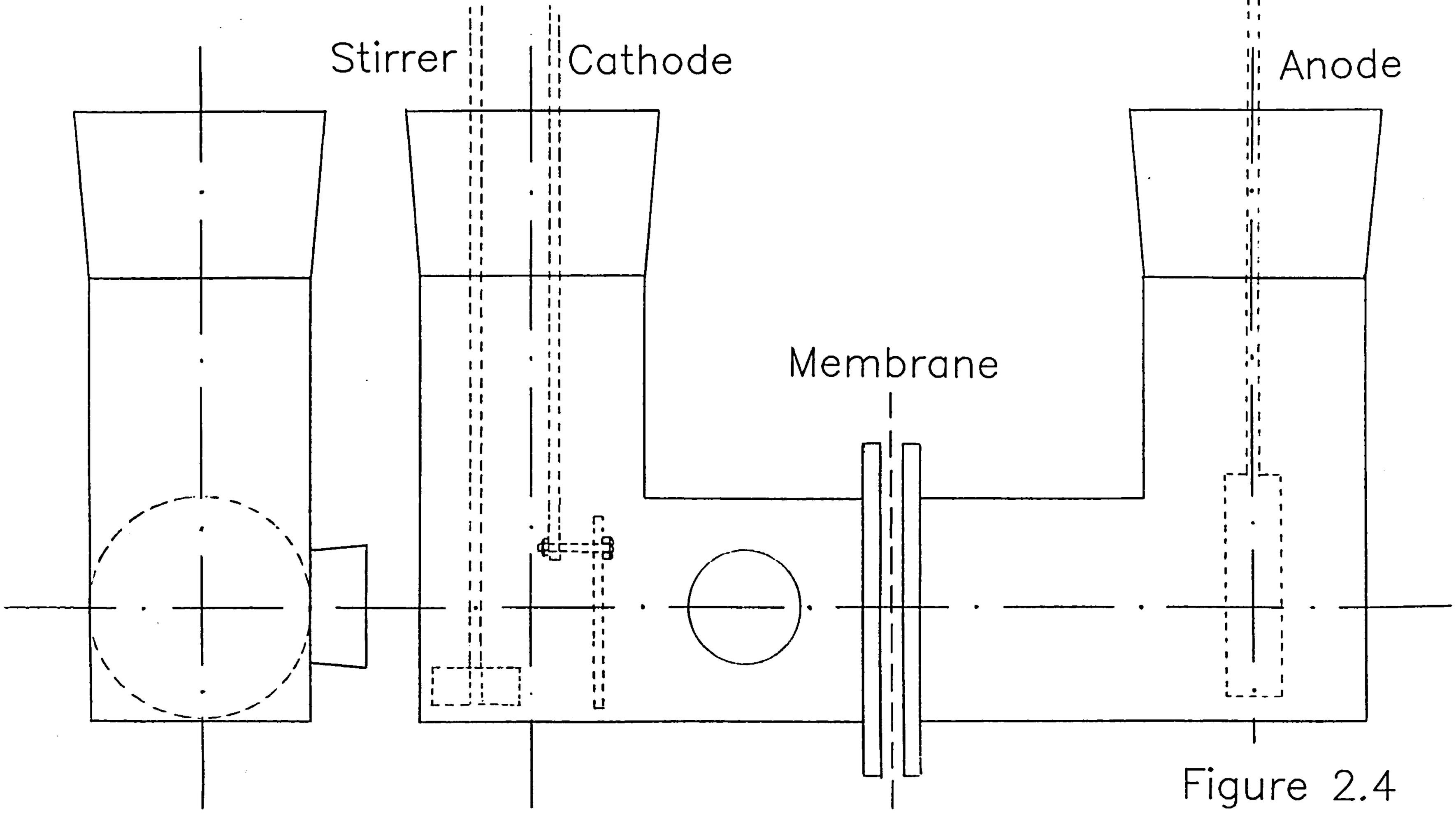

Figure 2.4

DETAIL ON H–CELL ATTACHMENTS

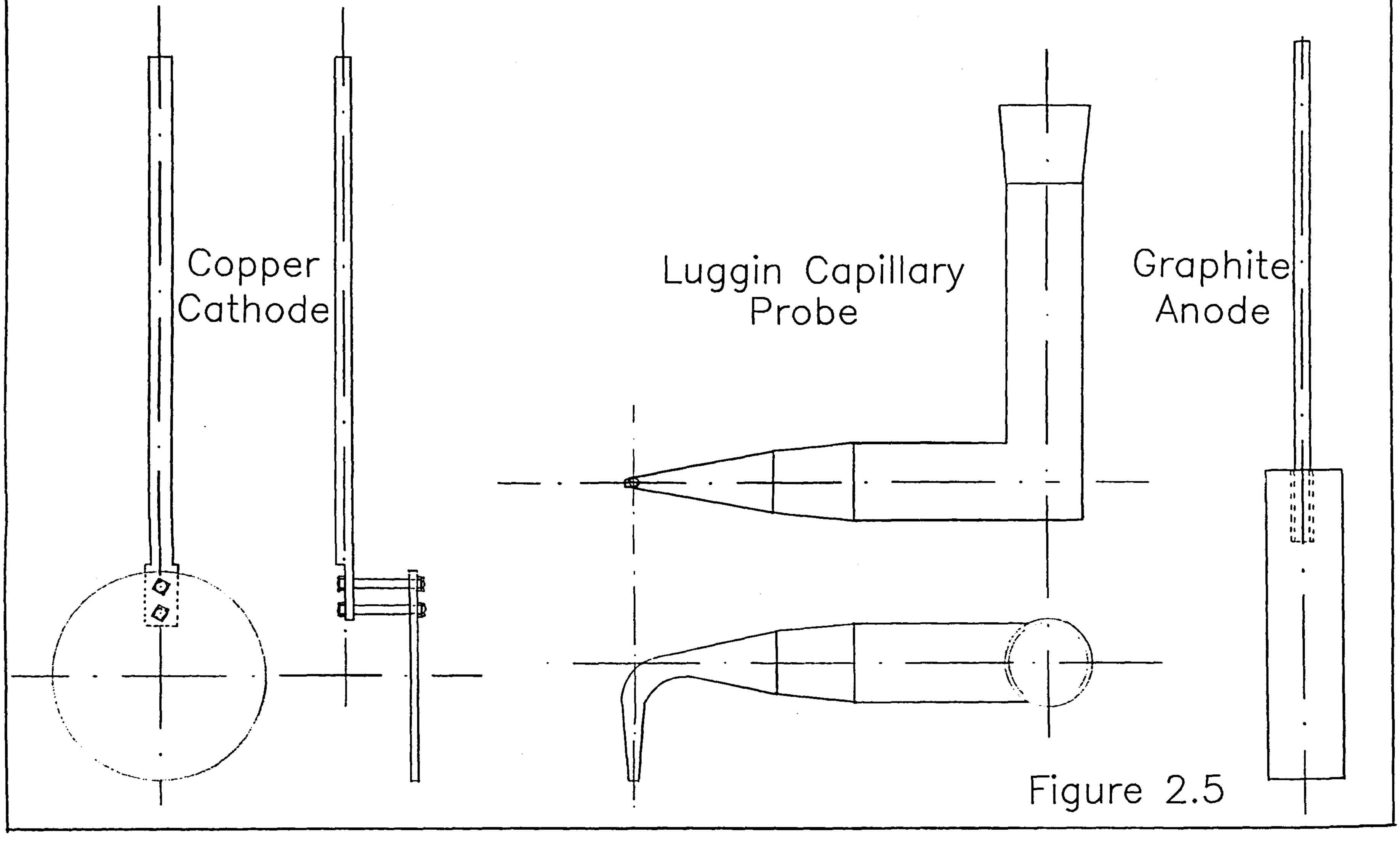

Figure 2.5

impeller was inserted through the top of the cell. Care was taken to insulate the impeller shaft with heat shrinkable tubing and Lacromite.

The instrumentation used is listed below and the circuit diagram is shown in figure 2.6.

Instrumentation.

Power Supplies:	Potentiostats from Sycopel, Station Rd., East Bolden, Tyne and Wear: a) Model 251 Output 1.2A, 28V or b) Model 2510(IR) Output 10A, 28V.
Voltmeters / Ammeters:	Thandar DVM models TM351 or TM 350, or Sinclair Multimeter DM350.
Coulometer:	Time Electronics Type TS 100A Digital Coulometer.
Reference Electrodes:	Saturated Calomel Electrodes made up in our own laboratory (for details see Goodridge and King[67]).

2.1.3 Experimental Procedure – Rotating Disk.

The investigations carried out in collaboration with Dr. Harrison involved steady state current-potential and steady state high frequency impedance-potential measurements in order to accurately determine IR drop, and to correct for it, continuously during an experiment. In addition, linear potential sweeps were also used to investigate the reaction.

Experiments were performed at both 20 and 55°C using a copper electrode of area 0.2 cm^2, which was prepared by mechanical polishing. Two concentrations of nitrobenzene (0.03M and 0.3M) were studied as well as the background electrolyte of 10% sulphuric acid in methanol. The catholyte was routinely degassed with nitrogen before the start of a run.

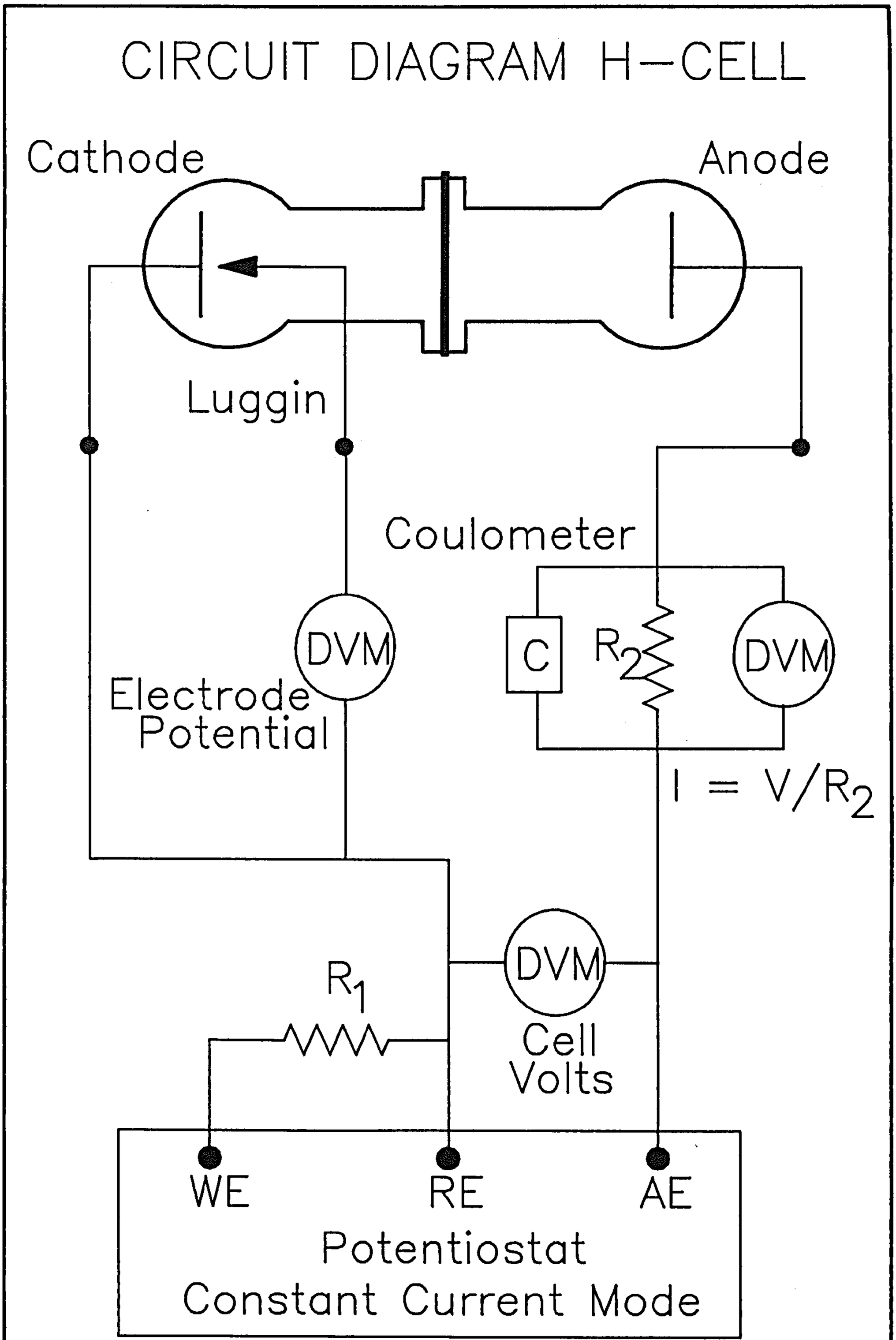
CIRCUIT DIAGRAM H-CELL
Cathode
Anode
Luggin
Coulometer
DVM
Electrode
Potential
C
R_2
DVM
$I = V/R_2$
R_1
DVM
Cell
Volts
WE
RE
AE
Potentiostat
Constant Current Mode

Figure 2.6

During each experiment the potential was increased and then decreased in a series of discrete steps. At each step a range of high frequency signals was imposed over the potential and the resulting output analysed to produce the impedance - potential plot. The methods used and the software to perform them are more fully described by Dr. Harrison[64]. Briefly, the impedance was curve fitted, at each potential, ϕ, to the equation below. The equation was derived by analogy with the well known equivalent electrical circuit of a capacitance in parallel with an electrochemical process, characterised by a resistance and a Warburg coefficient.

$$\frac{1}{Z(\omega) - R_\omega} = \frac{1}{R_{ct} + (1-j).\sigma.\omega^{-1/2}} + j.\omega.C_{dl}$$

Where $Z(\omega)$ is the impedance, R_ω, the Ohmic loss resistance, R_{ct}, the charge transfer resistance, σ, the Warburg impedance parameter, ω the ac potential frequency and C_{dl} the differential capacity of the electrical double-layer.

The graphical display of these parameters ie. plots of $C_{dl} - \phi$, $R_{ct} - \phi$, $R_\omega - \phi$ and $\sigma - \phi$, was used to help characterise the electrochemical process[68]. The potential was corrected at each point using the Ohmic resistance to give the variation of the true electrode potential against the current density.

2.1.4 Experimental Procedure - "H"- Cell.

Prior to a series of experiments the glass cell and attachments were cleaned in 50:50 mixture of HNO_3 and H_2SO_4, rinsed with water and dried. The cell was assembled, with the membrane sandwiched between the two flanges, sealed with a Dow Corning adhesive sealant and then left for several days for the sealant to cure. After a run, providing the flange seals were intact, the cell was rinsed well with water and then methanol. To prevent shrinking and cracking of the membrane, the cell was kept filled with dilute H_2SO_4 in methanol.

The whole cell was mounted in a supporting framework and placed in a thermostatically controlled water bath. The two chambers were filled with

previously mixed methanol and H_2SO_4 (10% by volume) and left to reach operating temperature (55°C), while the electrodes were cleaned.

The cathode was cleaned by careful rubbing with a fine wet-and- dry paper, until the surface was clean and free from scratches. Then the electrode was briefly dipped into 50% aqueous HNO_3 to try and create a reproducible surface. After copious rinsing with methanol, the cathode was placed directly into the cell, the anode having already been cleaned using fine emery paper. As soon as the cathode came into contact with the electrolyte, the current was switched on to maintain cathodic protection.

Due to the relatively low conductivity of the electrolyte and the high currents needed for product synthesis, there was a significant potential drop between the Luggin tip and the cathode. This potential difference, called Ohmic or IR drop, meant that the potential sensed by the potentiostat was not the true electrode potential (see Appendix B). The IR drop is usually compensated by placing the Luggin tip very close to the electrode. However, if it is placed too close current and mass transfer distributions can be seriously affected. In all the experiments using this H-cell the IR drop was compensated using the method described in Appendix B. In addition all runs were performed using constant current (and hence a constant IR drop) conditions. In practice the IR drop proved extremely troublesome in synthesis experiments. The reasons for this lie in the fact that high cell currents were used for the these experiments and the accuracy of the correction can be poor under these conditions. However for polarisation studies a much smaller cathode area, and hence current, was used, resulting in a very small, almost negligible, IR correction.

After the "acid only" electrolysis described in Appendix B to determine the IR correction, the run was started. Being careful not to move the cell or the cathode position, enough nitrobenzene was intoduced to give the required concentration. In synthesis runs this was always 41 g/l. During the run regular measurements of potential, current, and temperature were made. The number of coulombs passed were also noted. The potentiostat was operated in constant current mode. To determine the dependance of products on potential, synthesis runs were performed at various current densities, but a constant number of coulombs was passed during each run. The potential was recorded continuously on a chart recorder. At each chosen

current three runs were performed, while all other conditions were kept as constant as possible.

The electrode area for polarisation studies using the H-cell was between 0.25 and 12 cm^2 and the nitrobenzene concentrations between 0.41 and 41 g/l. Studies using the smaller areas and concentrations could be performed under constant potential conditions, since the IR drop proved almost negligible, or as constant current experiments using the IR correction method described earlier and in Appendix B. Several methods were used, with the H-cell, to determine the polarisation characteristics. Potential or current sweeps using a linear sweep generator were used with a variety of sweep rates. These sweeps were also performed manually. Steady state conditions were investigated by manually stepping the potential or current and then taking readings during several minutes at each step. The number of coulombs passed was always measured to estimate the nitrobenzene consumption, since the nitrobenzene concentration was assumed unchanged during a polarisation study.

2.2 Proposed Reaction Model

2.2.1 Reaction Scheme

It can be seen from the reaction scheme presented earlier (figure 2.1), that the nitrobenzene reduction may be represented as two consecutive electrochemical reductions with the intermediate also open to a competing chemical rearrangement. This is shown diagrammatically in the scheme below. The nitrobenzene, "A", is transported to the electrode surface where it undergoes a four electron reduction to the intermediate "B". "B" may be further reduced at the electrode to aniline, "D", or pass into the bulk and be rearranged to form species "C". "C" represents all the possible rearrangement products which were mainly para-anisidine, para-aminophenol and ortho-anisidine.

Analysis by HPLC and mass spectroscopy (Appendix A) revealed that the main reaction products were ortho- and para-anisidine, para-aminophenol and aniline. Small amounts of azo- and azoxybenzenes were detected, together

with other unidentified di-aromatics. These by-products were difficult to analyse routinely but since they appeared to account for less than 10% of the total products, they were ignored. These observations were consistent with the proposed reaction scheme.

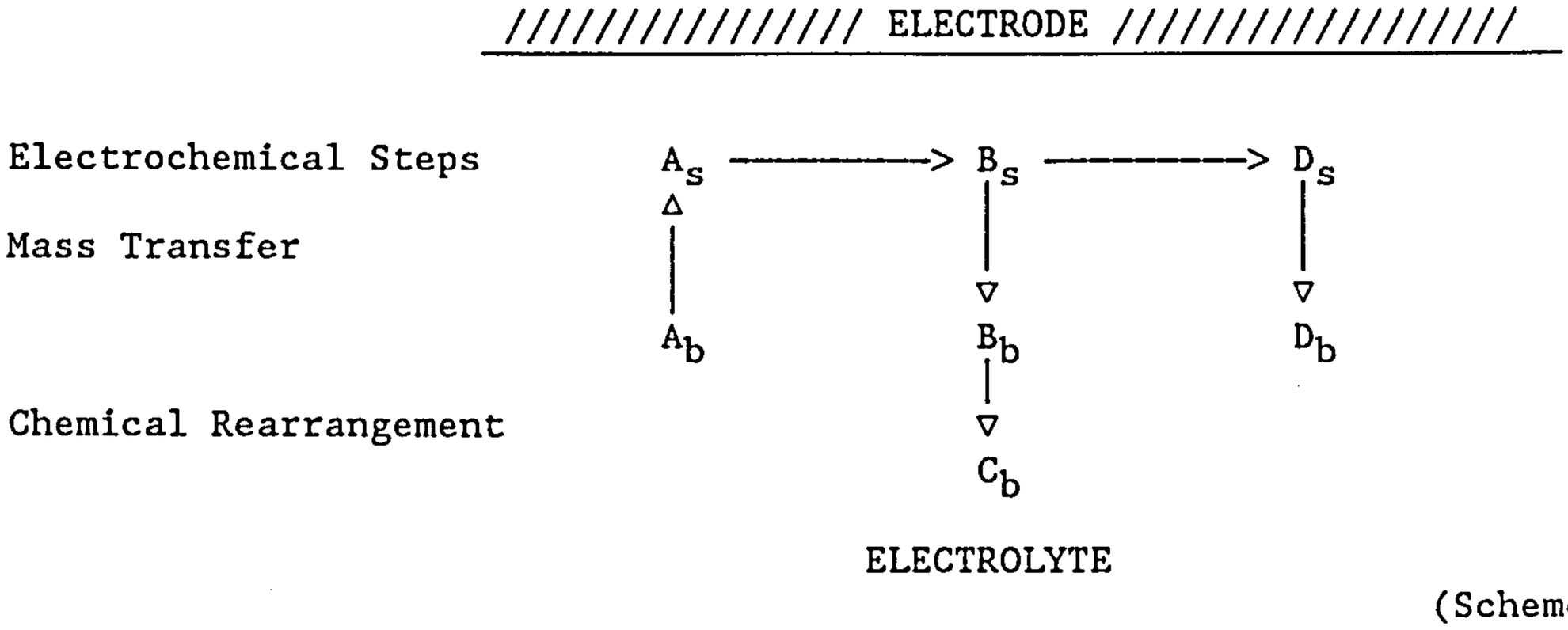

(Scheme 1)

The subscripts s and b refer to the electrode surface and the bulk electrolyte respectively.

For the derivation of the model the possibility of hydrogen evolution was also included, although this was negligible under the experimental conditions used throughout this work (Appendix D). Addition of the hydrogen reaction to the overall scheme allowed the model to be extended to conditions where significant evolution would be expected to occur ie. at high conversions or very high electrode potentials.

Considering the scheme above, it is clear that by removing the intermediate "B" from the electrode surface, further reduction to "D" is prevented and an increase in the yield of "C" will result. Thus, increased mass transfer will favour production of "C" and the ratio of "D" to "C" will decrease. This effect of mass transport has been previously reported by many authors (see section 1.2.2, also Bachurina and Yankovskii[69].

Before continuing, a possible alternative should first be mentioned. If the rate of chemical rearrangement of species "B" is fast, compared to the rate of mass transfer of "B" away from the electrode surface, it is possible that the chemical rearrangement could take place at the electrode surface (Scheme 2 below). In this case the rate of removal of "B" from the electrode would have little effect on the production of "C". The ratio of "D" to "C" produced would depend solely on the relative rates of the

chemical rearrangement and the second two electron electrochemical process and not the rate of mass transfer.

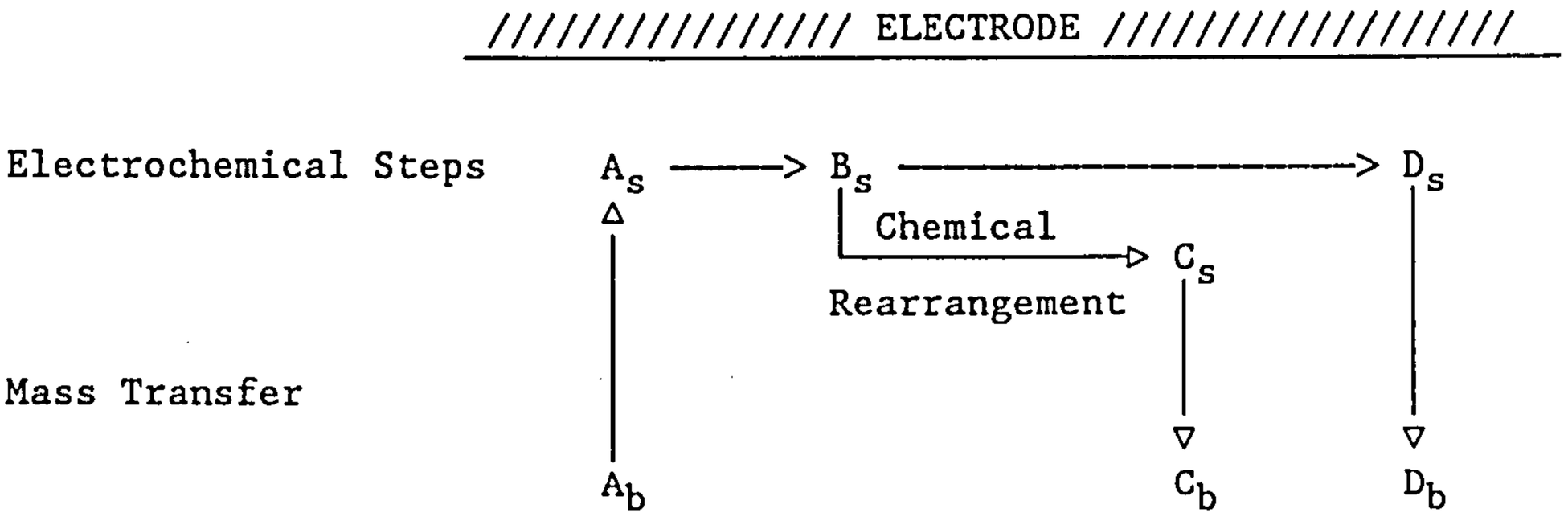

(Scheme 2)

Considering the weight of evidence that the production of para-aminophenol is indeed highly dependant on mass transfer rate, this scheme seemed unlikely for the reduction in aqueous media. Considering the reaction in methanol, several authors[18,19] have demonstrated that the Bamberger rearrangement involving water as the nucleophile proceeded very much faster than for methanol or ethanol. This was confirmed by our own observations that significant para-aminophenol (around 1/5 of anisidine product) was produced during an experiment, although the water content was estimated at around 500 ppm. Further, a strong dependance on mass transport was also observed for the production of para-anisidine. It seemed highly unlikely, therefore, that scheme 2 would be valid for the system under consideration.

From the foregoing discussion and the wealth of published work on the mechanism of the nitrobenzene reduction it is clear that, for the purposes of deriving a reaction model, Scheme 1 above adequately describes the processes involved and it is this scheme which forms the basis for the subsequent derivation of the reaction model.

2.2.2 Initial Polarographic Studies

The first polarisation studies carried out on the reduction of nitrobenzene in methanol / 10% sulphuric acid at a copper cathode in the H-Cell showed what seemed to be a single wave. Furthermore, when replotted as log(current density) versus electrode potential a well-defined linear region was identified with a slope of 170 mV / decade (see figure 2.7). A similar linear "Tafel" region was reported by Goodridge and Hamilton[58,62] using aqueous sulphuric acid. He interpreted this as evidence for activation control over the linear portion. Furthermore, on this evidence he assumed that the electrochemical process could be described by a simple Tafel approximation, implying a single electrode reaction.

Previously some authors[18,25] have reported a "two-wave" reduction of nitrobenzene. In other words a point was reached where the first reaction (A to B) was limited by mass transfer whilst the second reaction (B to D) was prevented from occurring ie. the surface concentration of "B" became zero. Even from the preliminary current - potential studies it became clear that this could not be reproduced for the methanol / 10% H_2SO_4 / nitrobenzene system. The preparative studies, described later in this chapter, confirmed that aniline was produced at potentials lower than the half-wave potential and that the limiting current plateau corresponded to a transfer of six electrons. Therefore, what appeared from the polarograms to be a single electrochemical process was, in fact, two consecutive electrode reactions superimposed onto each other. The same conclusion was reached by Marquez and Pletcher[19] in their extensive study of the aqueous reduction to para-aminophenol at a copper cathode. Considering this further it was not difficult to imagine a situation where mass transfer could affect the product formation without significantly altering the polarisation behaviour of the reaction. So that a change in mass transfer, which had little or no effect on the current and electrode potential, would nevertheless affect the ratio of "D" to "C" ie. the ratio of aniline to para-anisidine.

For these reasons the model derived in Appendix C and presented in the next section attempts to describe the nitrobenzene reduction as two consecutive electrochemical processes subject to the effects of mass transport and a secondary parallel hydrogen evolution process.

Initial Polarisation Data

("H"– cell, 1 cm^2 copper electrode, 55 °C,
0.3 M nitrobenzene, agitation by stirring)

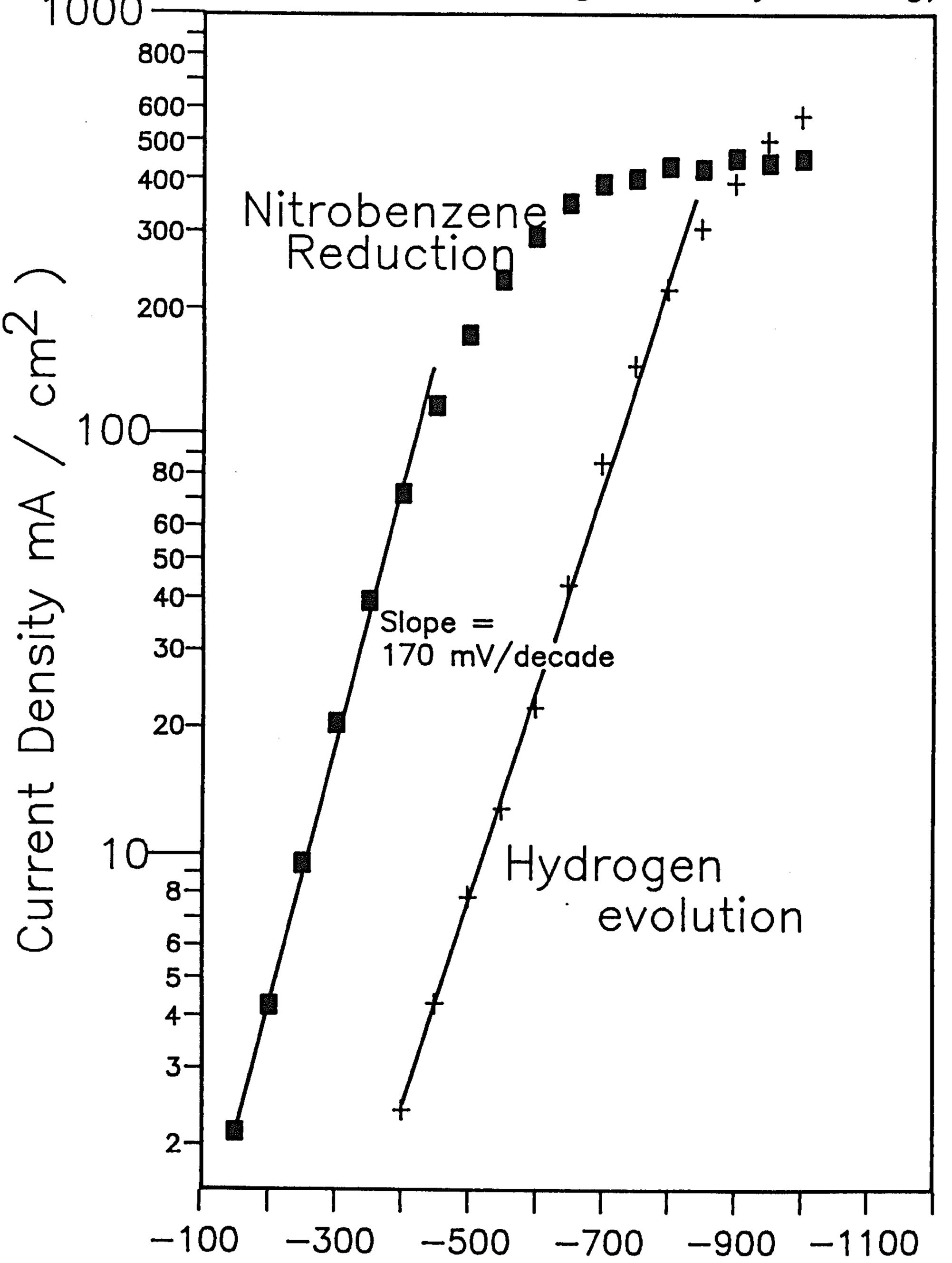

Figure 2.7

2.2.3 Model Derivation

Referring to the scheme below and to Appendix C for a full derivation, the following relationships may be written down to describe the partial current densities due to the first electrochemical process, i_A, the second consecutive process, i_B, and the competing hydrogen process, i_H:

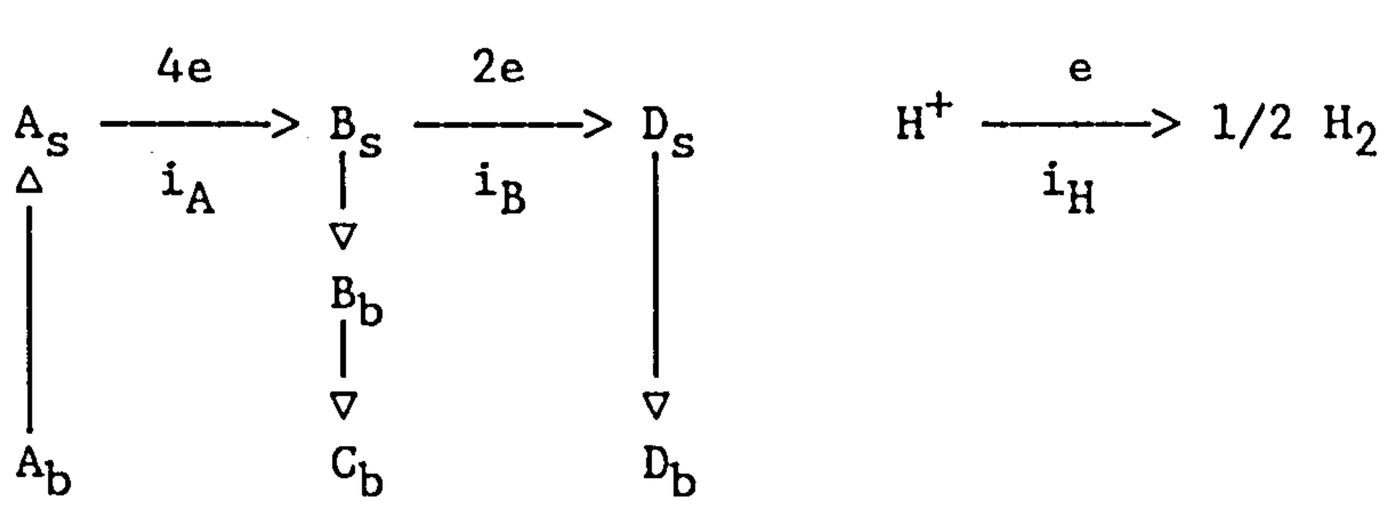

$$i_A = \frac{[A]_b}{\frac{1}{4Fk_L} + \frac{1}{k_A e^{-b_A \phi}}}$$

$$i_B = i_A \times \frac{k_B e^{-b_B \phi}}{4Fk_L + 2k_B e^{-b_B \phi}}$$

$$i_H = k_H e^{-b_H \phi}$$

and $$i = i_A + i_B + i_H$$

where $[A]_b$ is the concentration of species "A" in the bulk electrolyte; i_A, i_B, and i_H are the partial current densities for the primary, consecutive secondary and parallel secondary electrode reactions respectively; ϕ, the electrode potential; k_L, the mass transfer coefficient for the transport of "A" to the electrode and "B" away from the electrode; and k_A, k_B, k_H, b_A, b_B, b_H are the electrochemical kinetic constants.

To arrive at the equations above certain assumptions were made. These are stated fully in Appendix C2.0 but the important ones will be discussed here.

Firstly, it was assumed that the two consecutive electrochemical processes were first order, irreversible and could be described by Tafel relationships. Steady state conditions were also assumed to prevail with negligible accumulation of both reactants or products at the electrode surface. As a first approximation, the concentration of intermediate "B" in the bulk was considered negligible compared to its concentration at the electrode surface. Mass transport in the system was assumed to be adequately described by a single mass transfer coefficient, k_L.

Considering the work done by others in modelling the nitrobenzene reduction the first assumptions seem reasonable. The concentration of the phenylhydroxylamine, "B", was never measured in the bulk electrolyte due to its chemical instability and the great difficulty in analysing this compound. During the routine analysis procedure it was, however, noted that on standing for several hours at 55 ^{o}C some 10 to 15% more rearrangement products were formed. The presence of some unconverted phenylhydroxylamine in the bulk electrolyte was certainly implied. Due to the overwhelming difficulties mentioned in analysing for the hydroxylamine, this was considered an acceptable inaccuracy. It was probably the last of the above assumptions which proved the most difficult to meet in practice.

Measurements of the mass transfer rate in the glass "H" cell were reasonably accurate and great care was taken to ensure an even and reproducible stirring rate for all the experiments. The correlation used for the larger scale cell described in chapter three, however, included implicit assumptions of fully developed flow and absence of entry effects that were difficult to verify or allow for. This was noted as a limitation in extending the model to the larger cell.

It was found from initial rotating disk work that polarisation studies alone were not sufficient to determine the kinetic constants in the model. For this reason a series of preparative experiments were performed, during which the electrode potential and current density was recorded. The rate of mass transfer was kept constant throughout all the experiments. By analysis of the reaction products the amount of current consumed in forming each of the products could be calculated and hence the two partial currents, i_A and i_B, directly determined. The glass "H" cell described earlier in section 2.1.2 was used for these experiments. To complement this work polarisation studies at various rates of mass transfer were carried out using a rotating

disk electrode. The remainder of this chapter is devoted to the results and discussion of this work.

2.3 Results and Discussion - Determination of the Kinetic Constants

2.3.1 Polarisation Studies - Determination of k_H, b_H and b_A

To complement the preparative experiments, further polarisation studies were undertaken and the results used to determine the kinetic constants for the hydrogen evolution reaction and the Tafel constant, b_A, for the primary reaction. These were done with the help of Dr. J. Harrison, whose sophisticated and specialised equipment exceeded our own capabilities. In particular, Dr. Harrison's equipment could accurately determine Ohmic or IR losses, which were significant for the relatively low conductivity electrolyte used throughout this work. Further discussion of this point can be found in Appendix B. Studies were made of the nitrobenzene reduction at two different nitrobenzene concentrations and also when no reactant was present. This latter case is dealt with first.

A) Background Hydrogen Evolution

The polarisation curve for methanol / 10% sulphuric acid determined using the equipment described in section 2.1.1 is shown in figure 2.11. Insufficient degassing prior to the experiment meant that there was some dissolved oxygen in the electrolyte, which was reduced during the run. Nevertheless, the polarisation plot showed a clear linear portion due to hydrogen evolution. Noting that the model for hydrogen evolution predicts a linear log(i) vs ϕ (equation E1, Appendix E1.0), analysis of the slope and intercept gave the kinetic constants, k_H and b_H, associated with this reaction. Thus we have:

$$k_H = 1.01\text{x}10^{-10}\ \text{A/m}^2 \text{ per kmol/m}^3 \quad \text{and} \quad b_H = 0.0359\ \text{mV}^{-1}$$

The charge transfer resistance showed that the hydrogen evolution reaction started at around -600 mV in both the methanol / sulphuric acid

Polarisation Studies

MeOH / 10% H_2SO_4 at copper rotating disk electrode, area 0.2 cm^2 , 55°C

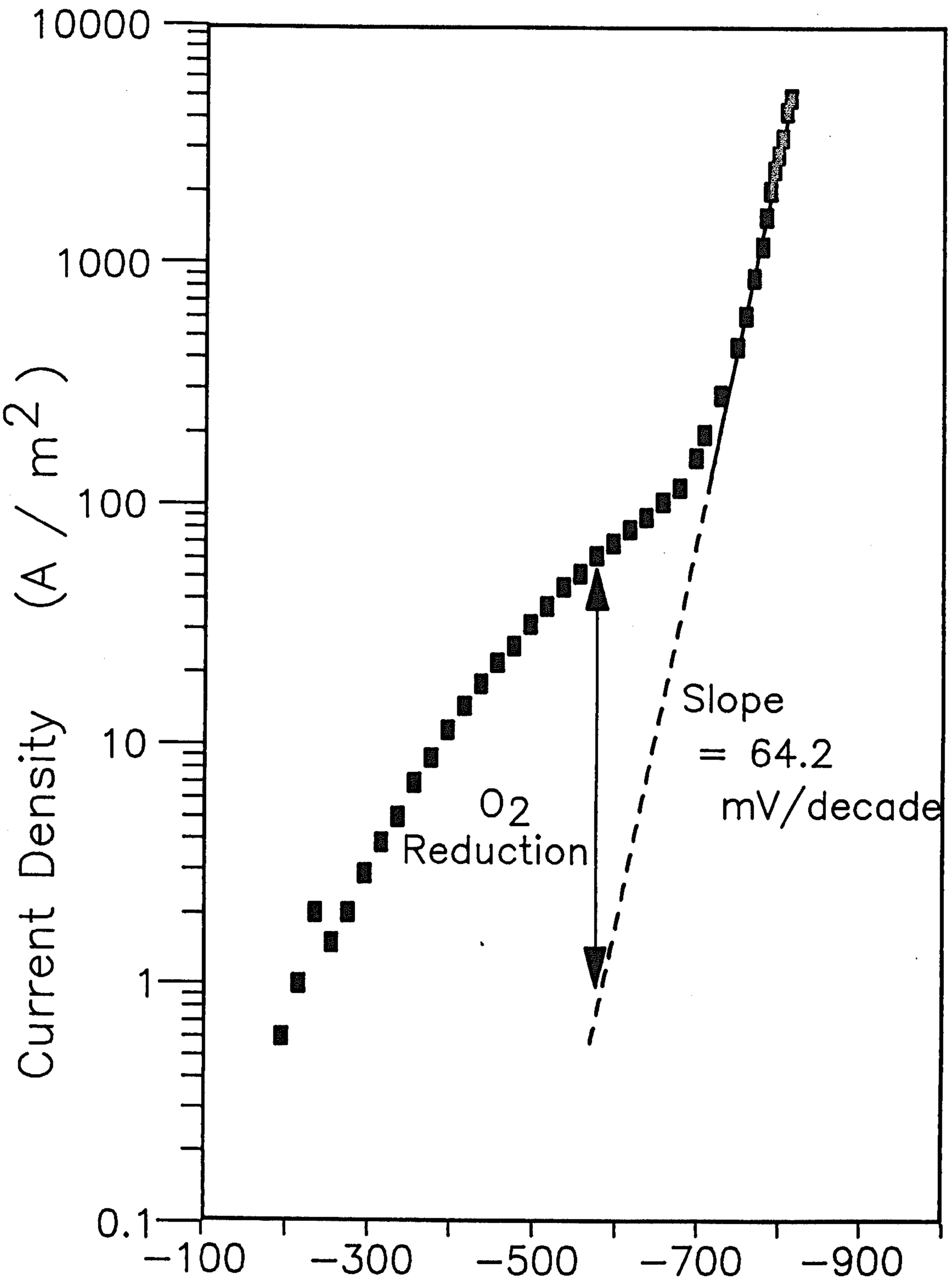

Figure 2.11

electrolyte and the aqueous electrolyte. What was interesting, however, was the initial portion of the curves at low potentials. For methanol R_{ct} was constant until the reduction process began, but the aqueous electrolyte showed a steep rise between -100 and -200 mV. The only likely explanation was that at potentials more anodic than -200 mV dissolution of the copper electrode into the aqueous electrolyte was taking place. This was not the case when methanol was used, the copper was cathodically protected over the whole range (-100 -> -800 mV) when methanol was used.

B) Nitrobenzene Reduction

Figures 2.12 show polarisation curves obtained at two electrode stirring rates using 0.03 M nitrobenzene. A limiting current is clearly visible, which is proportional to the square root of rotation speed. The limiting current plateau at 580 A/m^2 for the 10 Hz experiment was identified as being limited by mass transport after examination of the change in Warburg impedance and charge transfer resistance with potential during the run. The Warburg impedance became significant between -550 and -750 whilst the charge transfer resistance remained constant, indicating that mass transport was dominant over this range. Figure 2.13 compares polarisation curves obtained at 20°C and 55°C, showing the effect of temperature on the current - potential relationship.

Referring to the well known theory of the rotating disk electrode assuming a six electron transfer (See Appendix F1.4), the limiting current data can be used to calculate the value below for the diffusion coefficient, D, for nitrobenzene in 10% sulphuric acid / methanol. Direct comparison with the literature values is impossible since this system has not been studied before, however, the results are certainly within the range normally found for nitrobenzene. (cf. 5.5×10^{-6} cm^2/s for 0.1 M HCl in 70% ethanol / 30% water at 20°C[71]; 4.4×10^{-6} cm^2/s for 1.0 M H_2SO_4 in 50% ethanol / 50% water at 20°C[70]; 8.8×10^{-6} cm^2/s for 3 M H_2SO_4 in 50% acetone / 50% water at 20°C[19].)

$D = 6.9 \times 10^{-6}$ cm^2 / s at 20°C and $D = 1.1 \times 10^{-5}$ cm^2 / s at 55°C

Polarisation Studies

0.03 M nitrobenzene at rotating copper disk electrode, area 0.2 cm^2, 20°C.

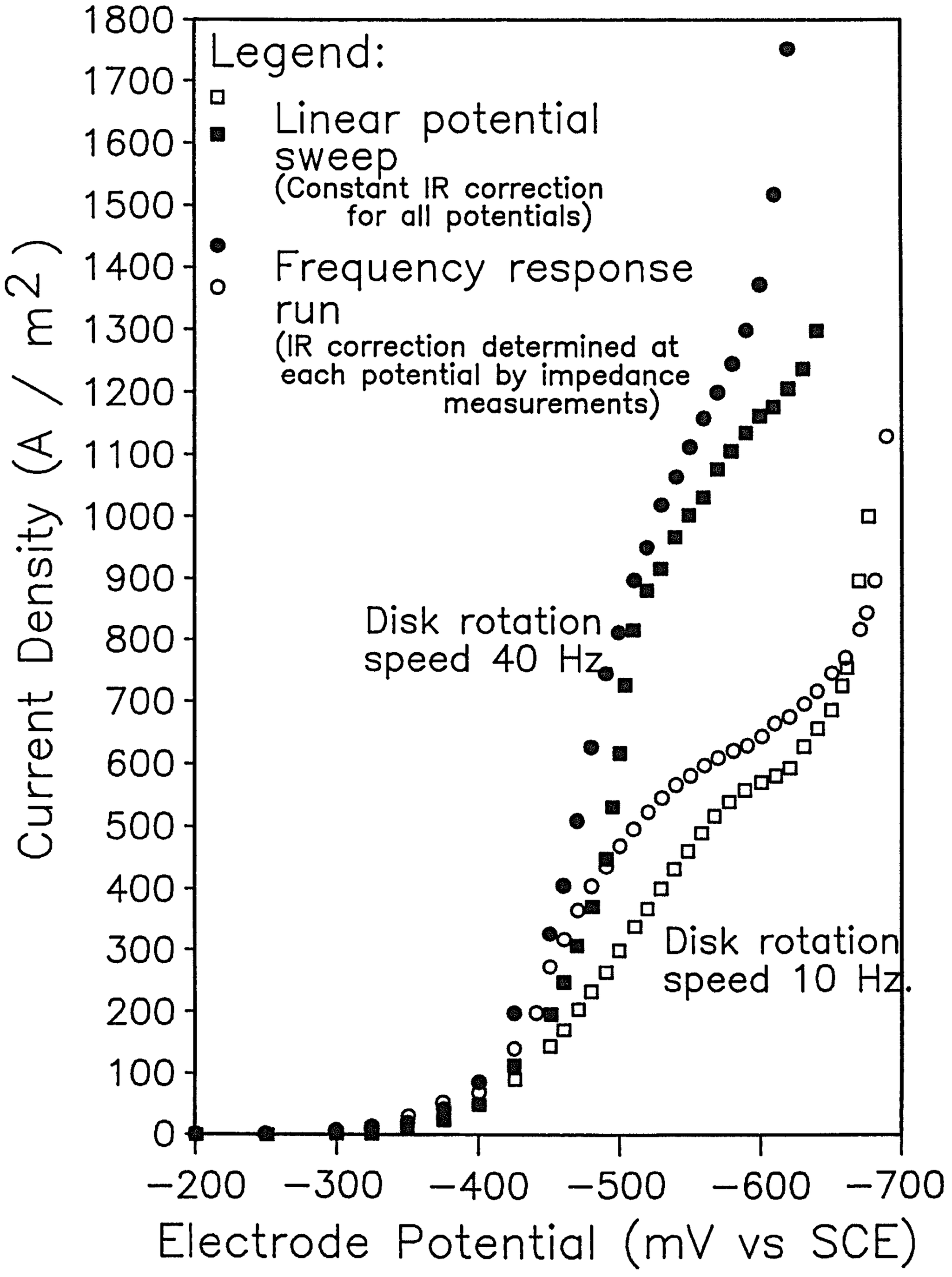

Figure 2.12

Polarisation Studies

0.03 M nitrobenzene at rotating copper disk electrode, area 0.2 cm^2, 55 and 20°C.

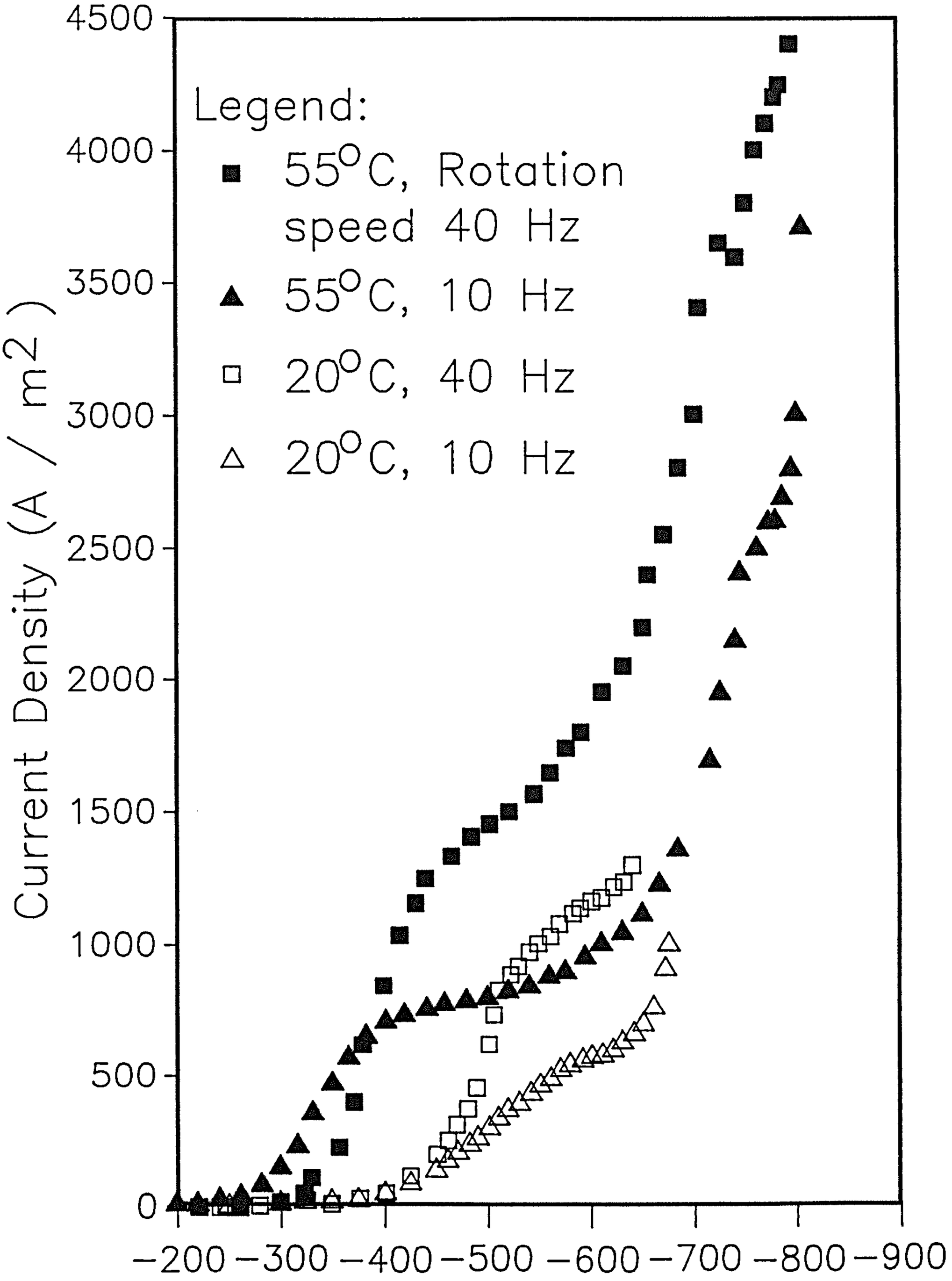

Figure 2.13

Polarisation Studies

0.3 M nitrobenzene at rotating copper disk electrode, area 0.2 cm^2, 55 and 20°C.

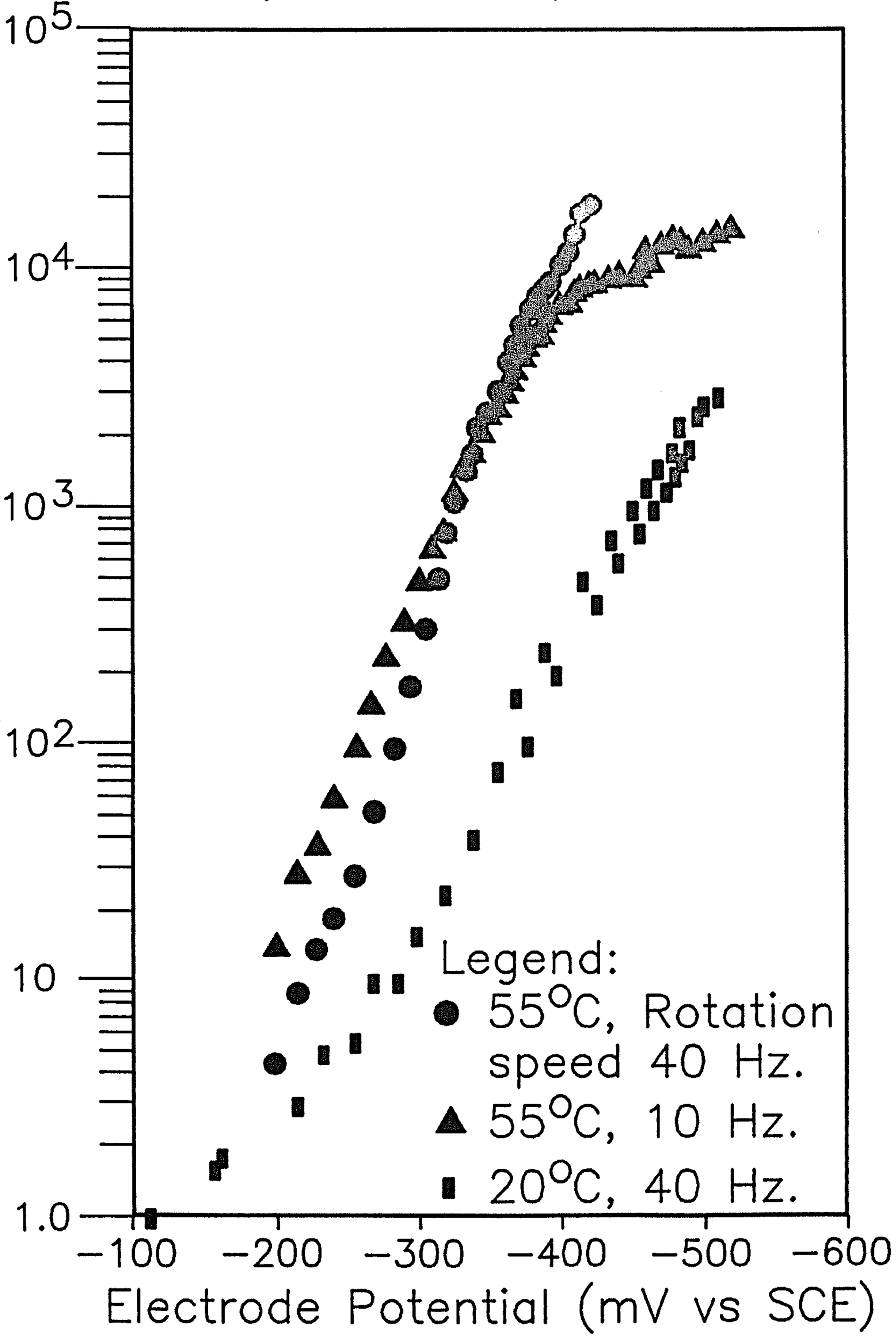

Figure 2.14

Figure 2.14 shows the polarisation data determined for a 0.3 M nitrobenzene concentration at two different temperatures. Quite why there was some difference at lower potentials between the two rotation speeds is unknown. Possibly the surface of the rotating disk was slightly different for the two runs, giving rise to a different electrochemical rate constant.

The data obtained at 55°C for 0.03 and 0.3 M nitrobenzene concentrations allowed one of the kinetic constants, b_A, to be determined. At low cathodic potentials the model (see Appendix E1.0) showed that the expressions for the partial current densities reduced to:

$$\log \frac{i_A}{[A]_b} = \log k_A - b_A.\phi \quad \text{and} \quad i_B \rightarrow 0, \text{ thus } i = i_A$$

Figure 2.15 shows the plot of the relationship above obtained using results from the polarisation curves determined at 55°C and 40 Hz. The slope of which gave the constant b_A. Note that whilst k_A could also be determined from this data it would only be applicable to the special case of a polished electrode where negligible reaction was taking place. To be able to apply the model to a preparative situation, k_A must be determined under conditions of significant product formation ie. during a preparative process. Thus we have:

$$b_A = 0.0348 \text{ mV}^{-1}$$

2.3.2 Preparative Study – Determination of k_A, b_B and k_B

The results described below were obtained using the glass "H" cell described in section 2.1.3. The aim of the study was to provide the necessary kinetic constants for the reaction model. Under constant current conditions (for reasons of IR drop*) experiments were run to about 10% nitrobenzene conversion (30,000 Coulombs). During the experiment electrode potential was recorded, and the products formed were determined

---

*Only under constant current conditions would the IR drop also be constant during an experiment.

Polarisation Studies

Determination of Kinetic Constant, b_B for the First Reaction.

(Copper rotating disk, area 0.2 cm^2, 55°C)

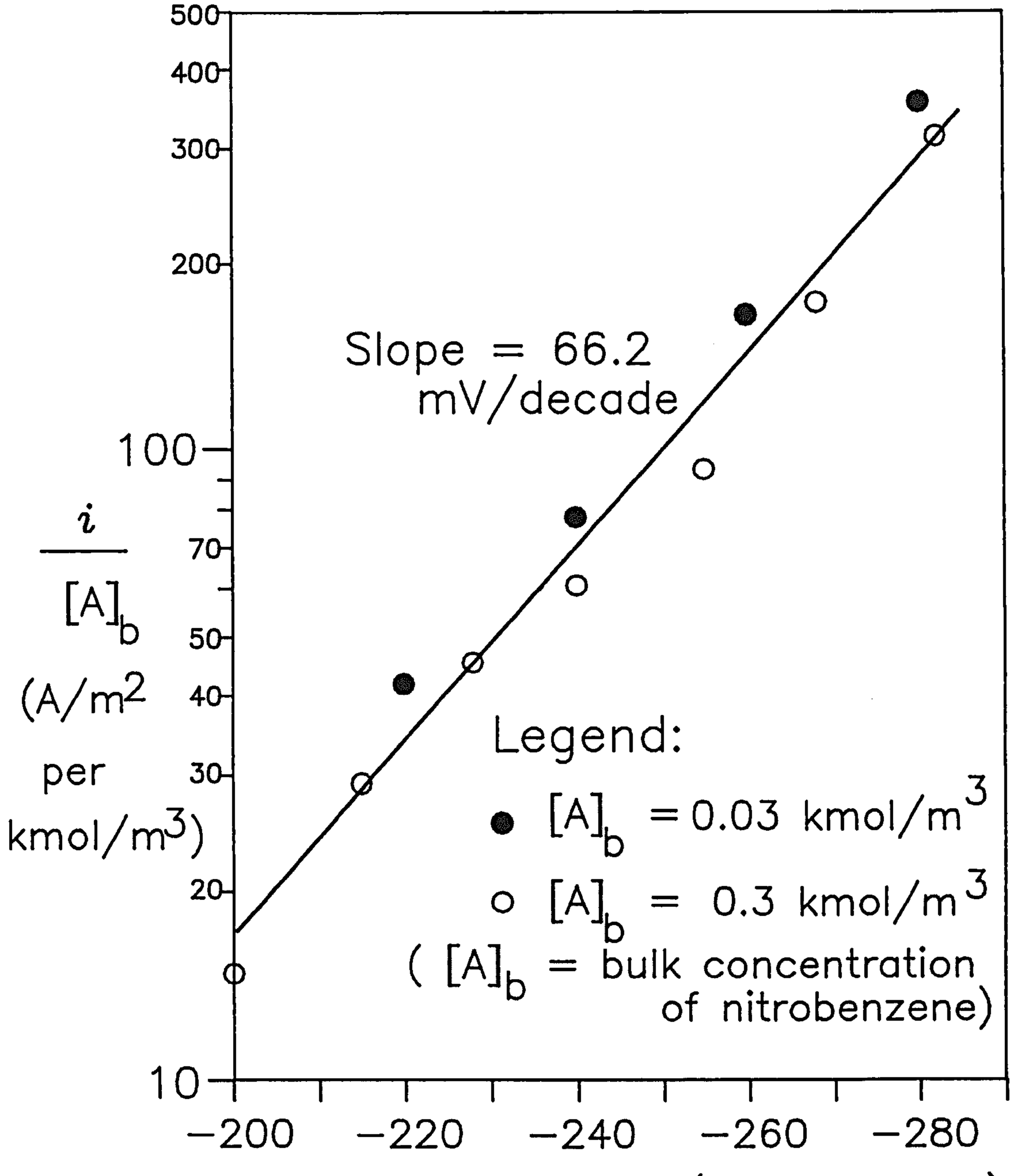

Figure 2.15

quantitatively by HPLC. In this way the two partial currents, i_A and i_B, were obtained as a function of electrode potential, which allowed the remaining kinetic constants to be calculated. Full experimental results may be found tabulated in Appendix G. The validity and accuracy of measurements made using the H-Cell results are discussed first in this section. The results are then presented and discussed before they are finally used to determine the remaining kinetic constants.

Current Potential Reproducibility.

Two similar glass cells and several copper electrodes were used for this study. In order to assess the effects of this upon results and to test the reproducibility of measurements, a series of polarisation studies were made for each cell and electrode. Also investigated was the effect of electrode preparation. Figure 2.18 shows polarisation curves obtained using cell no. 2 where the electrode was cleaned between each run 1 to 8. Figure 2.19 shows results from cell 1 when consecutive polarisation studies were carried out with no electrode cleaning between runs 1 to 8. There was considerable scatter of results, particularly at higher potentials, but this was attributed to inaccuracies in the determination of IR drop, which were more significant at higher current densities. Overall the results are not greatly affected by the method of electrode preparation.

Figure 2.20 shows the average polarisation data from cells 1 and 2. A difference in potentials of up to 75 mV between the two cells was noted for the same current density (Note all experiments were run under conditions of constant current density). This, however, is of the same order of accuracy found in the results for each individual cell (figures 2.18 and 2.19), suggesting that there was no great difference between the cells. Finally, figure 2.21 shows polarisation curves determined before and after preparative runs. These results showed that the preparative process had no significant effect on the current - potential behaviour, up to at least 10% conversion.

Thus the conclusion was that although there was some degree of error in the measurement of electrode potential, this was not due to methods of electrode preparation, electrode changes during the preparative process or to which cell was used for an experiment. The most likely source of the

H–Cell Polarisation Curves

Cell #2– electrode cleaned between each run 1–8

(55°C, 10 cm^2 electrode area, 0.3 M nitrobenzene)

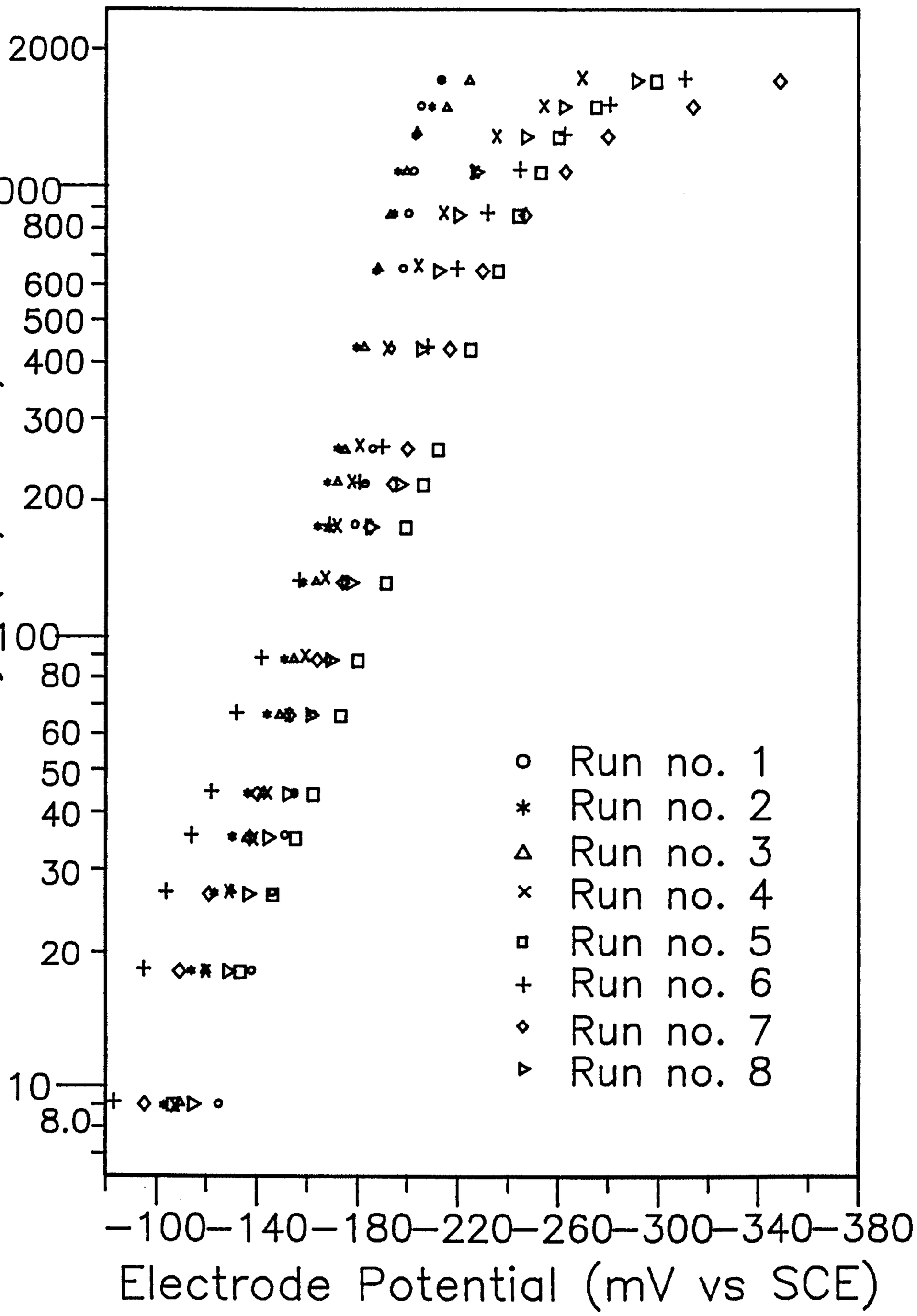

Figure 2.18

H–Cell Polarisation Curves

Cell #1– no electrode cleaning between the runs 1–8

(55°C, 10 cm^2 electrode area, 0.3 M nitrobenzene)

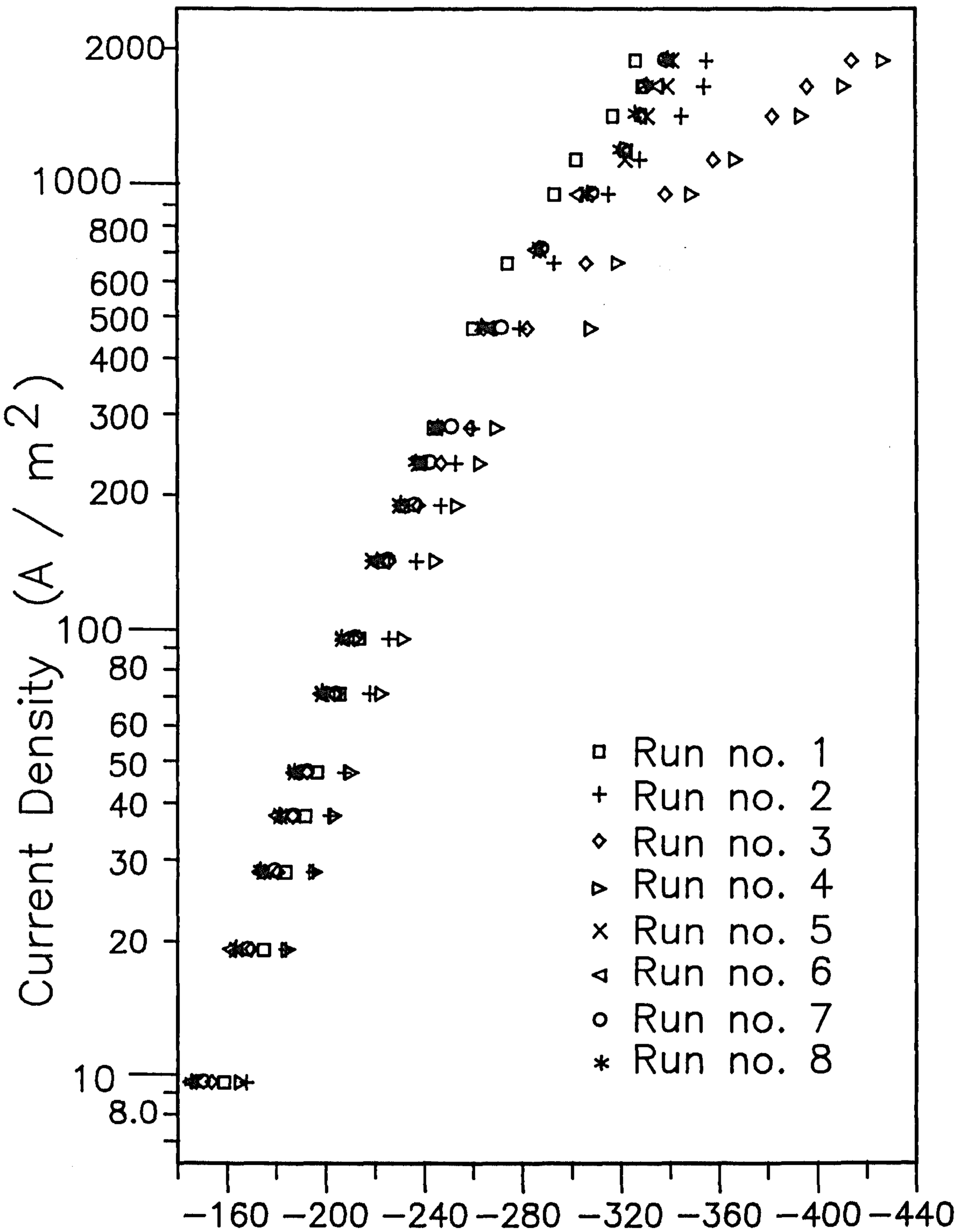

Figure 2.19

H–Cell Polarisation Curves

Average results for cell #1 and #2

(55°C, 10 cm^2 electrode area, 0.3 M nitrobenzene)

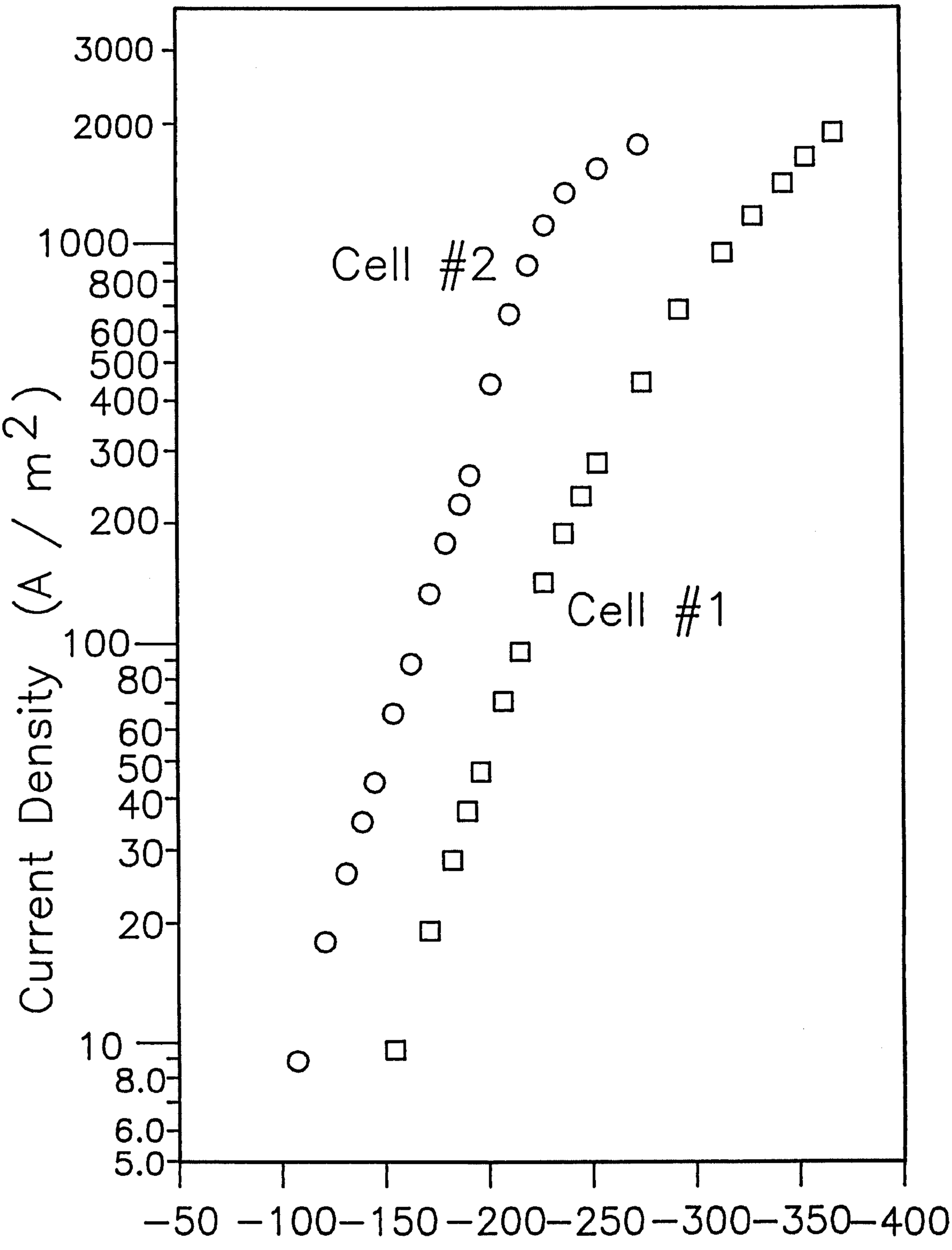

Figure 2.20

H—Cell Polarisation Curves

Before and after bulk electrolysis runs 1—4 (electrode cleaned between each run)

(55°C, 10 cm^2 electrode area, 0.3 M nitrobenzene)

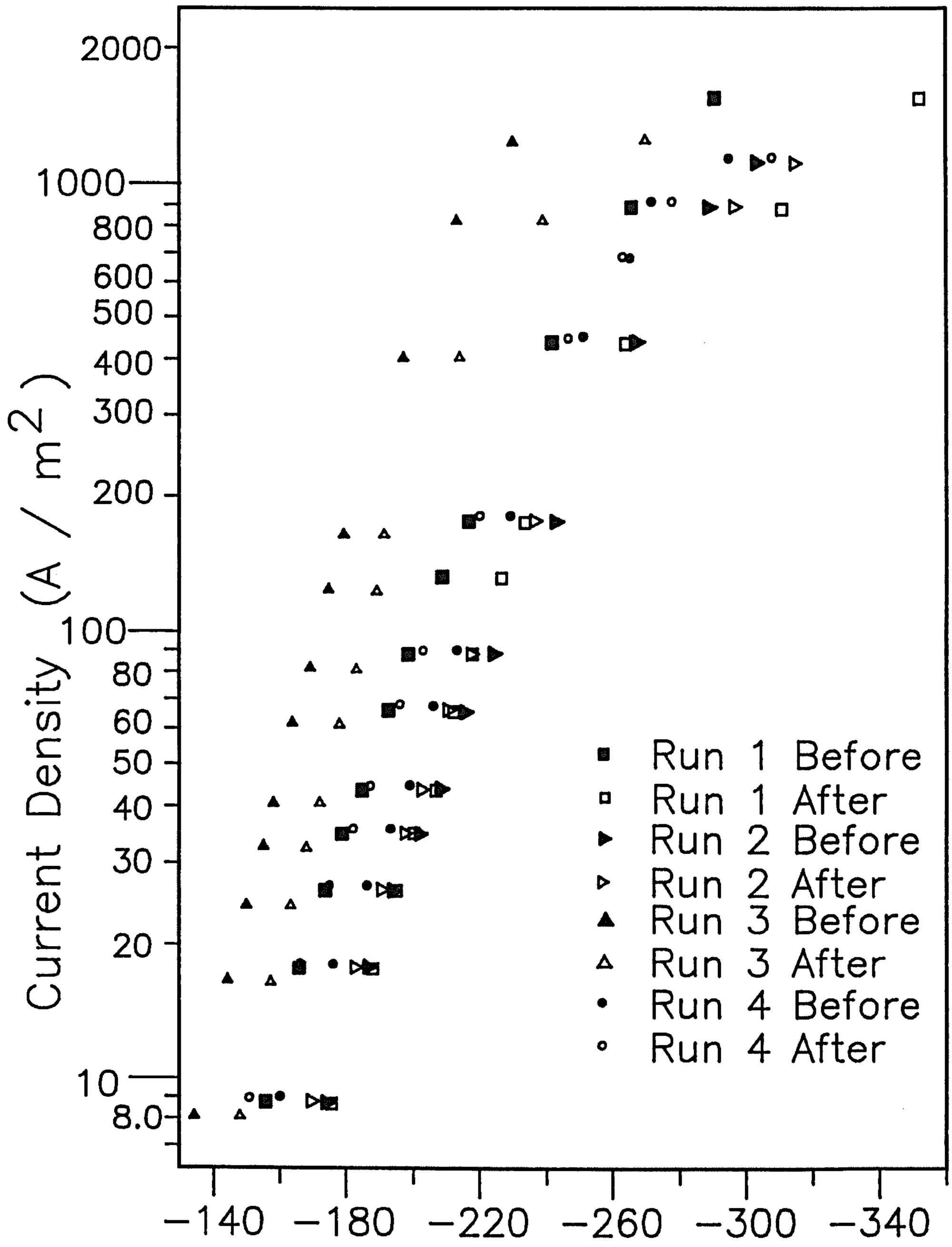

Figure 2.21

error was in the correction for IR drop implicit in the measurement of the electrode potential. This problem is further discussed in Appendix B. Comparison of all the polarisation curves indicated that the slope of linear portion of the curves (on a log(i) vs ϕ plot) remained constant, whilst the curves were "shifted" to more or less cathodic potentials. This observation suggested that small surface changes were responsible for any differences rather than a change in the nature of the electrochemical process.

Effect of Potential and Current Density on Reaction Products

The results from the preparative experiments with the H-cell are tabulated in Appendix G2. The products are expressed as moles formed after 5000 coulombs had been passed at a constant current density as detailed in section 2.1.4. Figure 2.22 shows these results plotted as the 4e- products (that is ortho- and para-anisidine and para-aminophenol) versus current density. The six electron product, aniline, is plotted together with the total 4e- products in figure 2.23. It is clear from these graphs that aniline production is, as expected, increasingly favoured at higher current densities, corresponding to a decrease in the rearrangement products.

During the H-Cell experiments the electrode potential was recorded and the average potential over the experiment determined. Due to the size of the correction for IR drop that was required, these potentials were subject to considerable doubt. Figure 2.24 compares the current density - electrode potential data so obtained from the preparative runs with the average polarisation curves for cells 1 and 2. The good agreement between these results indicates, within experimental error and despite the difficulties with IR drop, that the average potentials were meaningful and can be used with confidence in determining the kinetic constants. Further confirmation of these measurements can be found in Appendix B, where figure B2 compares these H-Cell results with those from the rotating disk work, in which IR drop was precisely determined. Despite the difference in mass transport between the rotating disk cell and the H-Cell and considering that no significant preparative process occurred at the rotating disk, there was good agreement.

H–Cell Preparative Results

4e– reduction products

(55°C, 10 cm^2 electrode area, 0.3 M nitrobenzene)

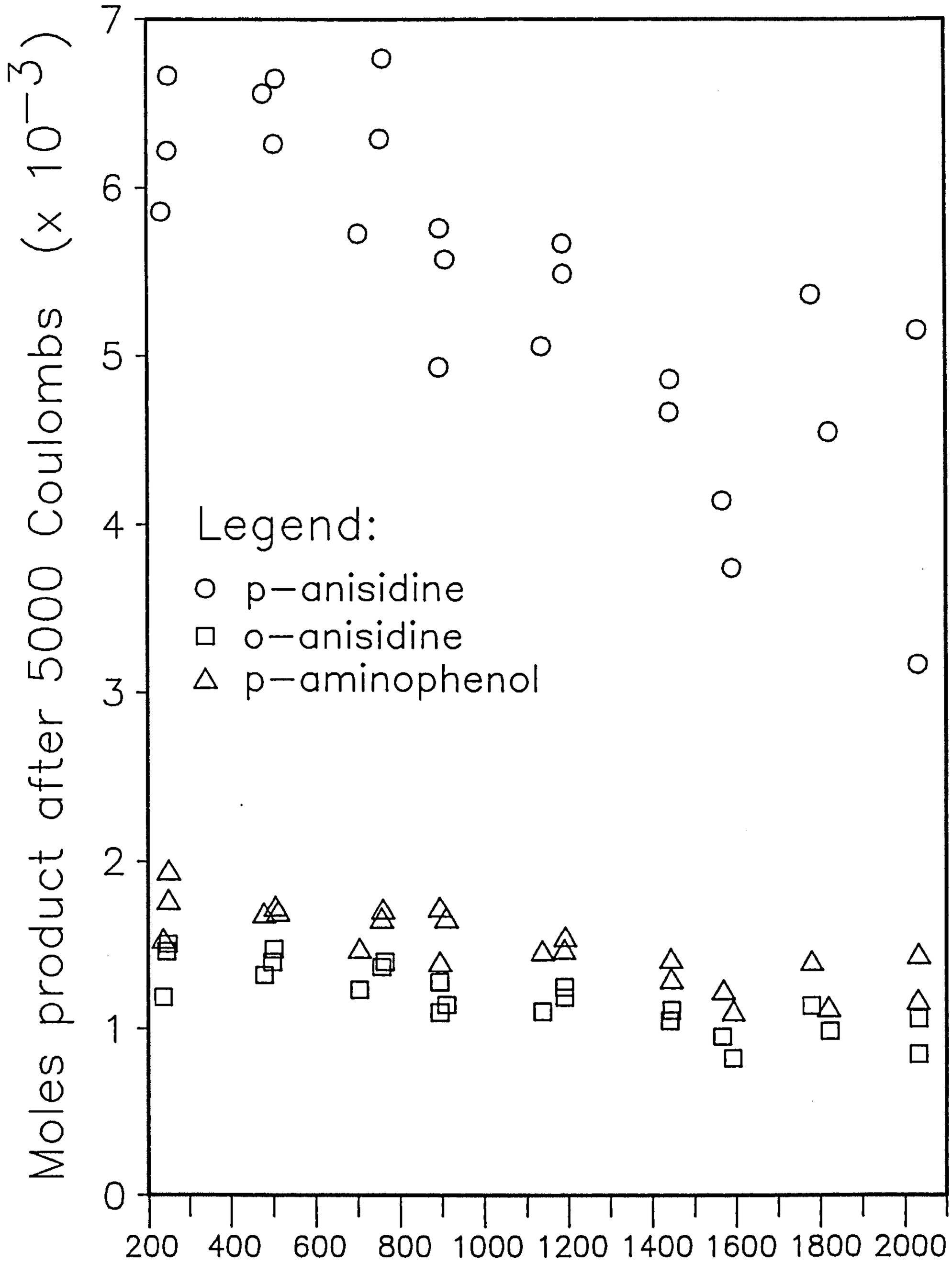

Figure 2.22

H—Cell Preparative Results

4e— and 6e— reduction products

(55°C, 10 cm^2 electrode area, 0.3 M nitrobenzene)

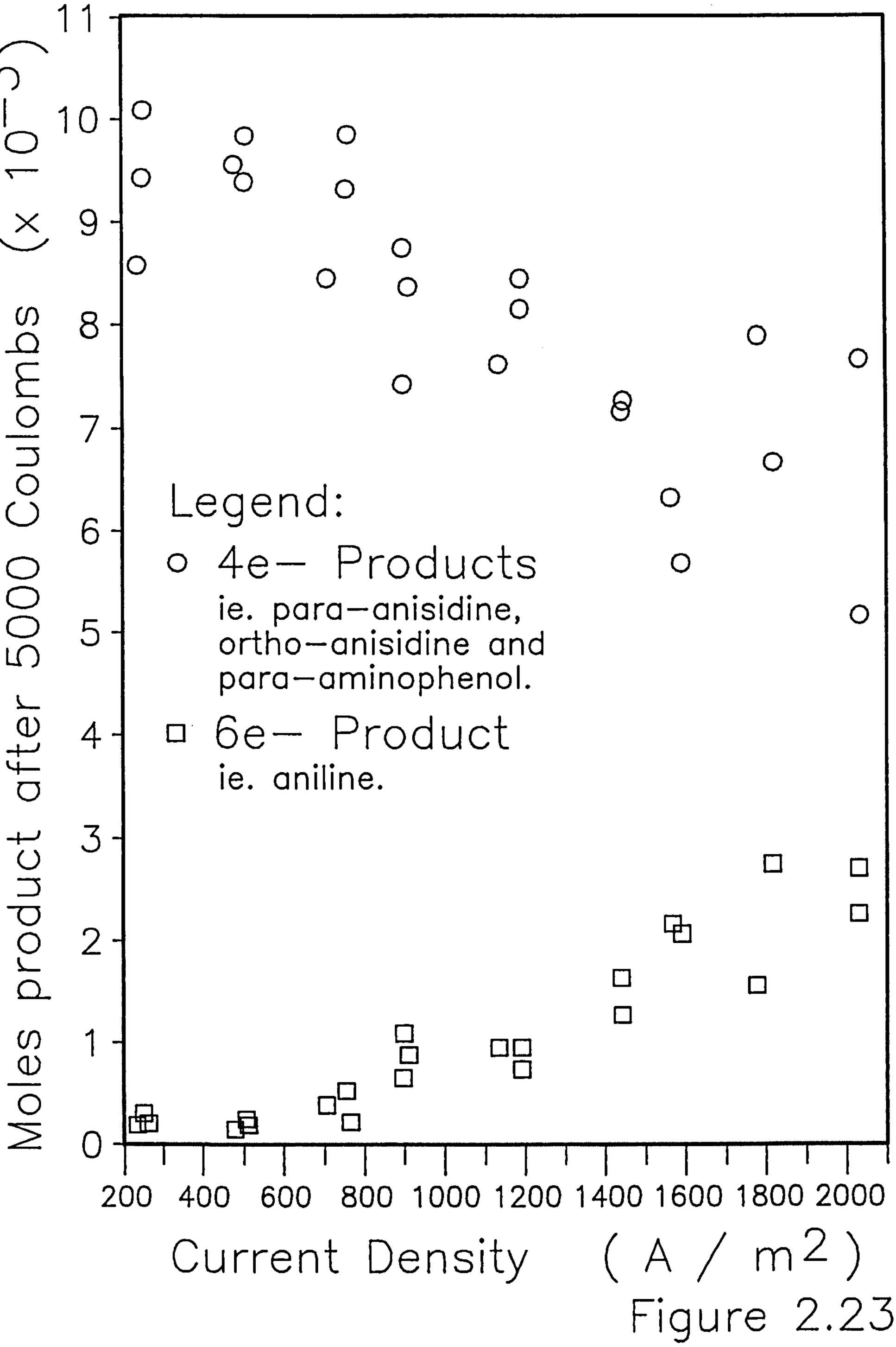

Figure 2.23

H—Cell Polarisation Curves

Results from preparative runs compared to average cell #1 and #2 results

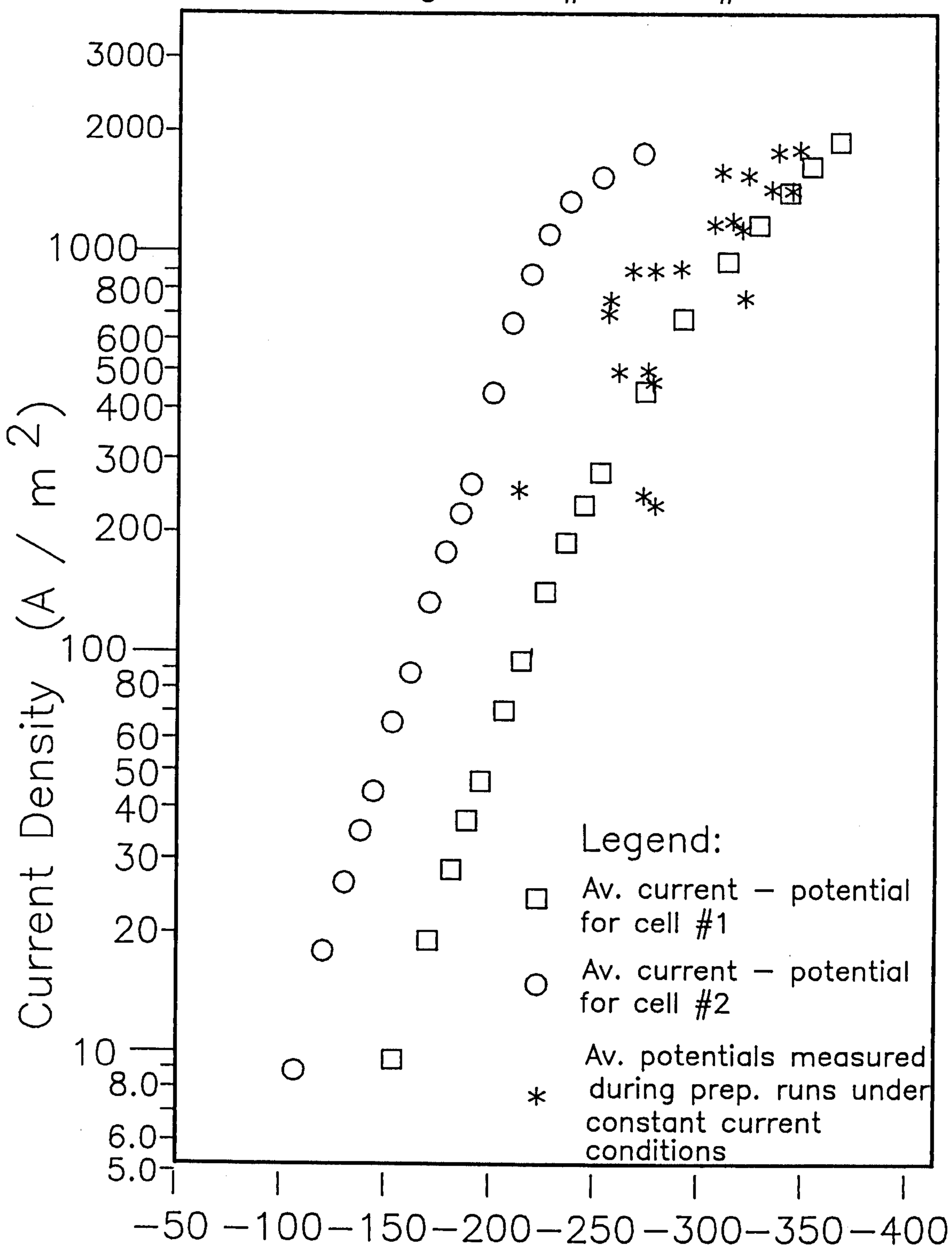

Figure 2.24

Before continuing, mention should be made of the method used to calculate i_A and i_B from the preparative results. The table below shows results from two H-cell experiments expressed as current efficiencies, CE, defined as:

$$CE = \frac{\text{Coulombs required to produce each product}}{\text{Total Coulombs passed (ie. 5000)}} \times 100\%$$

The average value for the current efficiency for all products over all the experiments is also shown.

Current Density (A/m^2)	Current Efficiency				
	4e- Products			6e-	Total
	o-anisidine	p-anisidine	p-aminophenol	aniline	
1140	8.5%	39.2%	11.4%	10.9%	70.0%
2040	8.3%	40.8%	11.5%	31.4%	92.0%

Average total of all experiments: 76.1%

These results show that the measured products using the HPLC analysis did not account for all of the current passed during the experiment, indeed in the worst case only 70%. Under the conditions of the experiments no hydrogen was evolved (Appendix D) so the only explanation for this "lost" current was either inaccurate analysis or undetected by-products. A full discussion of this point can be found in Appendix A4.0 onwards. Briefly, the conclusion was reached that the analysis gave acceptable values for the ratio of four to six electron products, but that an absolute quantitative determination of the products was not possible. Coupling reactions or adsorption effects were blamed for this problem. The implication for the determination of the kinetic constants was that only the measured ratio of products from the preparative results was used.

Referring to Appendix E2.0 it is shown there that:

$$i_A \propto 4F \times \text{measured total production rate}$$

and

$$i_B \propto 2F \times \text{measured production rate of aniline}$$

Hence,

$$i_A / i_B = \frac{2 \text{ x measured rate (total products)}}{\text{measured rate (aniline)}}$$

Further, given that during the experiment $i = i_A + i_B$, that is to say that the current efficiency for the total products is corrected for errors in the analysis to 100%, i_A and i_B are given by:

$$i_A = i / (i_B/i_A + 1)$$

and

$$i_B = i / (i_A/i_B + 1)$$

Figure 2.25 summarises the H-Cell preparative results in a plot of the partial current densities against the average electrode potential. These results were used to calculate the remaining constants as described below:

Determination of Kinetic Constants – k_A

Rearrangement of equation (C8) (Appendix E2.0) results in:

$$Y = \frac{1}{\frac{1}{i_A} - \frac{1}{4.F.k_L.[A]_b}} = k_A.[A]_b.e^{-b_A\phi}$$

Using the preparative results to determine i_A/i_B and, hence, i_A ,Y and the corresponding values of $e^{-(b_A\phi)}$ (noting $b_A = 0.0348\ mV^{-1}$ and $k_L = 1.6 \times 10^{-5}$ m/ s) were calculated. This data is tabulated in Appendix G. In plotting Y against $e^{-(b_A\phi)}$ for the determination of k_A, only data in which mass transport was relatively insignificant were used. The resulting straight line through the origin is shown in figure 2.26. Least squares analysis gave the slope and, hence, k_A:

$$k_A = 0.191 \text{ A / m}^2 \text{ per kmol / m}^3$$

H–Cell Polarisation Curves

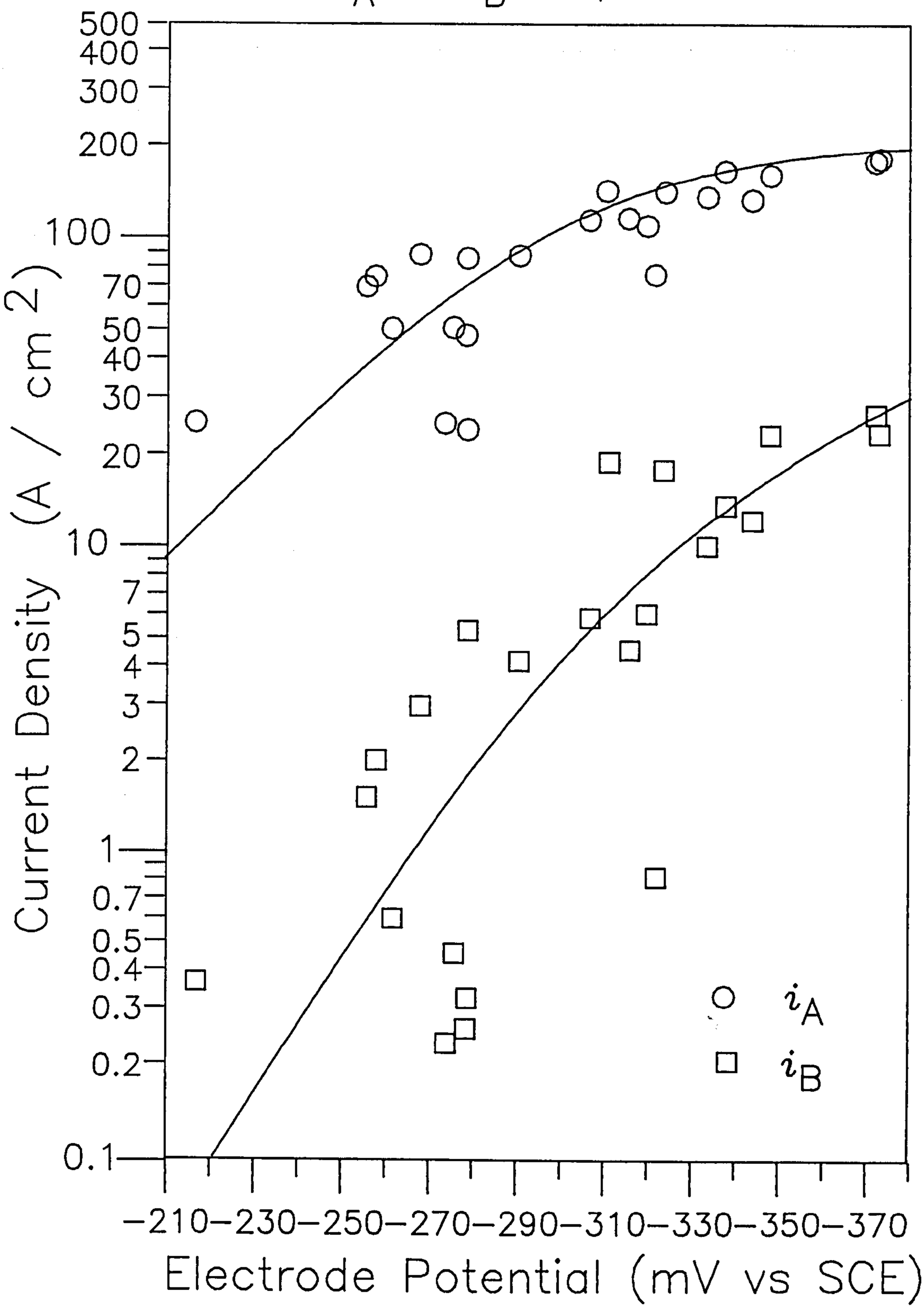

Figure 2.25

H—Cell Preparative Results

Calculation of rate constant k_A

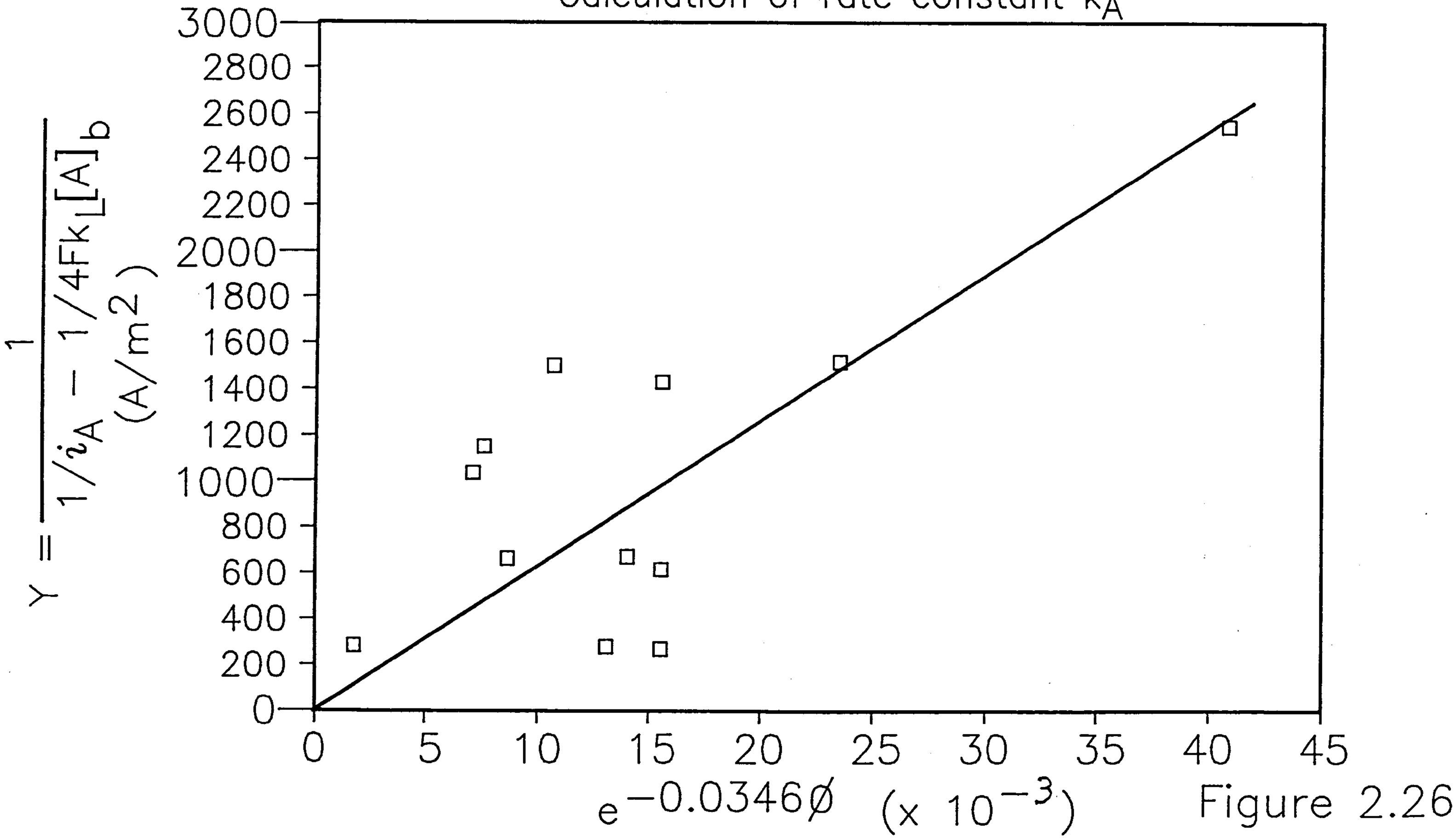

Figure 2.26

H—Cell Preparative Results

Determination of kinetic constants for the consecutive secondary reaction (b_B , k_B)

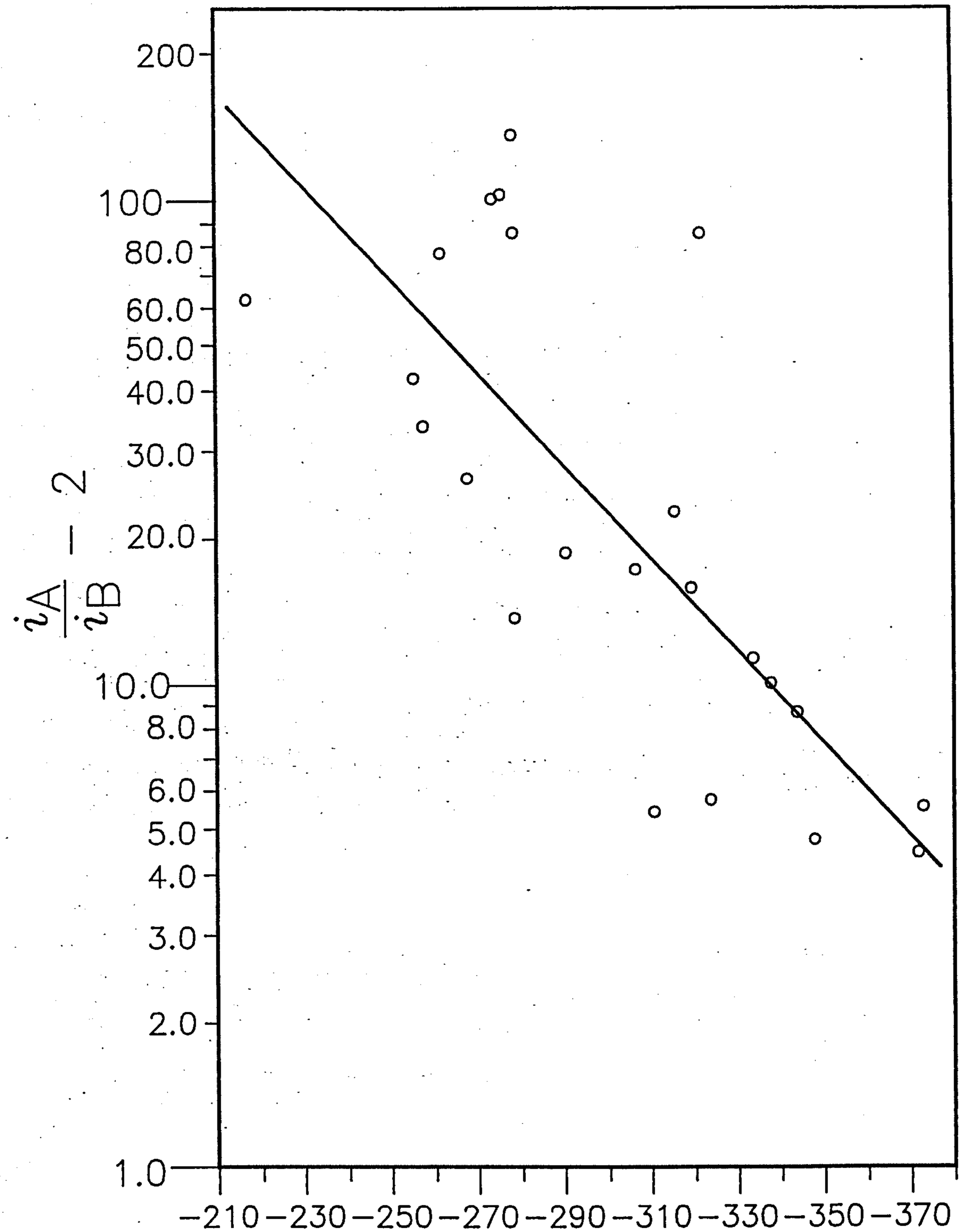

Figure 2.27

Determination of Kinetic Constants - k_B and b_B

Rearrangement of the expression for the consecutive partial current density, i_B (Appendix E2.0) gives:

$$\frac{i_A}{i_B} - 2 = \frac{4.F.k_L}{k_B} \times e^{b_B\phi}$$

Again using the preparative results, tabulated in Appendix G, log (i_A / i_B - 2) is plotted against the electrode potential in Figure 2.27, from which linear regression analysis gives the slope and intercept and, hence, b_B and k_B (noting k_L = 1.6 x 10^{-5} m/ s):

b_B = 0.0208 mV^{-1} and k_B = 0.505 A / m^2 per kmol / m^3

2.4 Conclusions

A model for the reduction of nitrobenzene at a planar electrode has been derived and the kinetic constants, associated with it, determined.

Figures 2.29 and 2.30 compare the actual results with those calculated by the model under the same conditions. Although, of course, the kinetic constants for the model have been determined using these same results, the degree of agreement is encouraging since the model was proposed using a simplified reaction scheme. The good correlation indicates this scheme to be valid and the model to be capable of describing the variation of products with electrode potential and current density. Figure 2.31 shows a model prediction for the polarisation behaviour in the H-Cell under the same conditions as the experimentally determined curves. Within the general experimental error, there is excellent agreement between the results. We can conclude, therefore, that the theoretical model of the electrode processes is an accurate description of observed behaviour.

The model allows prediction, not only of the current - potential relationship (figure 2.32), but also the product formation as a function of the rate of mass transfer and current density or electrode potential (figures 2.33 and 2.34). (A study of the hydroxylamine rearrangement

Reaction Model Results

Comparison between model predictions for H–Cell conditions and the measured results

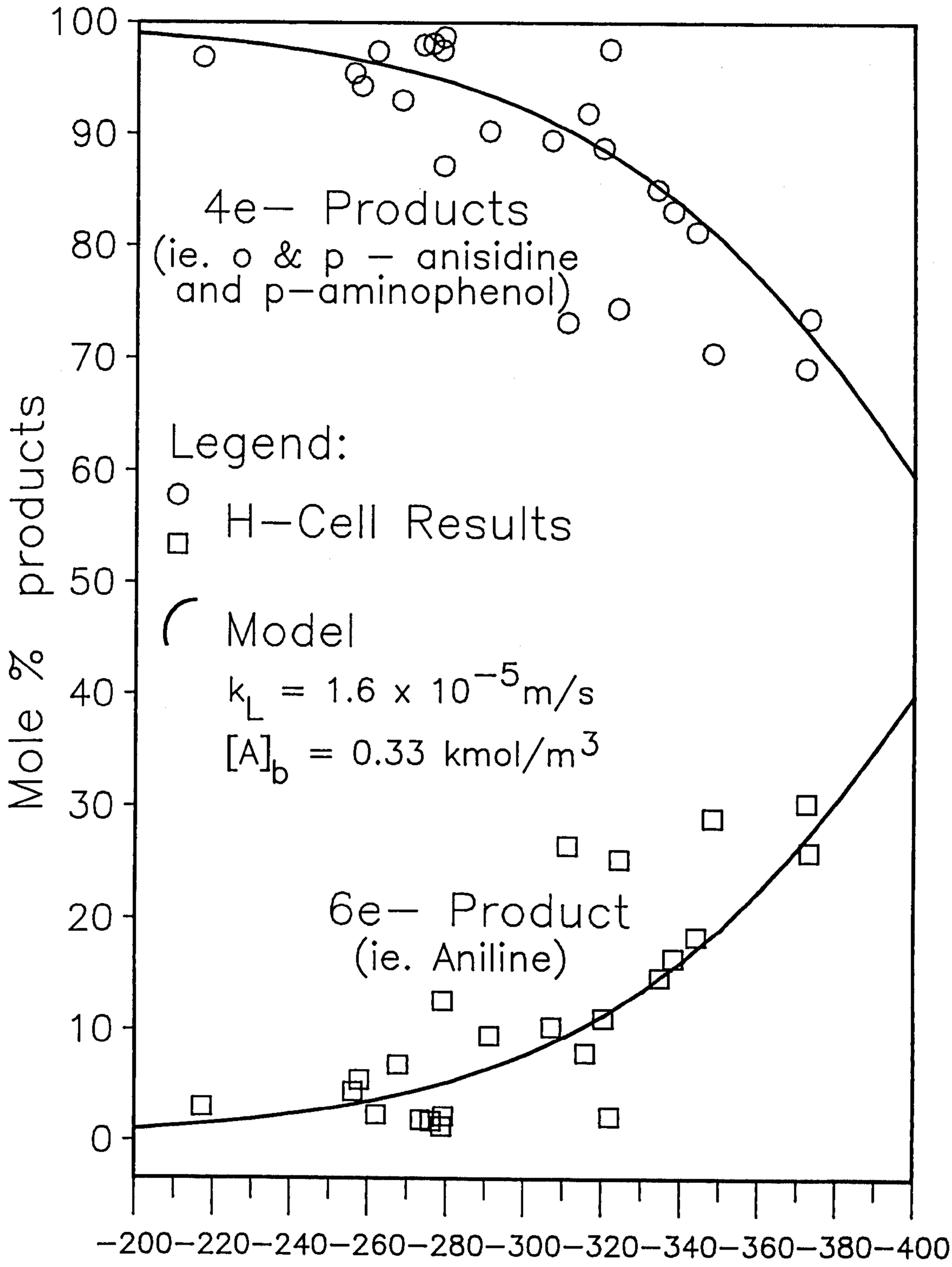

Figure 2.29

Reaction Model Results

H–Cell preparative results compared to model prediction for same conditions

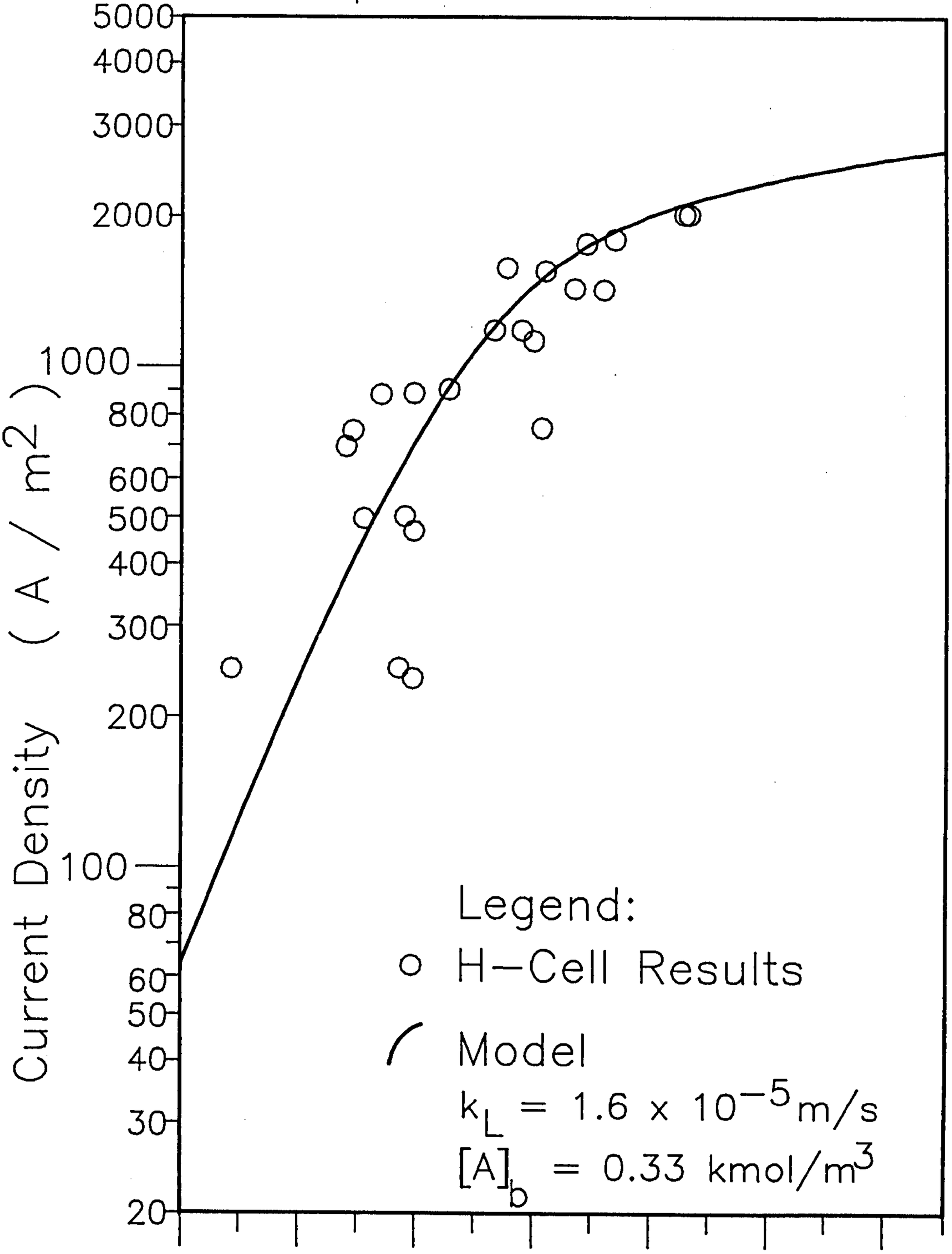

Figure 2.30

Reaction Model Results

Comparison between model polarisation curve and experimental results.

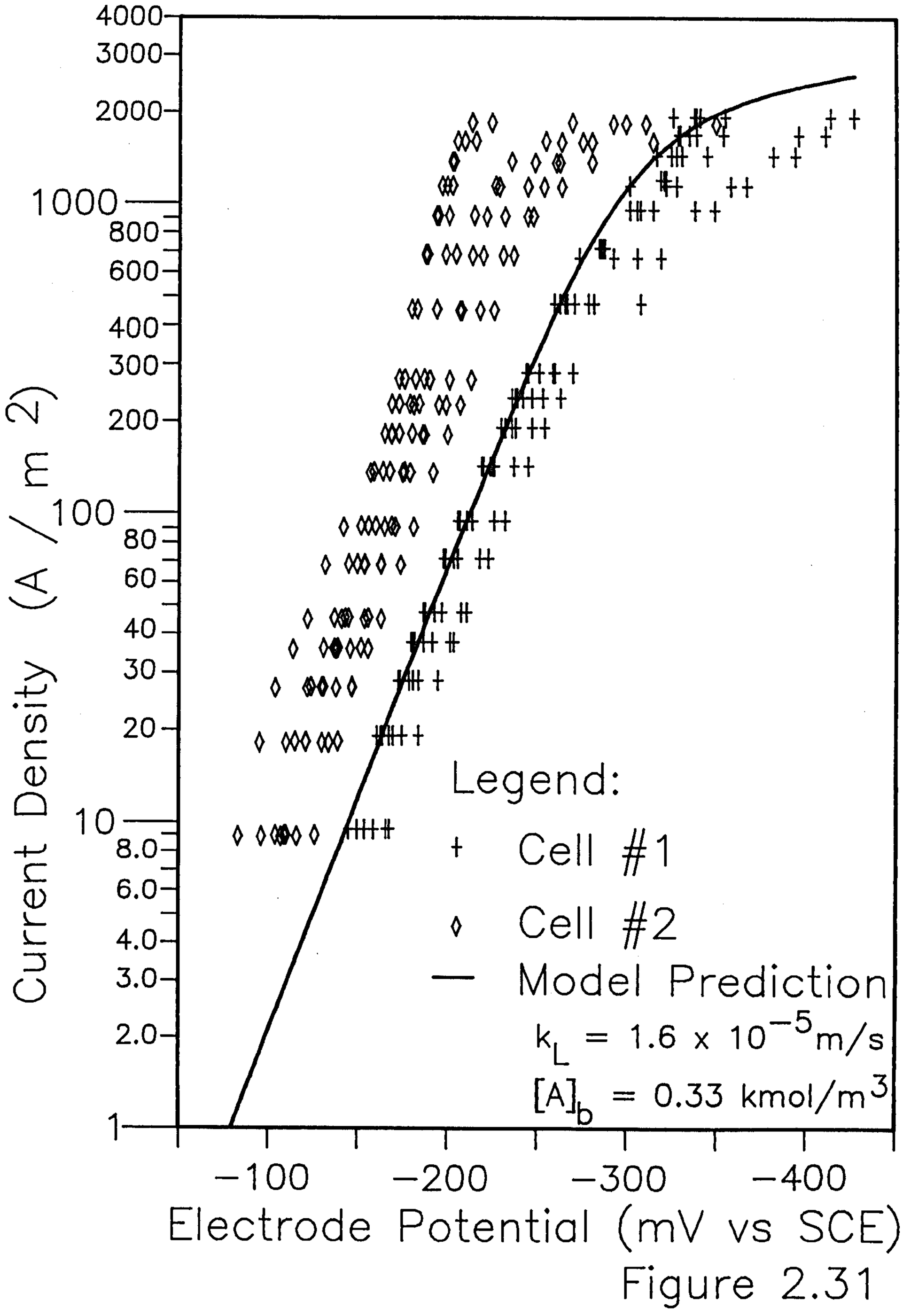

Figure 2.31

Reaction Model Results

Polarisation curves at varying rates of mass transport, k_L

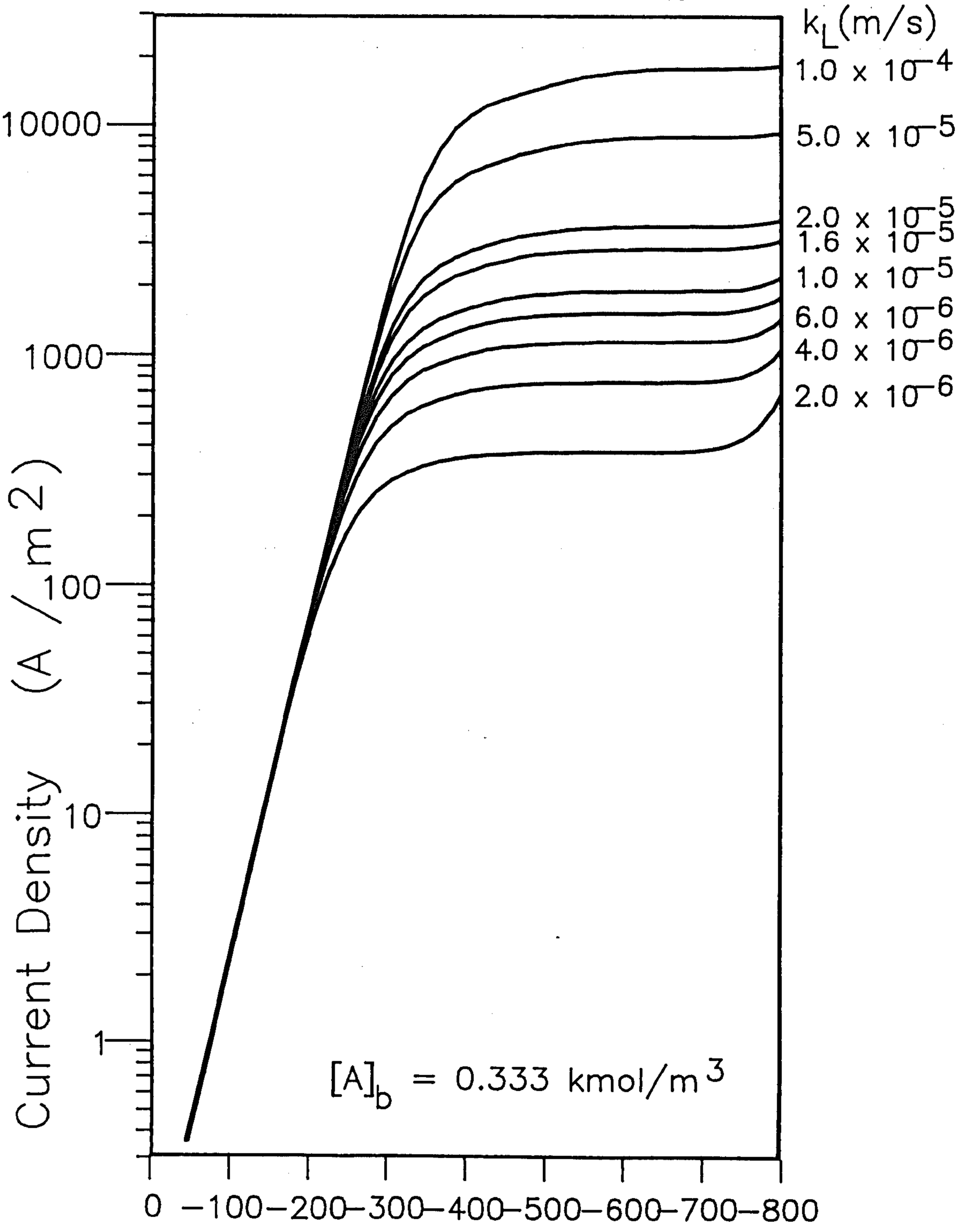

Figure 2.32

Reaction Model Results

Variation of aniline production with current density and mass transfer coefficient, k_L

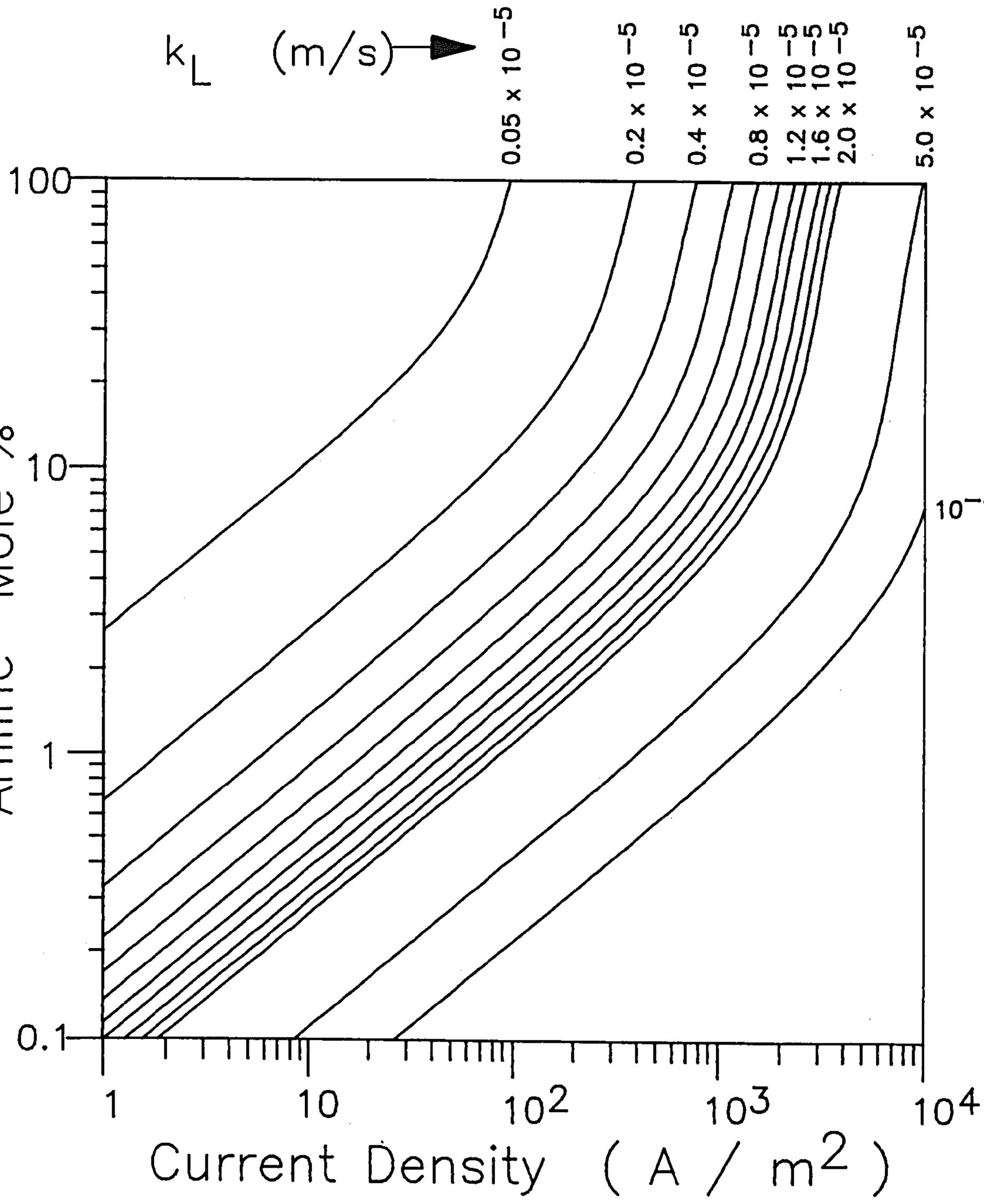

Figure 2.33

Reaction Model Results

Variation of reaction products with electrode potential and mass transfer coefficient, k_L.

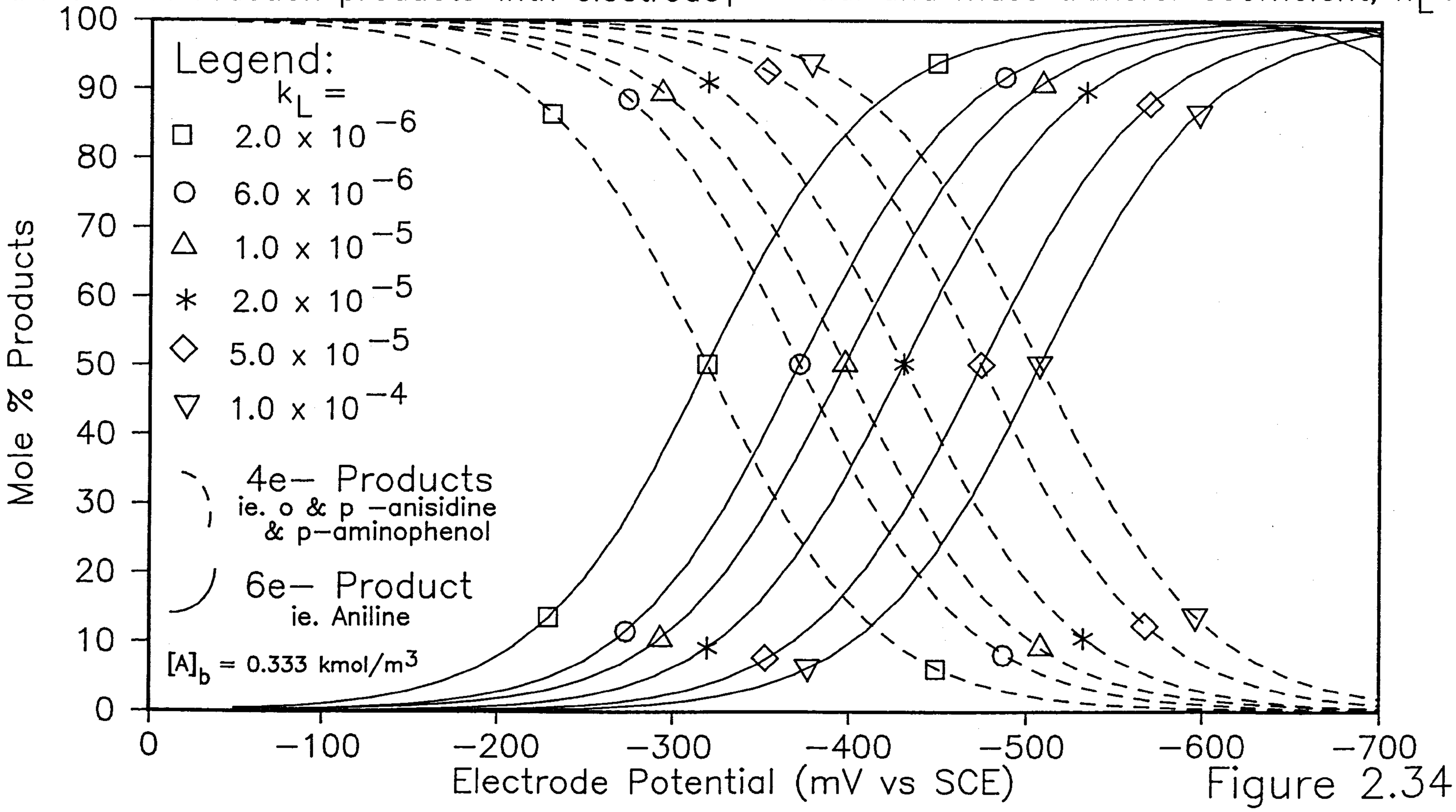

Figure 2.34

reaction was beyond the scope of the present work, so that a prediction of individual four electron products was impossible.) It must not be forgotten, however, that the model is limited by the assumptions that were made in its derivation and by the limits of experimental accuracy.

The model can also be used to study the effect of process conditions such as mass transport, current density and conversion on the products obtained and, thus, help design optimum operating conditions. As was mentioned in the introduction (section 1.2.1) the balance between a low current density and a high rate of mass transfer for minimum aniline formation is critical for this reaction. This can be clearly seen in figure 2.33. A possible method of achieving this aim at relatively low cell costs, proposed in section 1.3, was the use of three dimensional electrodes. The next chapter concerns the use of such designs of cells for the production of p-anisidine.

CHAPTER THREE

BENCH SCALE CELL DESIGN

It has been shown by BASF[2] that the electrochemical reduction of nitrobenzene in methanol can give a high selectivity to para-anisidine. However, the results presented in the previous chapter demonstrate that selectivity to the anisidine is very dependant on the electrode potential or current density. A high current density, whilst giving good space-time yields of products, would result, therefore, in a lower selectivity to the anisidine. The aim of the work described in this chapter was to investigate the effect of cell design on the nitrobenzene reduction, with a view to increasing space-time yields, whilst maintaining high selectivity to the anisidine product. The reaction model was to be used as the basis for reactor models of the different cells used. Three cell configurations were chosen according to the type of cathode used, namely a parallel plate electrode, a packed bed electrode and a fluidised bed electrode.

A cell was designed so that it could be used, without serious modification, for experiments with all three types of electrode. The first part of this chapter deals with the design of this cell, the equipment used and the experimental procedure.

The experimental results for the parallel plate electrode are presented and discussed. A comparison between the model predictions for this cell and the actual results is also made. Results obtained using the packed bed and fluidised bed electrodes are then described in the next section and the performance compared to that of the parallel plate cell. Reasons for the poor performance of the copper particulate electrodes are then suggested and the experimental evidence for them discussed. Due to this poor performance the use of Monel as an alternative electrode material is discussed and some experimental results presented. The chapter ends with a short conclusion of the bench scale work. As will become clear the problems encountered in this work with the three dimensional electrodes meant that the original aim of modelling the different cell types could not be achieved.

3.1 Experimental

3.1.1 Cell Design.

The cell used was similar to that of Hamilton[58] who worked previously in the same department. The design allowed the cell to operate with a parallel plate or packed or fluidised bed electrodes. For this reason the flow in the bed was from bottom to top, thus the use of a bed retainer for the packed bed configuration was necessary. The cell was constructed in polypropylene "sandwich" sections, which were sealed with O-rings and bolted together (Plate 3.1). Diagrams of the cell and its attachments are shown in figures 3.1 and 3.3.

Current was fed to the bed via a feeder electrode, which also served as the cathode when the cell was used in the parallel plate mode. This feeder extended from the top of the cell to 6.5cm above the flow distributor and was made of 0.3 cm thick copper plate or later, 0.1 cm thick Monel 400. The gap of 6.5cm between the point at which the catholyte entered the cell and the bottom of the feeder was to ensure that the electrolyte flow was fully developed before contact with the electrode. The feeder was imbedded in a polypropylene backing plate, flush fitting to minimise electrolyte flow disturbances. Electrical connection was made to the top of the electrode, which protruded from just below the lid.

The catholyte was pumped through a flow distributor up the catholyte chamber and out via a weir designed to trap any escaping bed particles. The inverted V-shaped distributor (figure 3.3) provided even flow into the packed bed and also allowed fluidisation. Liquid entered an initial chamber through a blanked off section of polypropylene pipe, drilled with holes. To prevent channelling these holes pointed downwards. Flow was then directed through four rows of closely spaced slots, machined into the distributor. This arrangement gave good flow distributions for both the packed and fluidised beds. The pressure drop across the distributor proved quite large, however, and for the high flowrate parallel plate experiment, where flow was expected to develop quickly in the chamber, this slotted part of the distributor was removed.

PLATE 3.1

PACKED BED CELL SHOWING CATHODE WITH ELECTROLYTE PROBES, CATHOLYTE CHAMBER, WINDOWS, BED RETAINER, MEMBRANE SUPPORT AND ANODE COMPARTMENT.

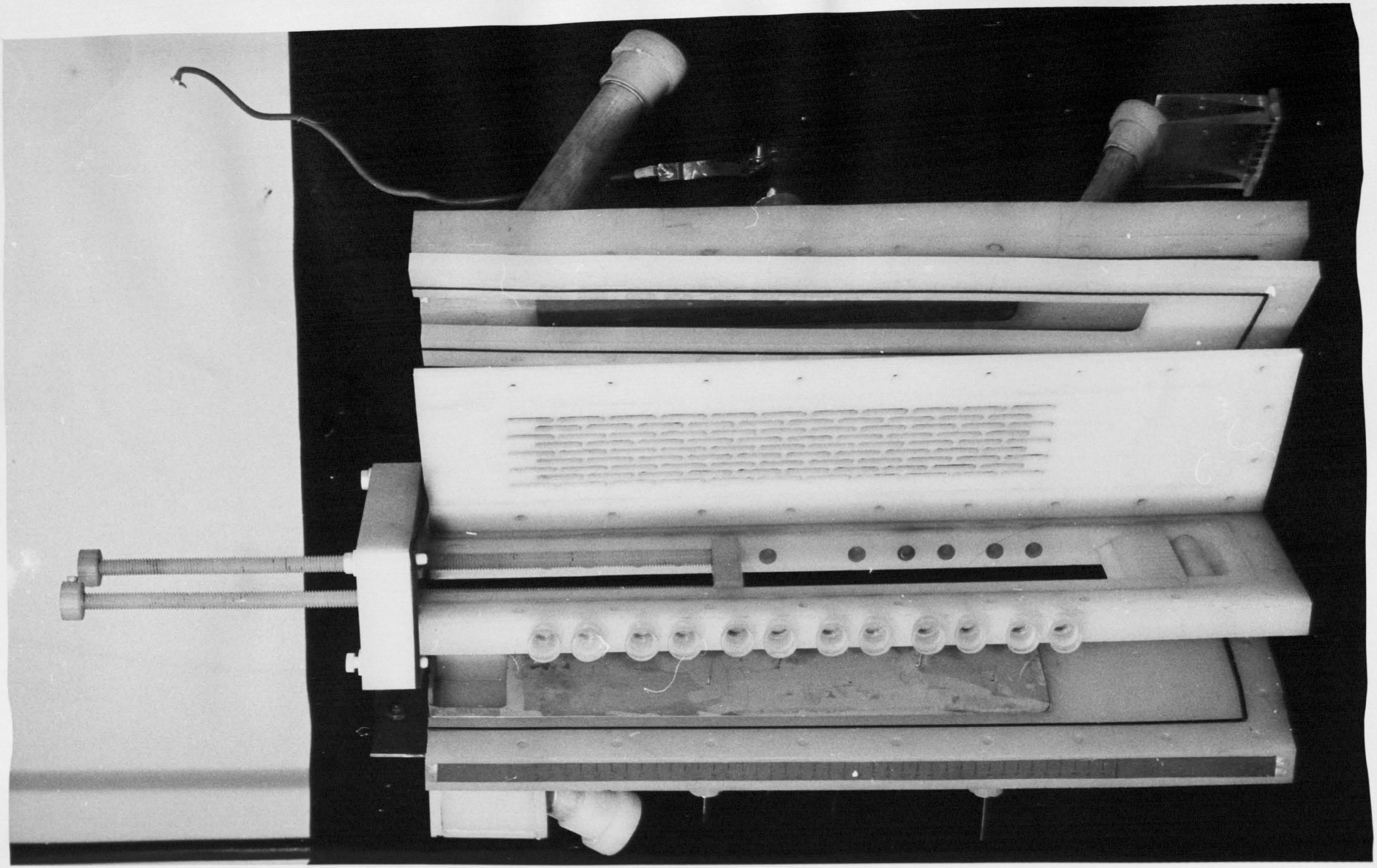

BENCH SCALE CELL

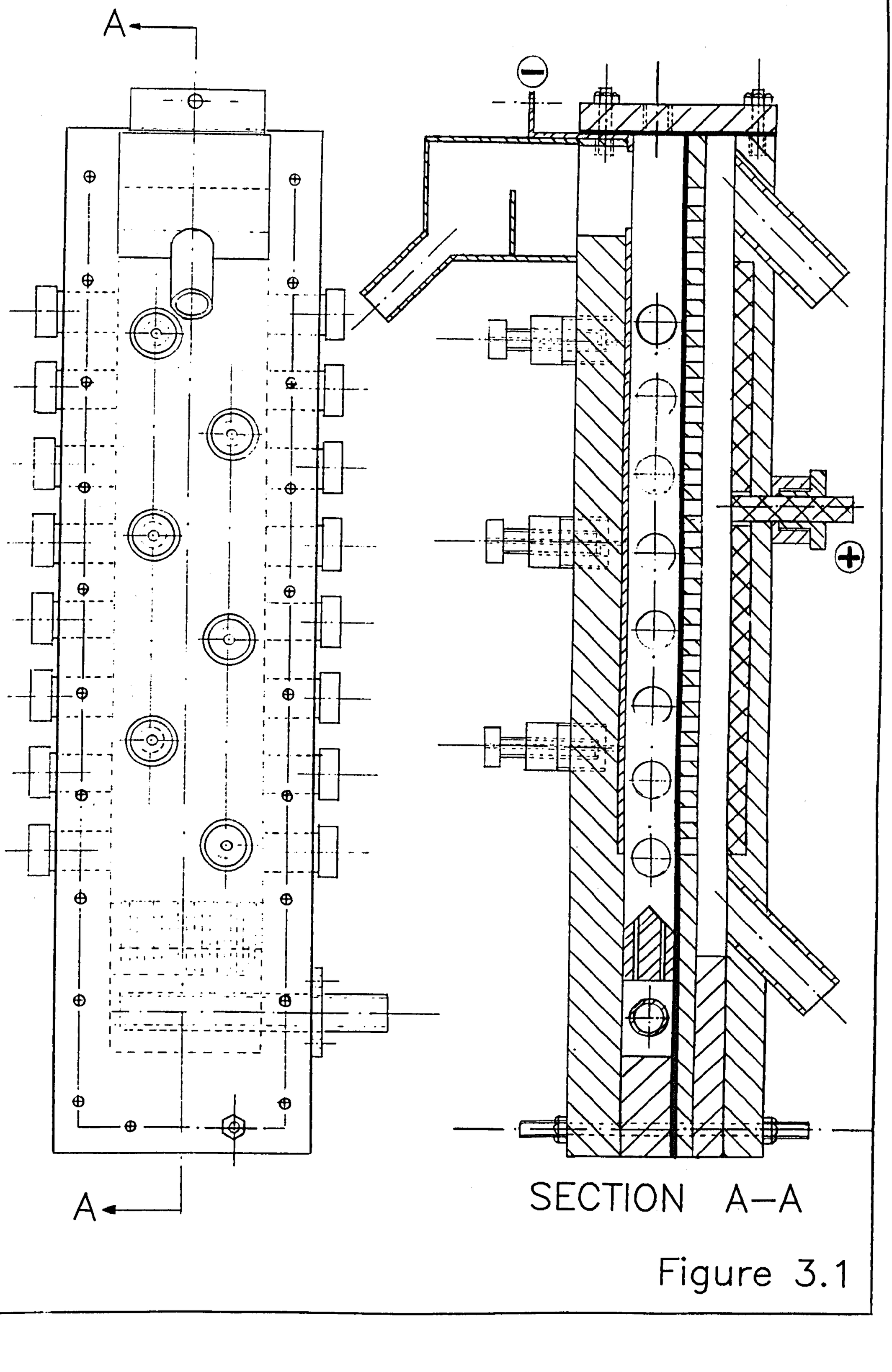

Figure 3.1

DETAIL ON BENCH SCALE CELL

BED RETAINER UNIT

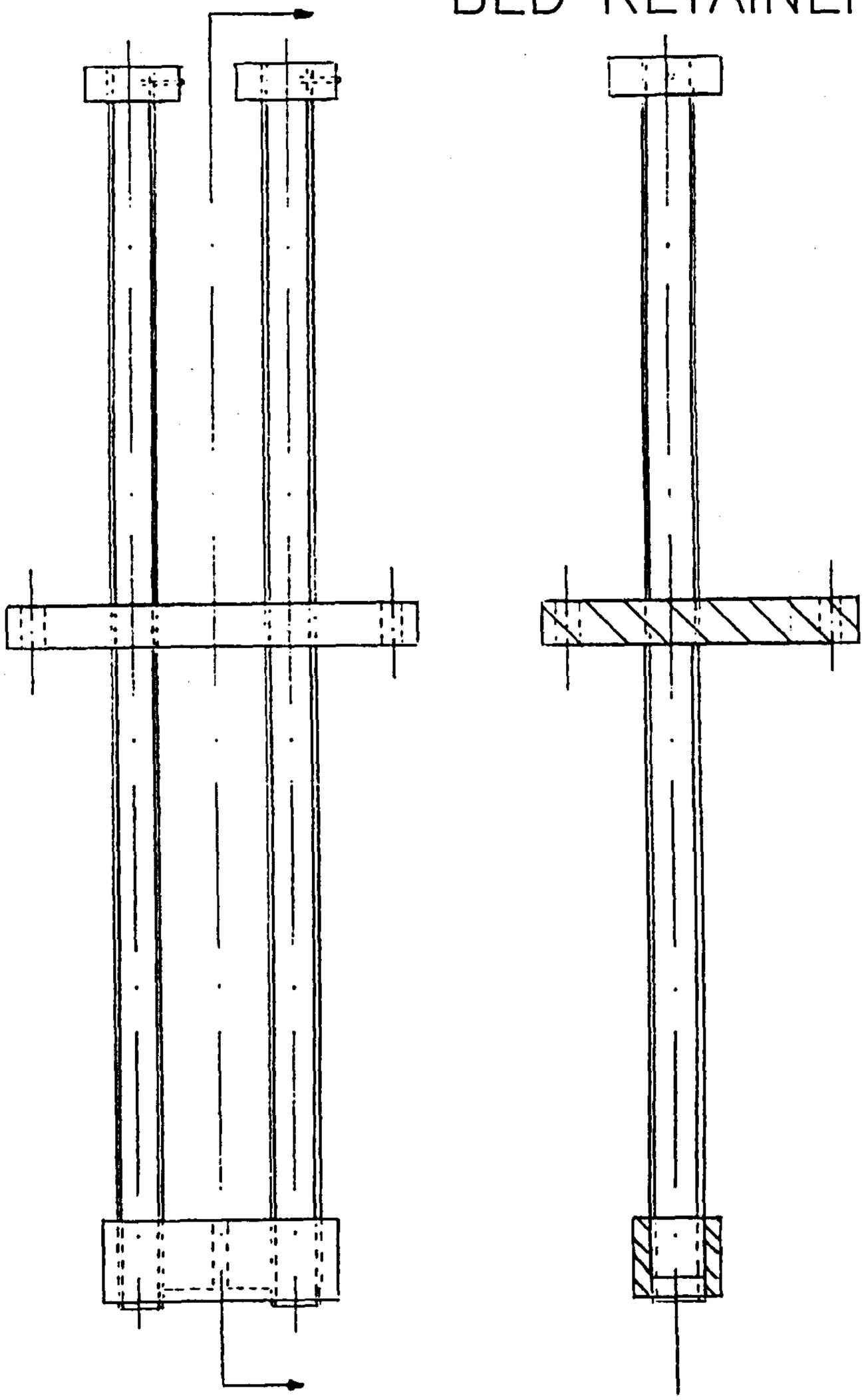

FLOW DISTRIBUTOR

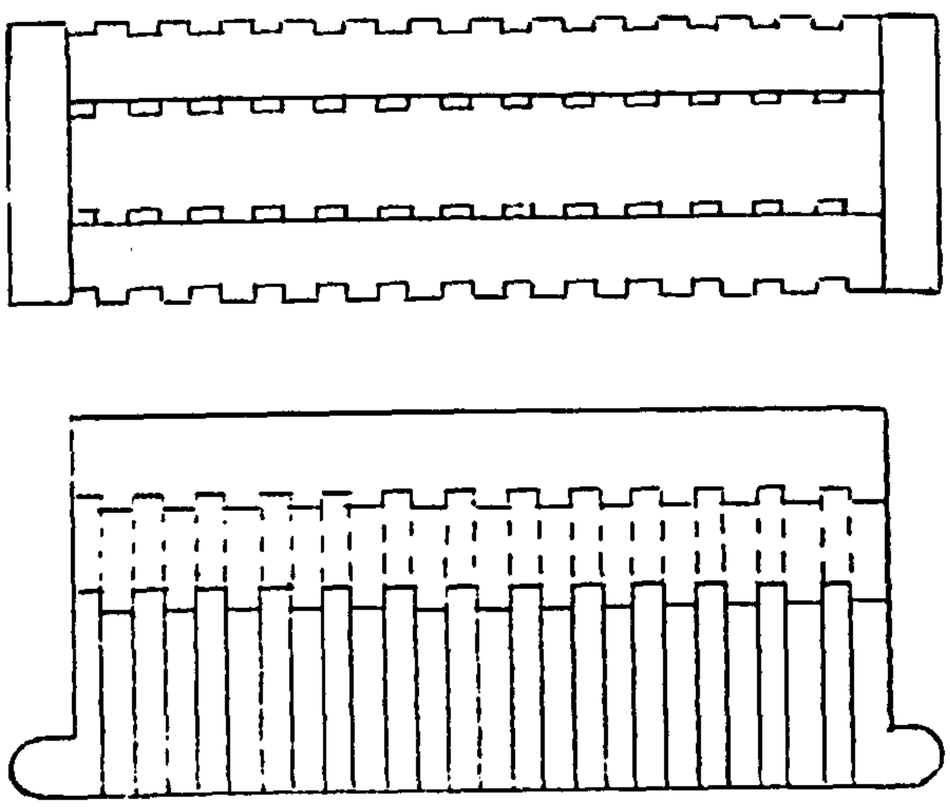

Figure 3.3

When used in the packed bed configuration, the cell was provided with a bed retainer (Figure 3.3) introduced through the lid of the cell. The retainer consisted of a polypropylene block with dimensions slightly smaller than the catholyte chamber, to allow movement up and down the chamber whilst preventing any particles escaping. Two holes were drilled through the block and a polypropylene gauze, with a grid size smaller than the particle diameters, fixed over them. The retainer was positioned and held secure by two long threaded shafts, screwed through the lid of the cell.

The catholyte backing plate also had holes drilled and tapped to accommodate up to six potential probes. The probes, when used, were inserted through the back of the feeder, allowing the electrolyte potential to be measured at various points within the cell. The probes were connected via 3mm PVC flexible tubing, a loose fitting 3-way tap and a salt bridge, to the reference electrode, a saturated calomel electrode.

Catholyte and anolyte were separated by a cationic ion-exchange membrane supported on a grid. Initially Nafion 423[65] was used, but later Ionac MC-3470[66] proved more successful. The support prevented the membrane from bulging into the anolyte compartment, altering the bed thickness. It consisted of an array of closely spaced holes, 0.64cm in diameter, drilled into 0.64 cm thick polypropylene sheet. In this way 60% of the area of the membrane was unobstructed to current flow.

The anolyte flowed from bottom to top through inlet and outlet tubes mounted into the anolyte backing plate. The anode was a graphite block 1.0 cm thick imbedded into and flush with the backing plate and matching the feeder in position. Electrical connection was made via a threaded graphite rod screwed through the backing plate into the anode.

Finally, the catholyte chamber was provided with windows to view the bed during a run. The windows were made in two sections; the inner one made from TPX (polymethylpentene), which is chemically resistant to nitrobenzene and sulphuric acid, and the outer section from Perspex, which is not. The inner sections were sealed with O-rings and the threaded Perspex sections were screwed in after them to secure and seal the windows.

3.1.2 Electrolyte Flow Circuit

The anolyte and catholyte were pumped through two separate but very similar flow circuits. The whole system was kept closed to minimise the loss of methanol due to evaporation at the operating temperature of 55°C. Thermostatically controlled water flowed through the tube sides of the heat exchangers to allow heating up to this temperature. Bypass loops around the pumps were provided for electrolyte mixing prior to a run, and to give greater flexibility in the flow control. The pumps used were of centrifugal design and magnetically driven. Thermometer pockets were provided before and after the cell for each flow circuit. The holding tanks were made from polypropylene and had a maximum capacity of 18 litres. The catholyte tank was later replaced by a smaller 10 litre tank. The flow circuit is shown schematically in figure 3.5 and the whole apparatus shown in Plate 2.2. The details of the items of equipment used are listed below:

Pumps, Catholyte:	Wade Type HDH, centrifugal, or later, Beresford Type 121 1.5HP.
Anolyte:	TEP Type PC 50/7, centrifugal.
Heat Exchangers:	QVF Glass Models HE 1.5 for anolyte, and HE 2.0 for catholyte.
Flowmeters, Catholyte:	Metric Type 24, Korranite float, or Metric Type 35P, Korranite float.
Anolyte:	Metric Type 14, Stainless Steel float.
Pipework and Valves:	Polypropylene throughout.

3.1.3 Materials

The nitrobenzene, sulphuric acid and methanol were used as supplied by B.D.H. Ltd. and were "AnalaR" grade. Reagent grade methanol and sulphuric acid and singly distilled water were also used for cleaning the system.

99% pure copper sheet was used for the feeder, but later replaced by Monel 400; an alloy specified, by the manufacturers, as 66% Ni, 30% Cu, 3% Fe and 1% others. The particles used for the packed and fluidised bed

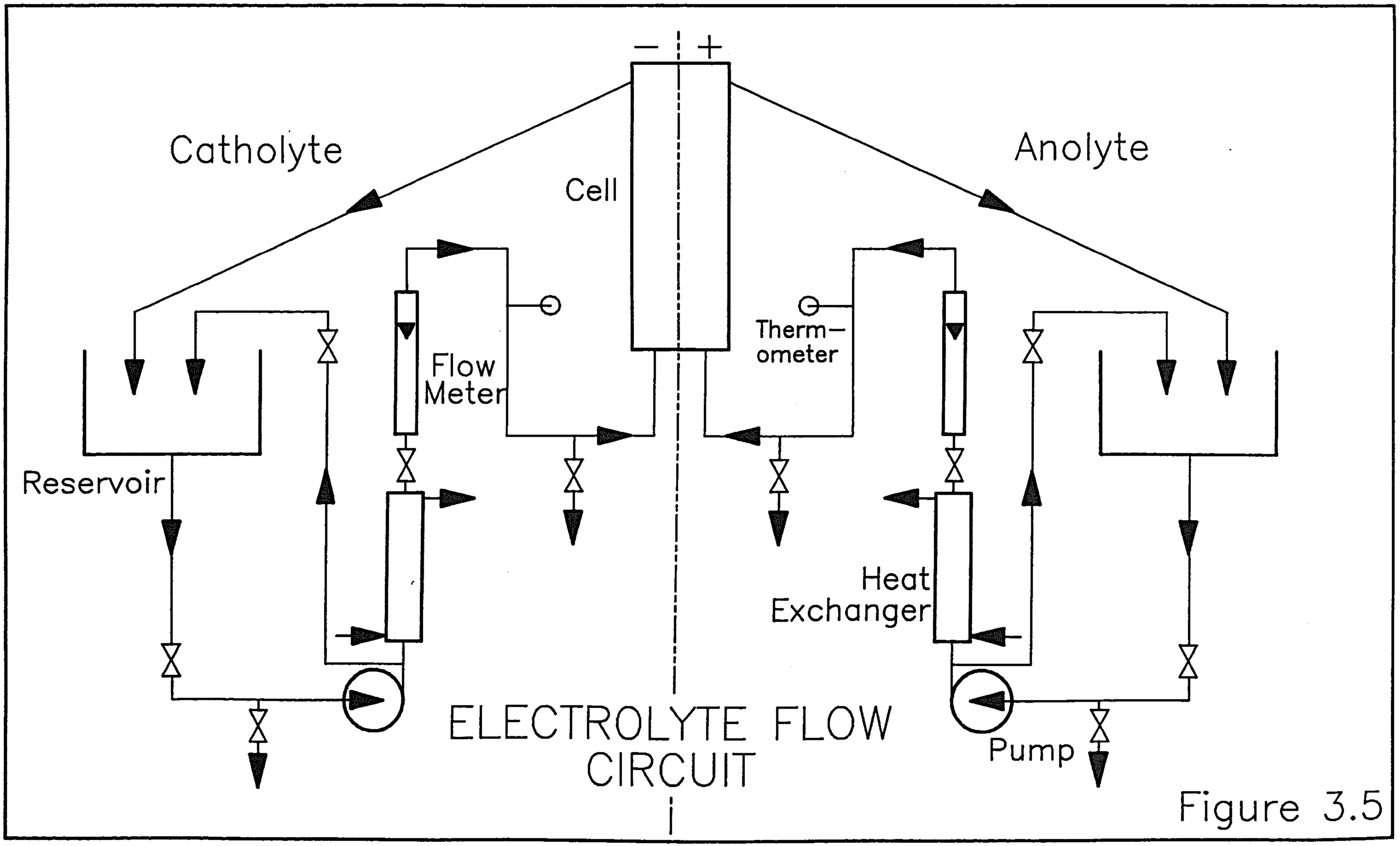
−
+
Catholyte
Anolyte
Cell
Flow
Meter
Therm–
ometer
Reservoir
Heat
Exchanger
Pump
ELECTROLYTE FLOW
CIRCUIT

Figure 3.5

Plate 3.2

EXPERIMENTAL RIG SHOWING CELL, ELECTROLYTE FLOW CIRCUIT AND THE REFERENCE ELECTRODE ARRANGEMENT ALL ENCLOSED IN THE FUME HOOD.

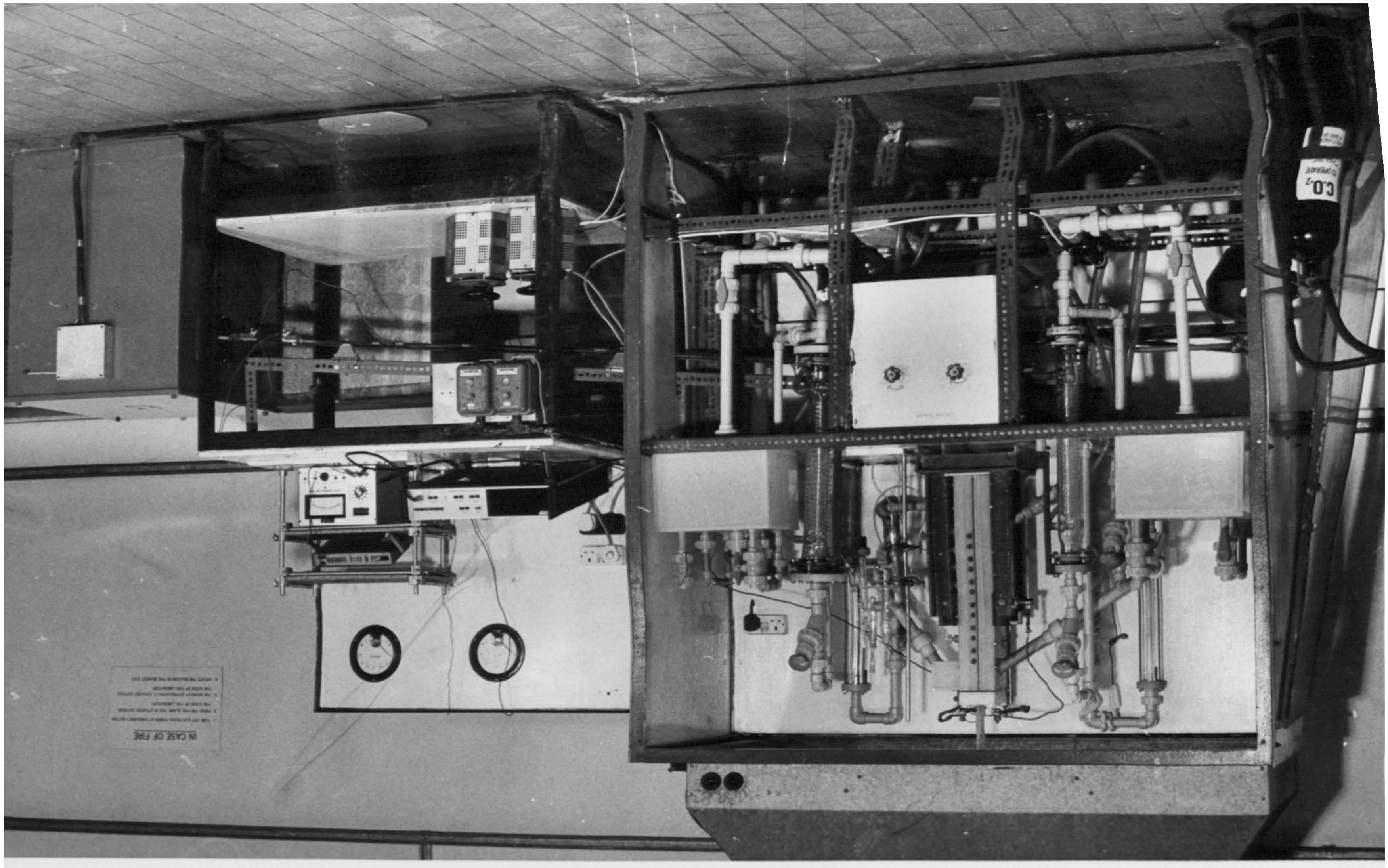
C.O.2
IN CASE OF FIRE

electrodes were copper or Monel. All the particles were sieved to a nominal size range of 800–1200 microns. The mean particle diameters were 1100 microns for the copper and 1000 microns for the Monel.

3.1.4 Instrumentation

The circuit diagram of the instrumentation is shown in figure 3.6. The equipment used listed below:

Power Supply:	3 Phase Transformer–rectifier from Sturdy Electric Co. Ltd. Output 20V, 250A.
Voltmeters / Ammeters:	Thandar DVM models TM 351 or TM 350.
Coulometer:	Time Electronics Type TS 100A Digital Coulometer. Installed across a 0.002502 shunt resistance.
Reference Electrodes:	Saturated Calomel Electrodes made up in our own laboratory (for details see Goodridge and King[67]).

3.1.5 Experimental Procedure

Before each experiment the entire flow circuit was rinsed with singly distilled water several times and, finally, with reagent grade methanol. The system was then drained. The cell was similarly cleaned and rinsed before assembly.

Before assembly of the cell, methanol and sulphuric acid were added to the anolyte and catholyte holding tanks and circulated through the bypass system to ensure good mixing. The electrolyte always contained 10% sulphuric acid by volume. Typically 10 litres were added to the anolyte tank and 12 litres to the catholyte. Later, however, the catholyte volume was reduced to 6 litres to shorten the running time of an experiment.

The feeder electrode was prepared just prior to a run using, first, emery paper and then fine wet–and–dry paper, until the surface was clean,

CIRCUIT DIAGRAM FOR BENCH SCALE CELL

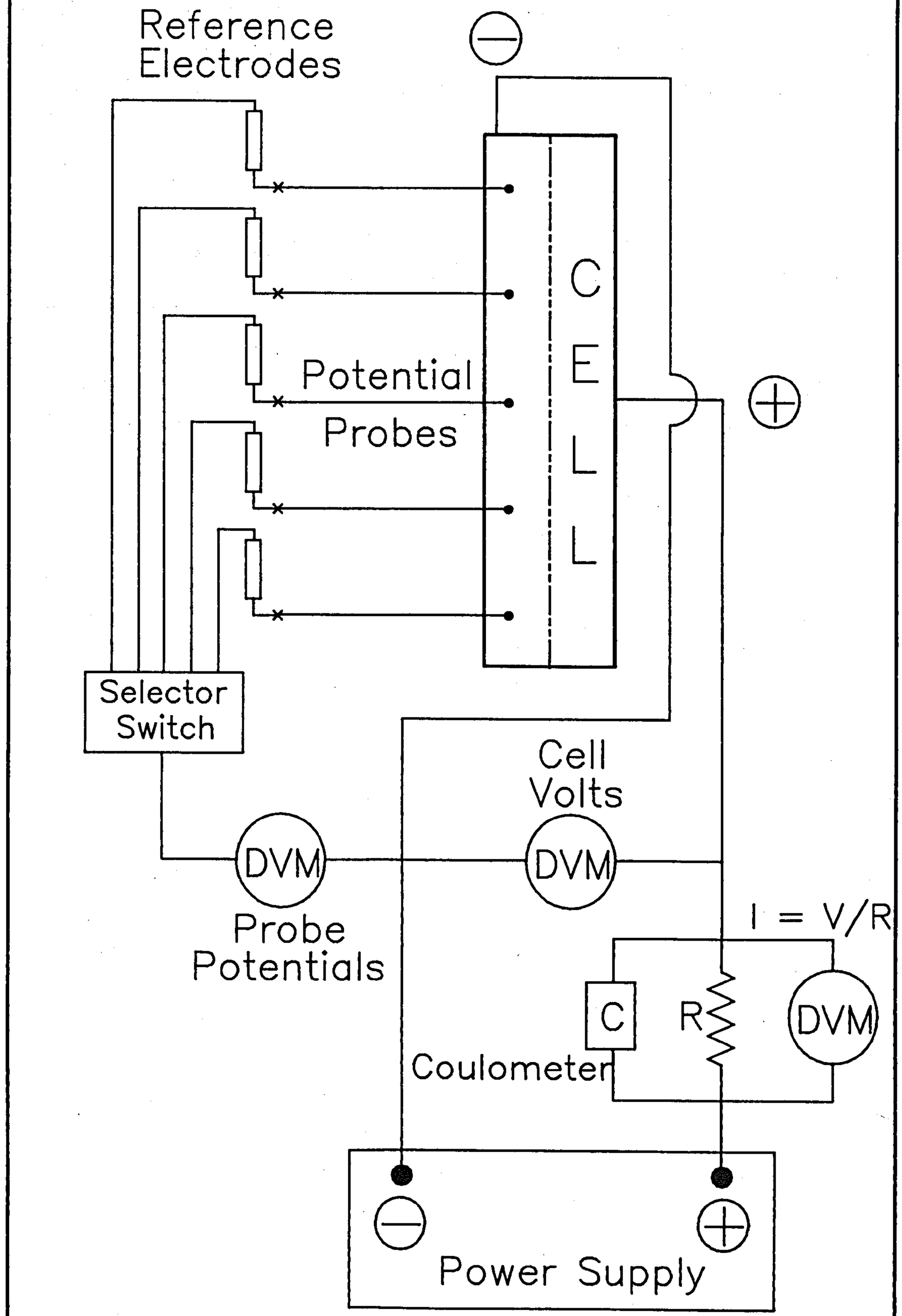

Figure 3.6

bright and free from scratches. The electrode was degreased with acetone and finally rinsed with methanol and dried. The graphite anode was carefully rubbed with emery paper to remove any loose surface and then rinsed with methanol. The electrical connection points on both electrodes were cleaned and checked for low resistivity.

When used, the potential probes were cleaned by carefully passing a thin wire through the capillary. Then they were mounted in their holders and inserted through the back of the feeder backing plate. Their initial positions were accurately measured using a micrometer depth gauge and a marker placed on the end of the probe. In this way the position during an experiment could be measured by a travelling microscope focused on this marker.

The ion-exchange membrane was soaked in methanol overnight prior to the run to minimise swelling, and subsequent sagging, during an experiment. The membrane was stretched tightly when assembled into the cell, care being taken to smooth out any wrinkles and creases in the membrane before finally closing the cell.

The assembly of the cell was straightforward; the sections were sandwiched together and the bolts inserted. The bolts were tightened carefully, in sequence, to ensure an even pressure on the O-rings, and hence a good seal. The cell was then mounted in a steel support and immediately placed into the flow system.

For the experiments requiring a packed or fluidised bed electrode, copper or Monel particles had to be prepared. The particles were first sieved and then cleaned by vigorously shaking with dilute sulphuric acid / methanol. If the particles were particularly dirty, they were cleaned in a fluidised bed apparatus. The particles were fluidised with aqueous sulphuric acid and current was fed to the bed. The simultaneous dissolution and plating of copper resulted in extremely clean particles of pure copper. Monel particles could not cleaned in this way, since the composition of the alloy would have changed during replating. After cleaning the particles were thoroughly rinsed with methanol and stored under methanol in a closed container until required.

The particles were added to the cell, at a low flowrate, during the initial "acid-only" electrolysis, thus ensuring cathodic protection for the bed at all times. When used as a fluidised bed electrode, no bed retainer was needed and the height of the bed measured by viewing through the Perspex windows. For the packed bed, the particles were briefly fluidised and then the flow reduced to the point of incipient fluidisation. The bed retainer was then introduced through the lid of the cell and screwed tightly down onto the bed. The catholyte flow was then alternately increased and decreased, whilst tightening the retainer down further, until no movement in the bed could be observed through the windows. The bed was then considered packed and its height noted.

As soon as the cell had been installed the anolyte and catholyte were circulated and immediately liquid was present in the cell the current supply was turned on to give cathodic protection to the electrode at all times. Hot water was circulated through the heat exchangers and the "acid-only" electrolysis continued until the system had reached the operating temperature of 55°C. This usually took about half an hour, during which time the potential probes were connected.

The PVC tubing, connecting the probes to the salt bridge and reference electrode, was allowed to fill using the pressure from the cell. In this way gas bubbles, which would seriously affect the potential measurement, were forced out of the system. This same procedure could also be used during a run, should a gas bubble enter the probes. The reference electrodes were checked against each other for reproducibility. If acceptable, they were placed into the measuring system. The reference electrodes were connected to the digital voltmeter via a multi-input switching device.

When the electrolyte had reached the required temperature and all the electrical connections had been made and checked, the run was started. The catholyte flow was greatly reduced, and a measured amount of nitrobenzene added to the catholyte holding tank, sufficient to give a concentration of 41 g/l. The catholyte was then circulated through the fully open bypass circuit to give fast, efficient mixing. After a short time the bypass valve was shut and the current and flow set to the required levels. The time was noted and the run started.

Temperature was kept constant by the thermostat in the heating water circuit. The flowrates and current were controlled manually. All experiments were carried out under constant current conditions. Periodically temperature, flowrate, potential, current, and coulombs passed were measured and recorded. The potential difference across the whole cell was measured continuously on a chart recorder.Samples for later analysis by HPLC, see Appendix A, were also taken regularly throughout an experiment.

If potential profiles were to be determined during an experiment the following procedure was adhered to. After an initial period of between 30 and 60 minutes had elapsed, to allow the system to settle down, the first measurements from the potential probes were taken. The measurement from each probe was allowed to stabilise for several minutes before the potential was noted, then the next probe was selected on the switch and so on. This was repeated 5 times before the probes were then moved to a new position. This new position was determined using the travelling microscope. Usually eight different positions for each of six probes were sampled in one experiment.

During operation two Perspex doors were placed in front of the apparatus and the exhaust fans above and in the laboratory were kept running for safety reasons.

After every run the cell and flow circuit were thoroughly flushed through and rinsed at least five times with water. The system was drained, dismantled and left to dry. The feeder electrode was cleaned, dried and then coated in silicone grease to prevent air oxidation between experiments. The particles were cleaned as described above and stored under methanol. As a precaution the membrane was usually discarded after each run, since 55^{o}C and the pressure across the cell limited the lifetime of the supporting fabric.

3.2 Results and Discussion

Tables of all the results can be found in Appendix H, under section numbers referring directly to the numbers below. In addition Appendix H contains these results expressed in the form of various performance

indicators namely: current efficiency, selectivity, chemical yield, energy consumption and space-time yield.

3.2.1 Planar Electrode - Parallel Plate Cell.

Table 3.1 shows the results of experiments using the parallel plate cell. The expected effects of current density and the rate of mass transfer on the product formation can be most clearly seen by considering the ratio of "four electron" (ie. o- and p-anisidine and p-aminophenol) to "six electron" (aniline) products, I_C/I_D. Lower current densities and faster mass transfer are seen to favour the "four electron" process.

Table 3.1 Parallel Plate Cell - Product Current Efficiencies (PP-1 & PP-2)

Mass Transfer Coeff-icient (m/s)	Current Density (A/m^2)	Current Efficiencies (%) p-anis-idine	o-anis-idine	p-amino-phenol	aniline = Total 6e-	Total 4e-	Total Organic	$I_C/I_D = \frac{I_{4e}}{I_{6e}}$
Experiment PP-1								
$4.4x10^{-6}$	570	27.25	4.59	8.19	33.26	40.03	63.29	1.20
$4.4x10^{-6}$	1130	23.30	4.84	5.30	45.02	33.43	78.45	0.74
$4.4x10^{-6}$	2270	14.09	2.92	3.32	62.39	20.34	82.73	0.33
Experiment PP-2								
$1.5x10^{-5}$	570	52.97	8.81	6.85	5.52	68.62	74.14	12.43
$1.5x10^{-5}$	1130	52.72	7.65	5.12	13.46	65.49	78.95	4.87
$1.5x10^{-5}$	2270	41.42	11.04	5.31	22.28	57.78	80.16	2.59

It can also be seen that the total products formed did not account for the amount of current passed during an experiment. This problem was briefly discussed in chapter 2 (2.3.3), but was present throughout the work contained in this thesis and is dealt with fully in Appendix A. It is thought that a combination of factors was to blame. Among these was the formation of by-products that were too difficult to analyse quantitatively and experimental error both in the analysis and in the measurement of the coulombs passed. During the course of the work considerable improvements

were made to the analysis technique, including routinely analysing for p-aminophenol, which turned out unexpectedly to be a relatively major product, as well as trying to eliminate possible sources of error. Comparison of the results in Table 3.1 with some early work, carried out before the "H" cell studies of the previous chapter (Table 3.2), shows the effect of these improvements. The reduction of nitrobenzene is well known for its diversity of products and it is not uncommon in the literature to find at least 10% of the current passed unaccounted for. Considering this and the acknowledged limitations in the analysis, it was thought that further improvements would be extremely difficult and rather pointless.

Table 3.2 Initial Bench Scale Work - Product Current Efficiencies (IPP-1, IPP-2 and IPB-1)

Experiment No.	Current Efficiencies (%)						$I_C/I_D = \frac{I_{4e}}{I_{6e}}$
	p-anisidine	o-anisidine	p-aminophenol (calculated) (see app. H)	aniline = Total 6e-	Total 4e-	Total Organic	
IPP-1	24.49	4.20	5.05	16.29	33.73	50.02	2.07
IPP-2	29.00	5.81	6.12	19.38	40.93	60.31	2.11
IPB-1	17.90	2.86	3.65	51.28	24.41	75.69	0.48

Nb. Current Density for IPP-1, IPP-2 and IPB-2 = 1000 A/m^2
Mass Transfer Coefficients estimated as: 3.5×10^{-6} m/s for IPP-1 & -2
1.7×10^{-4} m/s for IPB-1

3.2.2 Comparison of the Planar Results to the Model

Figure 3.7 shows the experimentally determined six electron products compared to the prediction of the reaction model derived in chapter two. In keeping with the assumptions made in the derivation of the model, the experimental results have been adjusted so that the four and six electron products together account for 100% of the current passed. In other words the measured ratio of products has been used (See Appendix E).

Reaction Model Results

Comparison of Model and Bench Scale Work

▲ Results from PP–1
● Results from PP–2

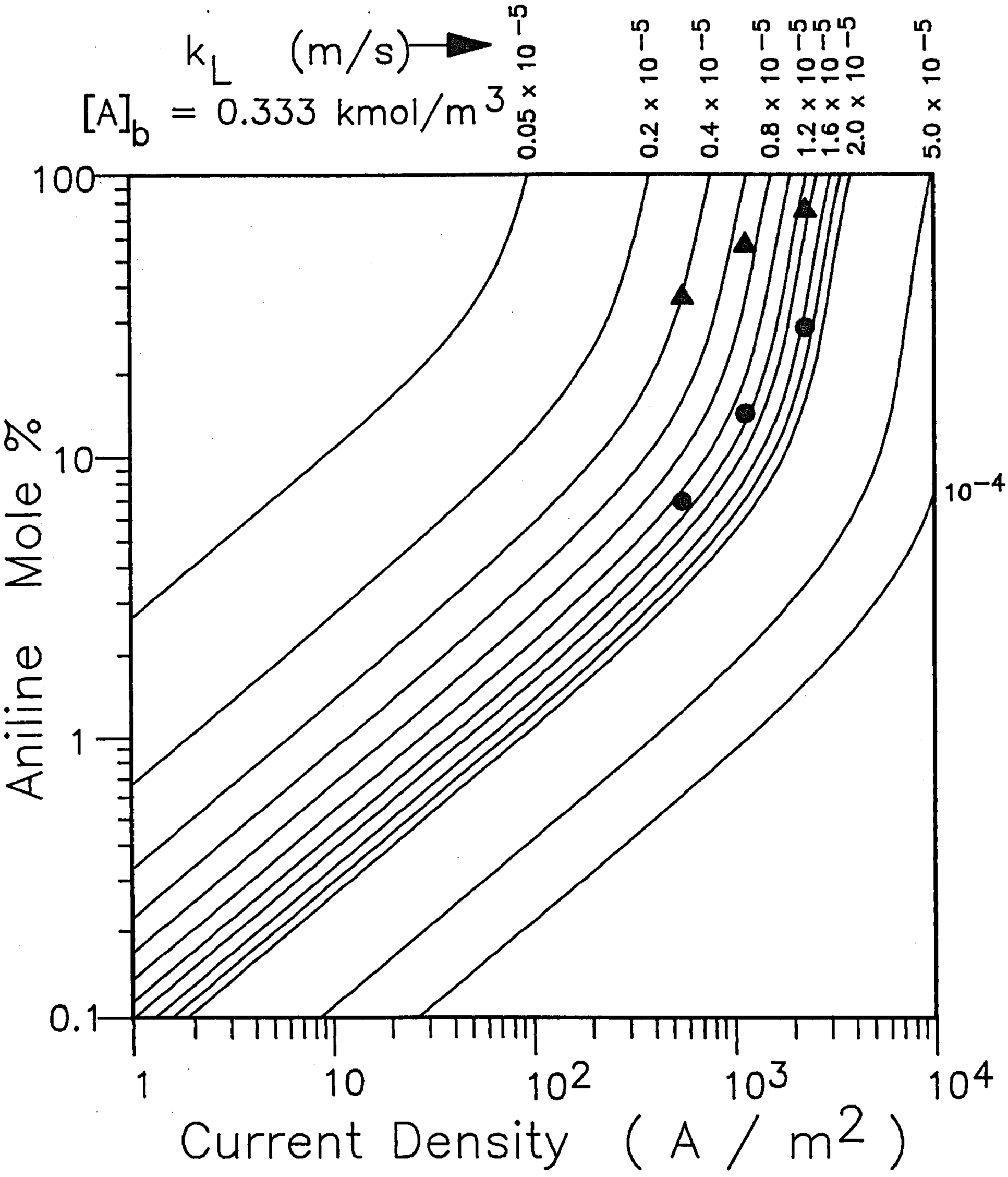

Figure 3.7

Considering the experimental errors and the errors in estimation of the mass transfer coefficient for the cell, there is good agreement between the model prediction and the experimental results from PP-2. These results seem to correlate to the model with a mass transfer coefficient of between 1.0 and 1.6 x 10^{-5} m/s, this compares well with the value of 1.5 x 10^{-5} estimated for the cell (Appendix F). Entrance effects and other local deviations, particularly for such a relatively small cell, were cited by **Mamoor et al.**[74] as possible reasons for deviations from the mass transfer correlation. Such effects probably account for the slight differences between the experimental product / current density relationship and the model predictions. Nevertheless the correlation was encouraging for the scale-up possibilities of the model.

Less encouraging was the poor correlation between the results from PP-1. One explanation is that at such low rates of mass transport, the assumption of steady state is no longer valid ie there is a change of nitrobenzene concentration over the length of the electrode. Even at the highest rate of production, a rough estimate shows that only 1.5% of the nitrobenzene is converted per pass. A steady state approximation would seem valid therefore.

A more likely explanation is the effects of uneven mass transfer in the cell. It is probable that at low flowrates, fully developed flow conditions were present in only a part of the cell, if at all. The rate of mass transfer in the entrance region of the catholyte chamber would then be expected to be significantly different to that at the exit. It is possible, even, that under the conditions of PP-1 the mass transport in the cell was in fact determined by entrance and exit effects only. If mass transport cannot be described by a single mass transfer coefficient then one of the assumptions implicit in the model derivation is invalid. Further, product formation would change with position in the cell; in the more turbulent entrance and exit of the cell, the local mass transfer coefficient will be higher and less aniline will be formed. The overall effect would be to lower the expected aniline formation.

From the studies carried out in this work it is not possible to determine if deviations from the model are indeed due to such effects described above or to deficiencies in the model at low rates of mass

transport and high rates of aniline production. This is clearly an area for future work.

3.2.3 Particulate Electrodes - Packed Bed Cell - Initial Study

An initial packed-bed experiment, IPB-1, compared with the initial parallel plate results, IPP-1 and -2, (Table 3.2) showed that far from increasing the selectivity to the four electron products, aniline was the major product. During the experiment, potential profiles were measured in the bed and are shown in Figure 3.8. It appears, therefore, that the maximum electrolyte cathodic potential was only around -160 mV, at which very little aniline would be expected to be formed (section 2.3.3). In addition the rate of mass transfer was estimated (see Appendix F3.0) to be some 50 times higher in the packed-bed than in the comparable parallel plate cell, which should result in a decreased yield of aniline. In order to explain this behaviour of the packed-bed it was supposed that due to the low conductivity of the electrolyte compared to the particles, the reduction took place only in the small space between the membrane and the layer of particles nearest the membrane. There would then be a large rate of charge transfer over a very small volume and the local mass transfer conditions would be expected to be very much lower than the rest of the bed. Hence, very close to the membrane high potentials and low rates of mass transfer were possible, resulting in increased reaction selectivity towards aniline. Due to the uncertainty of the analysis in these initial experiments, it was decided to carry out the basic H-Cell studies that are described in chapter two.

3.2.4 Particulate Electrodes - Packed and Fluidised Bed Cell

Following the improvement of the analysis technique and the H-Cell work, attention returned to the particulate electrodes. Packed and fluidised bed experiments were carried out according to the methods described earlier (section 3.1.5).

Measured Potential Profiles
for packed-bed experiment IPB-1
at different heights in the bed

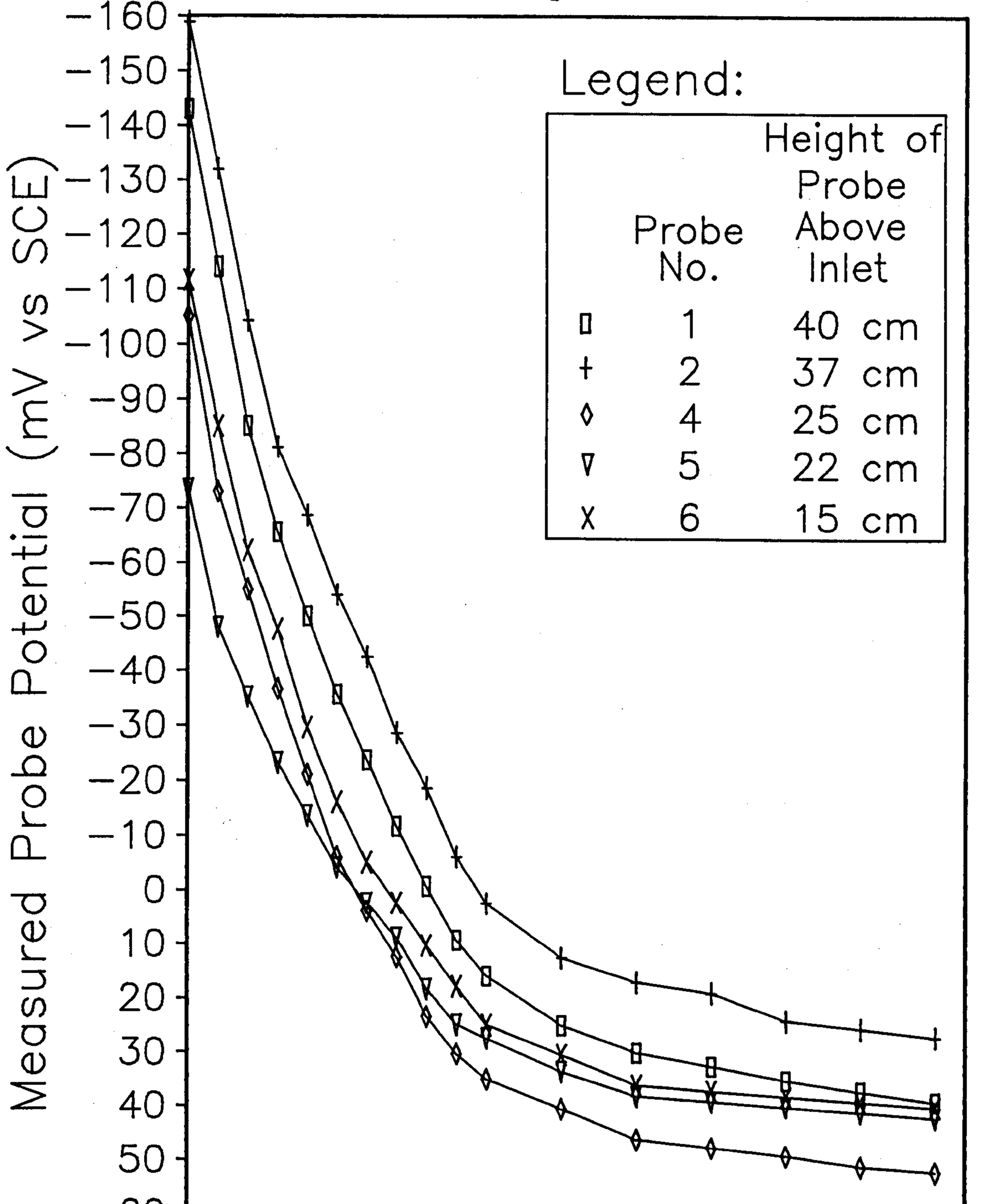

Figure 3.8

The results from these experiments are summarised in Table 3.3. It can immediately be seen, by comparison with the parallel plate, that the particulate electrodes afforded a very much lower selectivity to para-anisidine at a given geometric current density. From these results, it would seem that packed and fluidised bed cell design does not offer a better yield of para-anisidine, indeed it is considerably worse than a parallel plate configuration. A second glance reveals some curious phenomena: total current efficiencies at greater than 100%; differences between the results of experiments - for example, in PB-1 selectivity to aniline increases as expected with increasing current density, in PB-2, however, this trend is reversed!; Finally, in the fluidised bed experiments, the total current efficiency <u>increased</u> with increased current density. Clearly the performance of these two electrodes is entirely different to that which was expected. The rest of this section examines the reasons for these rather surprising results.

<u>Table 3.3 Packed and Fluidised Bed Cell - Product Current Efficiencies (PB-1, PB-2, FB-1 and FB-2)</u>

Experiment No.	Geometric Current Density (A/m^2)	Current Efficiencies (%)						$I_C/I_D = \frac{I_{4e}}{I_{6e}}$
		p-anisidine	o-anisidine	p-aminophenol	aniline = Total 6e-	Total 4e-	Total Organic	
PB-1	620	12.05	2.64	6.15	34.51	20.83	55.34	0.60
PB-1	1240	18.56	3.73	3.65	40.83	25.95	66.78	0.64
PB-1	2470	19.72	6.10	6.61	71.77	32.43	104.2	0.45
PB-2	2470	19.14	3.40	7.11	43.94	29.65	73.59	0.67
PB-2	1240	5.58	1.46	3:77	83.41	10.81	94.22	0.13
PB-2	620	5.15	1.97	4.97	102.3	12.09	114.4	0.12
FB-1	620	20.11	3.67	6.18	20.38	29.96	49.96	1.47
FB-1	1240	25.47	4.07	6.62	34.11	36.15	70.26	1.06
FB-1	2470	25.75	4.11	6.99	56.56	36.85	93.41	0.65
FB-2	2470	34.62	5.85	11.04	55.69	51.50	107.2	0.93
FB-2	1240	36.74	5.56	8.57	52.71	50.87	103.6	0.97
FB-2	620	16.61	5.18	10.18	47.25	31.98	79.23	0.68

After a packed-bed experiment, PB-1, it was noted that the layer of particles nearest the membrane were fused together and that copper had been deposited on the surface of the membrane. Clearly, there had been significant dissolution of the electrode into the electrolyte leading to replating under the cathodic conditions of an experiment. Using atomic absorption spectroscopy (Appendix A) the concentration of copper ions in the electrolyte was determined. There was found to be 800 mg/l at the start of an experiment, but a huge 5500 mg/l after 7 hours of the run (Table 3.4). It was obvious therefore, that during an experiment the electrode was being continuously dissolved. Noting some rather novel work by Gunawardena and Pletcher[41], where anilines were produced by reduction of the nitrobenzene enhanced by the continuous dissolution and replating of metal ions, it was suggested that this might explain the high aniline production and the other strange phenomena encountered. It must be born in mind that the presence of so many copper ions in the electrolyte certainly adversely affected the product analysis (see Appendix A). Consequently no quantitative comparison can be made and any conclusions must be somewhat tentative.

Table 3.4 Cu^{2+} Concentration In PB-1 and FB-1

Time (hrs)	Copper Ion Concentration	
	PB-1	FB-1
0	800 mg/l	600 mg/l
7	5500 mg/l	150 mg/l

3.2.5 Copper Dissolution

Table 3.5 shows the results of analysis of copper ions in the electrolyte during a packed and a fluidised bed experiment. The first thing to note is the difference in behaviour of the fluidised and packed beds. Similar electrode cleaning and experimental set-up procedure is reflected in the very similar starting concentrations. In the course of an experiment, however, the fluidised bed appears to remove most of the copper from the electrolyte, whilst the packed bed dissolves more into it.

Considering the bipolar mechanism suggested by Plimley and Wright[73] for charge transfer in a fluidised bed electrode the electrode material can be thought of as being continuously dissolved and re-deposited. The decrease in copper ion concentration during a fluidised bed experiment can be explained, therefore, by a greater rate of deposition over dissolution rather than the absence of dissolution. The dissolution / deposition mechanism was expected for the fluidised bed, many authors have found evidence for anodic regions in a "cathodic" fluidised bed. Its dramatic effect upon the nitrobenzene reduction was, however, less expected.

Table 3.5 Cu^{2+} Concentration In PB-2 and FB-2

Sample No.	Time (mins)	Current Density (A/m^2)	Copper Ion Concentration			
			PB-2		FB-2	
			mg/l	mmol/l	mg/l	mmol/l
1	0	-	750	11.81	1000	15.75
2	12	2470	375	5.91	425	6.69
3	24	2470	375	5.91	300	4.72
4	36	2470	500	7.87	400	6.30
5	48	2470	375	5.91	305	4.80
6	60	2470	500	7.87	130	2.05
7	84	1240	625	9.84	155	2.44
8	108	1240	875	13.78	185	2.91
9	132	1240	1125	17.72	165	2.60
10	156	1240	1375	21.65	198	3.12
11	180	1240	1500	23.62	235	3.70
12	228	620	4000	62.99	65	1.02
13	276	620	3250	51.18	95	1.50
14	324	620	2500	39.37	95	1.50
15	372	620	2500	39.37	120	1.89
16	420	620	3750	59.06	105	1.65

The packed bed should have been cathodically protected during an experiment ensuring that no dissolution of the electrode took place. Samples from parallel plate experiments were analysed for copper ions, but in no case was more than 50 mg/l found. Given the large difference in electrical conductivity between the electrolyte and the particles, current would be expected to flow through the path of least resistance, namely the particulate phase. The effect of this would be to create a potential profile which is flat for most of the bed but rises steeply close to the membrane. Consequently cathodic processes such as nitrobenzene reduction

and copper deposition would tend to occur only in a very small layer close to the membrane surface.

This is consistent with the observations of copper dissolution and subsequent deposition on or close to the membrane surface. It would appear that copper is dissolved from the particles in a sufficiently anodic part of the packed bed and replated in the cathodic regions close to the membrane. Measured potential profiles (for example figure 3.8) confirm these observations by showing that in large regions of the bed the potentials were, in fact, anodic with respect to SCE. Close to the membrane the potentials became cathodic.

Having established that the copper particles were dissolving during an experiment, the question was what effect did this have on the reduction of nitrobenzene? Could the seemingly strange results using particulate electrodes be explained by this phenomena?. In order to investigate this it was proposed that the presence of copper in solution or the dissolution of the copper led to increased aniline formation and an experiment, detailed in Appendix I, was designed.

A quantity of copper particles was stirred vigorously with a solution of nitrobenzene in methanol / sulphuric acid at 55°C for several hours. In 4 hours over 2 g/l aniline had been formed, whilst a large amount of copper had been dissolved (See table 3.6). The aniline formation was confirmed by mass spectroscopy and no other products were found.

Table 3.6 Copper Particle Dissolution Experiments

Time (hrs)	Cu^{2+} Conc. (mg/l)	Cu^{2+} Conc. (mmol/l)	Aniline Conc. (g/l)	Aniline Conc. (mmol/l)	Equivalent Coulombs for aniline prod.	Equivalent Coulombs for Cu dissol.
0	21.4	0.34	0.0	0.0	0	0
1	1241	19.54	0.44	4.73	639	754
2	1802	28.38	0.86	9.24	1151	1095
3	1300	20.47	1.98	21.27	2493	790
4	2293	36.11	2.11	22.66	2667	1393

These results clearly indicate the formation of aniline due to copper dissolution. It is also evident that the process is rather complicated. **Pletcher and Gunawardena**[41] found that certain metal redox systems enhanced the yield of aniline in the reduction of nitrobenzene. In particular they proposed the following mechanism for copper:

$$3Cu + 6H^+ + C_6H_5NO_2 \longrightarrow 3Cu^{2+} + 2H_2O + C_6H_5NH_2$$

This implies that 3 moles of copper ions are produced per mole of aniline. In Faradaic terms, the coulombs required to form the aniline must equal the coulombs lost in forming the copper ions. Bearing in mind the inaccuracies in the HPLC analysis for amines when copper ions are present and also in the AA analysis for copper when the concentrations are so high, reasonable agreement between the coulombs can be seen.

It is suggested, therefore, that the process described above occurs in the packed and fluidised bed electrodes during nitrobenzene reduction, giving rise to an increased aniline formation. Additional anodic copper dissolution is also probable. The copper ions in solution are available for deposition, which occurs rapidly in the fluidised bed and somewhat less effectively in the packed bed.

3.2.6 Effect of Copper Dissolution on Experimental Results

Table 3.7 shows how the averaged packed bed results are affected by copper dissolution during an experiment.

The packed bed results show a clear trend – the higher the copper ion concentration the higher the aniline formation. This is even more dramatic since it reverses the expected aniline dependance on current density, namely low aniline formation at low current densities. Current efficiency for aniline formation of over 100% indicates that an additional process other than the cathodic reduction of nitrobenzene is occurring. It seems most probable that the sort of reaction described by **Pletcher** is responsible.

Table 3.7 Effect of Cu^{2+} Concentration on PB-2 and FB-2

Geometric Current Density	Average Results PB-2				Average Results FB-2			
	Av. Cu^{2+} Conc.	Av. Current Efficiency		4e- / 6e-	Av. Cu^{2+} Conc.	Av. Current Efficiency		4e- / 6e-
A/m^2	mg/l	4e-	6e-		mg/l	4e-	6e-	
2470	425	29.65%	43.94%	0.67	312	51.50%	55.69%	0.92
1240	1100	10.81%	83.41%	0.13	188	50.87%	52.71%	0.97
620	3200	12.09%	102.32%	0.12	96	31.98%	47.25%	0.68

The effect of the copper ions on the fluidised bed results is less obvious, there seems to be little effect. The interesting point to note, though, is that geometric current density also had very little effect on the results. Without further detailed studies of potential profiles in the fluidised bed, no reasonable explanation can be offered for this behaviour.

3.2.7 Effect of Conversion on Experimental Results

One last odd feature of the particulate electrode work was the non-reproducibility between PB-1 and PB-2 and between FB-1 and FB-2. To save both time and money, it was decided to use three different geometric current densities during each run, just as was done with the parallel plate experiments. In this way three experiments could be performed, but without the lengthy down time between runs and the advantage of using only one batch of electrolyte. Results from the initial experiments showed that up to 30 to 40% conversion, rates of product formation were reasonably constant (Figure 3.9). The results so obtained should be the same, therefore, as if three separate experiments were performed. Further, no problems associated with conversion were found with PP-1 (Figure 3.10). As an additional precaution, one experiment was performed starting at the low current density and then increasing the current stepwise when the required coulombs had been passed (PB-1 and FB-1). The other experiment started at the high current density, decreasing stepwise with time (PB-2 and FB-2). No differences in results were expected between these two procedures.

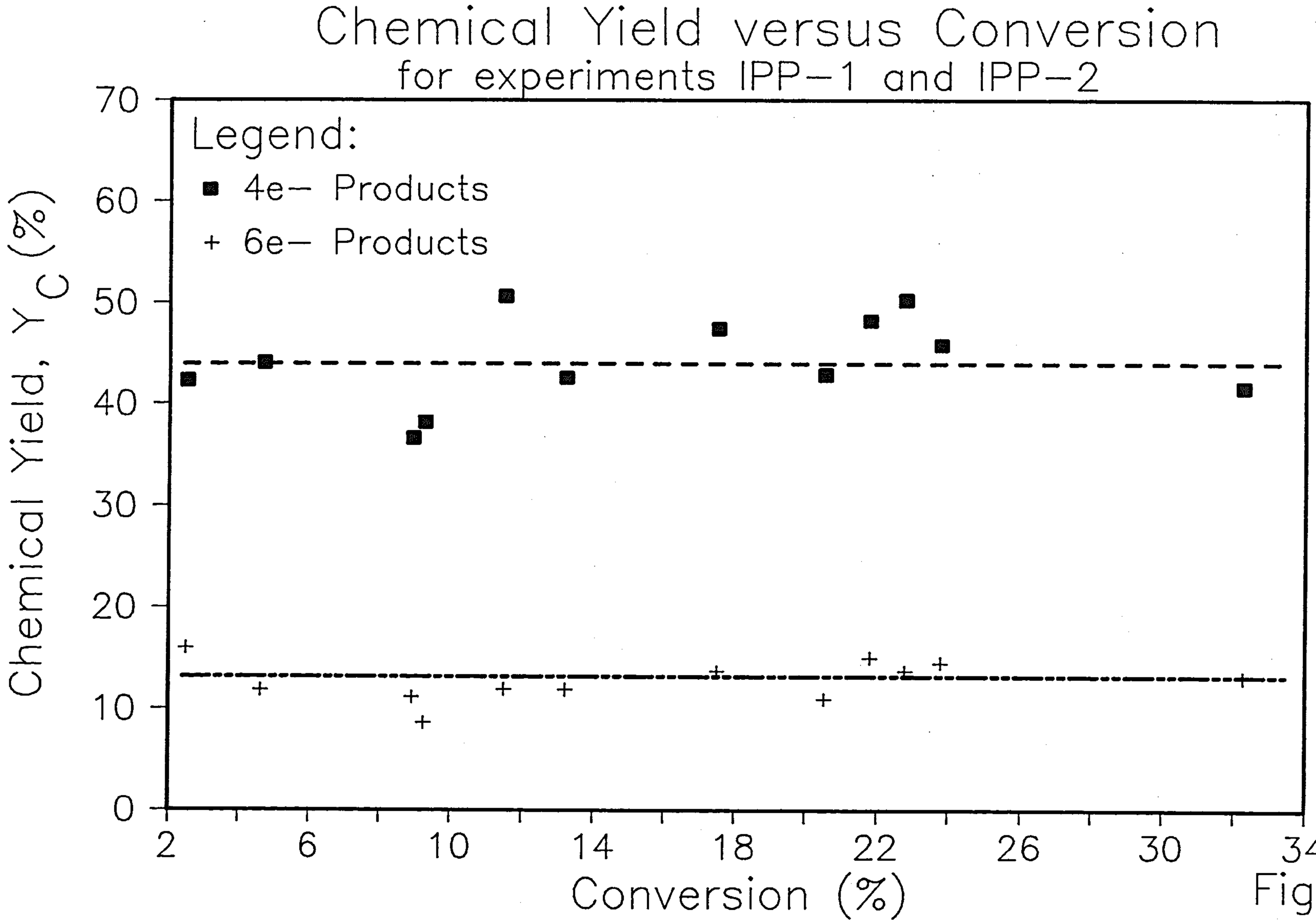
Chemical Yield versus Conversion
for experiments IPP-1 and IPP-2
Legend:
■ 4e- Products
+ 6e- Products
Chemical Yield, Y_C (%)
70
60
50
40
30
20
10
0
2
6
10
14
18
22
26
30
34
Conversion (%)

Figure 3.9

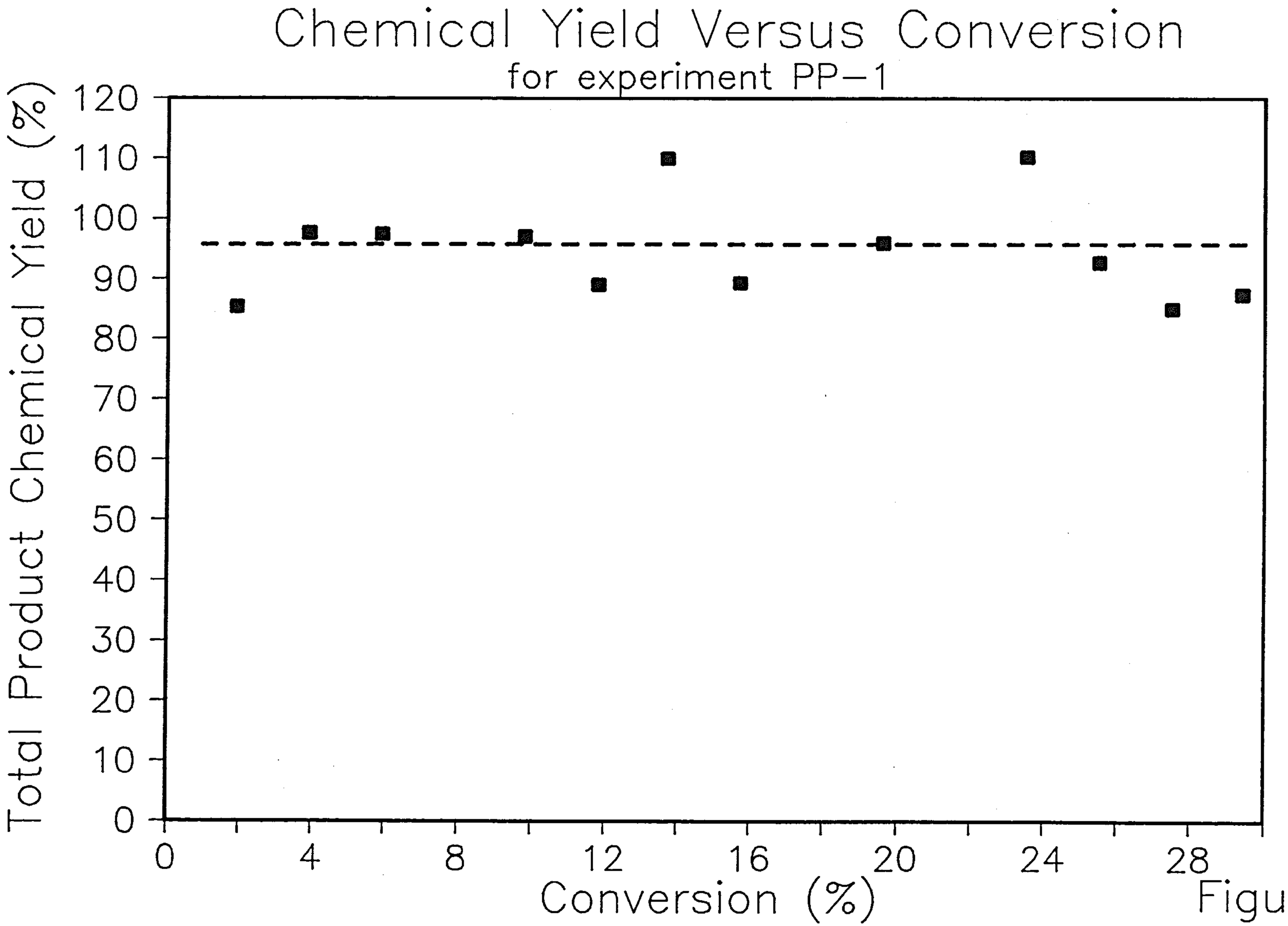
Chemical Yield Versus Conversion
for experiment PP-1
Total Product Chemical Yield (%)
120
110
100
90
80
70
60
50
40
30
20
10
0
0
4
8
12
16
20
24
28
Conversion (%)

Figure 3.10

Table 3.8 shows the average results from the packed and fluidised bed experiments with the percentage (calculated assuming 100% CE) conversion of nitrobenzene added.

Table 3.8 Effect of Conversion on PB-1, PB-2, FB-1 and FB-2

Geometric Current Density A/m^2	Average Results PB-1				Average Results PB-2			
	Conversion %	Av. Current Efficiency 4e-	Av. Current Efficiency 6e-	4e-/6e-	Conversion %	Av. Current Efficiency 4e-	Av. Current Efficiency 6e-	4e-/6e-
2470	30	32.43%	71.77%	0.45	10	29.65%	43.94%	0.67
1240	20	25.95%	40.83%	0.64	20	10.81%	83.41%	0.13
620	10	20.83%	34.51%	0.60	30	12.09%	102.3%	0.12

Geometric Current Density A/m^2	Average Results FB-1				Average Results FB-2			
	Conversion %	Av. Current Efficiency 4e-	Av. Current Efficiency 6e-	4e-/6e-	Conversion %	Av. Current Efficiency 4e-	Av. Current Efficiency 6e-	4e-/6e-
2470	30	36.85%	56.56%	0.65	10	51.50%	55.69%	0.93
1240	20	36.15%	34.11%	1.06	20	50.87%	52.71%	0.97
620	10	29.96%	20.38%	1.47	30	31.89%	47.25%	0.68

nb. Conversion was estimated assuming a 100% current efficiency for nitrobenzene consumption due to inaccuracies in the nitrobenzene analysis.

It can be seen that for the packed bed the aniline formation seems to correlate better with conversion than with current density (it would be expected that higher current densities would lead to higher rates of aniline formation). It is suggested that copper dissolution is responsible for this non-reproducibility. The dissolution of the electrode was shown earlier to be greatest at lower current densities, consequently in experiment PB-1 large amounts of copper were dissolved during the first few hours. The inefficiency of the packed bed in replating this copper meant

that copper ion concentrations in PB-1 were significantly higher than for PB-2, leading to more aniline formation.

The fluidised results are less easy to explain, there seem to be no trends in the results either with conversion or current density. It is pointless to further speculate as to the causes of these seemingly odd results without further work. The situation is clearly highly complex with simultaneous organic and inorganic, chemical and electrochemical processes occurring.

The primary aim of the bench scale work was to compare and assess the suitability of the different cell configurations for para-anisidine production. It seemed clear that electrodes which dissolved into the electrolyte during experiments were not going to be of much use. Further investigation into the causes of the electrode dissolution and the apparent non-reproducibility were not made. Instead an alternative electrode material was sought.

3.3 Monel as an Electrode Material

It is known that Monel (66% Ni, 33% Cu, 1% others) is a material less susceptible to anodic dissolution than either copper or nickel. Monel was also used, with some success, by **Goodridge and Hamilton**[62] for p-aminophenol production. In view of this and the dissolution problems described above, it was decided to try Monel as an alternative electrode material.

Preliminary results using the "H" cell with a Monel electrode showed some improvement in the ratio of four electron to six electron products when compared to copper. A similar particle dissolution experiment to the one carried out using copper particles was also performed (Appendix I). Although the particles dissolved, much fewer copper ions were found in solution and the formation of aniline considerably reduced (Table 3.9). This result was a little surprising considering the well known nickel-catalysed hydrogenation of nitrobenzene to aniline.

Table 3.9 Copper and Monel Particle Dissolution Experiments

Time (hrs)	Copper Particles			Monel Particles			
	Cu^{2+} Conc. (mg/l)	Aniline Conc. (g/l)	Equiv. Coulombs	Cu^{2+} Conc. (mg/l)	Ni^{2+} Conc. (mg/l)	Aniline Conc. (g/l)	Equiv. Coulombs
0	21.4	0.0	0	24.6	10.4	0.0	0
4	2293	2.11	2667	2080	1130	0.42	342

Encouraged by these results, a parallel plate, a packed and a fluidised bed experiment were performed. The aim being to show that copper dissolution was indeed responsible for the poor results obtained using copper electrodes, and demonstrate an advantage of Monel over copper as an electrode material.

The results obtained using equipment modified for the new electrode material are shown in Table 3.10. Only one experiment for each configuration was carried out, making it unwise to draw too many conclusions. However, Monel certainly seemed to give an advantage over copper for the production of para-anisidine.

Dissolution of the bed for the packed and fluidised bed cells was still a problem however. Table 3.11 shows the copper and nickel ion concentrations in the electrolyte during the runs; the nickel is clearly preferentially dissolved. Consequent formation of aniline seems, however, to have been greatly reduced using Monel particles as is also shown in Table 3.11. The aniline formation increased only slightly over the seven hours of the experiment and the Monel packed bed performed considerably better than its copper counterpart for the production of para-anisidine.

Table 3.10 Monel Parallel Plate, Packed and Fluidised Bed Cells - Product Current Efficiencies (MPP-1, MPB-1 and MFB-1)

Experiment No.	Geometric Current Density (A/m^2)	Current Efficiencies (%)						$I_C/I_D = \frac{I_{4e}}{I_{6e}}$
		p-anisidine	o-anisidine	p-aminophenol	aniline = Total 6e-	Total 4e-	Total Organic	
MPP-1	1080	54.93	9.38	14.63	14.04	78.93	92.97	5.62
MPB-1	1330	49.49	8.39	14.63	14.57	72.51	87.08	4.98
MFB-1	1070	19.46	1.56	7.10	46.22	28.12	74.12	0.61
PP-2	1130	52.72	7.65	5.12	13.46	65.49	78.95	4.86
PB-1	1240	18.56	3.73	3.65	40.83	25.95	66.78	0.64
PB-2	1240	5.58	1.46	3.77	83.41	10.81	94.22	0.13
FB-1	1240	25.47	4.07	6.62	34.11	36.15	70.26	1.06
FB-2	1240	36.74	5.56	8.57	52.71	50.87	103.58	0.97

Table 3.11 Cu^{2+} and Ni^{2+} Concentrations in MPB-1 and MFB-1

Time (hrs)	Ion Concentrations (mg/l)				Current Efficiencies (%)			
	MPB-1		MFB-1		MPB-1		MFB-1	
	Cu^{2+}	Ni^{2+}	Cu^{2+}	Ni^{2+}	4e-	6e-	4e-	6e-
0	73	278	149	275	0.0	0.0	0.0	0.0
1	31	708	254	878	80.95	9.65	47.92	38.56
2	40	936	278	1381	70.77	12.87	25.15	50.43
3	36	1248	286	1848	85.24	12.06	23.78	55.24
4	29	1573	305	2190	88.99	18.50	23.38	45.26
5	59	2063	283	2453	52.00	16.08	20.38	41.64
6	60	2428	295	3713	57.11	18.24	28.62	48.14
7	48	2793	260	4258	90.25	35.07	22.81	42.77
8			282	4595			29.73	59.23

The Monel fluidised bed experiment showed a constant, but considerably higher Cu^{2+} concentration than the comparable copper run. Perhaps this explained why the results using Monel as the electrode material were somewhat worse than the copper equivalent (Table 3.10) but that almost no

change was observed with time. There is a possibility that the cementation reaction:

$$Ni^{2+} + Cu \longrightarrow Ni + Cu^{2+}$$

could have played a part when Monel particles were used for the fluidised bed electrode. The copper ions would be preferentially electrodeposited, thus lowering the current available for the nitrobenzene reduction.

3.4 Conclusions

Experiments have shown that para-anisidine can be produced in a bench scale unit. A high rate of mass transport and low current densities have been confirmed as important for a high yield of the four electron reduction products. At a flowrate of about 20 l/min through the cell and a current density of between 600 and 1000 A/m^2, a 70% selectivity to para-anisidine at 53% current efficiency can be achieved. Space-Time yields are, as expected, relatively low and energy consumption high.

The results showed good agreement with the predictions of the model. Although this conclusion is based on a limited number of experiments, it is certainly encouraging for the scale-up of the model.

Changing to a copper packed or fluidised bed electrodes gave a much increased selectivity to aniline and in no case was performance better than the parallel plate in this respect. Serious dissolution of the electrode was shown to be the major problem, causing inaccuracies in analysis methods as well as increasing the aniline formation.

A limited study of the use of Monel as a possible electrode material showed very promising results. Not only was the Monel parallel plate superior to copper in respect of current efficiency for para-anisidine formation, but the packed-bed gave almost the same results. Indeed, selectivity to para-anisidine and its chemical yield were both somewhat better in the case of the packed-bed. A high space-time yield and low energy consumption, however, add to the advantages of the Monel packed-bed. Unfortunately, serious corrosion was also noted and, although this did not

adversely affect the para-anisidine formation, it suggests that such an electrode would not be suitable for production of para-anisidine.

Packed or fluidised bed electrodes could still be of industrial interest if a suitable electrode material, which does not dissolve, could be found.

CHAPTER FOUR

OVERALL CONCLUSIONS

1) The electrochemical reduction of nitrobenzene in methanol / 10% sulphuric acid in a divided cell has been shown to produce para-anisidine, ortho-anisidine, aniline and para-aminophenol as major products.

2) A reaction model has been developed which is capable of correlating experimental results in a laboratory scale cell. The model predicted chemical yield from a bench scale cell in a satisfactory manner.

3) Experiments with cells of different configurations showed that a parallel plate cell performed well but suffered from relatively low space-time yields.

4) Packed bed and fluidised bed cells performed badly due to corrosion of both the copper and Monel cathode materials. This corrosion was shown to give rise to increased formation of aniline by an electrocatalytic process.

CHAPTER FIVE

SUGGESTIONS FOR FURTHER WORK

1) Further work should employ a work-up procedure for product analysis, similar to that suggested in Appendix A, in addition to a "concentration" method such as GLC or HPLC.

2) Further bench scale work should use a narrow gap cell with a turbulence promoter to determine optimum chemical and space-time yields.

3) Before a packed or fluidised bed can be considered a suitable cathode material will have to be found. Measures to increase the electrolyte conductivity must also be studied to decrease the possibility of cathode corrosion.

4) Experimental work over a larger range of current densities and different temperatures should be undertaken in order to demonstrate the limitations of the model.

5) Investigation of the rearrangement reaction and determination of the chemical rate constants would allow the model to individually predict the formation of p- and o- anisidine and p-aminophenol.

NOMENCLATURE

A	Surface area.	cm^2 or m^2
A	Nitrobenzene.	
$[A]_b$	Concentration of nitrobenzene in the bulk electrolyte.	mol/l or $kmol/m^3$
B	Phenylhydroxylamine.	
C	Products by rearrangement of B ie. ortho- and para- anisidine and para- aminophenol.	
C_E, CE	Current Efficiency.	
C_b	Concentration in bulk.	mol/l or $kmol/m^3$
C_{dl}	Differential double-layer capacitance.	$\mu F/cm^2$
C_o	Bulk Concentration of species o.	mol/l or $kmol/m^3$
C_s	Concentration at electrode surface.	mol/l or $kmol/m^3$
D	Aniline.	
D	Diffusivity.	cm^2/s
E	Observed potential.	mV
F	Faradaic constant = 96500×10^3	C/kequiv
I	Current.	A
K_H	Electrolyte conductivity for MeOH / 10% H_2SO_4.	$\Omega^{-1}.cm^{-1}$
K_N	Electrolyte conductivity for MeOH / 10% H_2SO_4/ $PhNO_2$.	$\Omega^{-1}.cm^{-1}$
M	Molecular weight.	g/mol or kg/kmol
N_A	Flux of nitrobenzene to electrode.	$kmol/m^2/s$
N_B	Flux of phenylhydroxylamine away from electrode.	$kmol/m^2/s$
N_D	Flux of aniline away from electrode.	$kmol/m^2/s$
Q_E	Amount of product per unit charge.	kmol/coulomb
R_H	Ohmic resistance for MeOH / 10% H_2SO_4.	Ohms, Ω
R_N	Ohmic resistance for MeOH / 10% H_2SO_4/ $PhNO_2$.	Ohms, Ω
R_{ct}	Charge transfer resistance.	Ohms, Ω
Re	Reynolds number = $d_e U\rho/\mu$.	
Re_p	Reynolds number for particles = $d_p U\rho/\mu$.	
R_ω,R	Resistance due to ohmic loss.	Ohms, Ω
Sc	Schmidt number = $\mu/\rho D$.	
Sh	Sherwood number = $k_L d_e/D$.	

Sh_p	Sherwood number for particles = $k_L d_p/D$.	
V	Volume of titrate at end point (TA analysis).	ml
U	Superficial fluid velocity.	cm/s
Y_{ST}	Space-Time Yield = ajQ_EC_E.	kmol/hr/m^3
$Z(\omega)$	Impedance at frequency, ω.	Ohms, Ω
a	Superficial geometric electrode area per unit volume of cell.	m^2/m^3
b	Exponential coefficient (slope of Tafel plot).	mV
b_A, b_B, b_H	Exponential kinetic constants for the primary, secondary and hydrogen evolution reactions respectively (slope of Tafel plot).	mV^{-1}
c	Perchloric acid concentration (TA analysis).	mol/l
d_e	Equivalent diameter = $\frac{4 \times \text{flow area}}{\text{wetted perimeter}}$.	cm
d_p	Particle diameter.	cm
i	Current density.	mA/cm^2 or A/m^2
i_A	Partial current density associated with the primary consecutive electrochemical process.	mA/cm^2 or A/m^2
i_B	Partial current density associated with the secondary consecutive electrochemical process.	mA/cm^2 or A/m^2
i_H	Partial current density associated with the hydrogen evolution process.	mA/cm^2 or A/m^2
$i_{(\infty)}$	Current density at infinite rate of mass transport.	mA/cm^2 or A/m^2
j	Current density.	mA/cm^2 or A/m^2
k	Reaction rate constant.	mA/cm^2 or A/m^2
k_A, k_B, k_H	Pseudo electrochemical rate constants for the primary, secondary and hydrogen evolution reactions respectively.	mA/cm^2 per mol/l or A/m^2 per $kmol/m^3$
k_L	The individual mass transfer coefficient.	m/s
l	Distance between Luggin tip and the edge of double layer.	cm
m	Sample weight (TA analysis).	g
n	Number of electrons.	
w	Total amine content in sample (TA analysis).	weight%

r_A	Rate of first electrochemical reaction.	$kmol/m^2/s$
r_{B2}	Rate of second electrochemical reaction.	$kmol/m^2/s$
r_H	Rate of hydrogen evolution reaction.	$kmol/m^2/s$
r_{B1}	Rate of chemical rearrangement of phenylhydroxylamine.	$kmol/m^2/s$
δ	Thickness of diffusion layer.	cm
μ	Fluid viscosity.	g/cm/s
ν	Kinematic viscosity = μ/ρ	cm^2/s
ρ	Fluid density.	g/cm^3
σ	Warburg impedance parameter.	
ϕ	Electrode Potential.	mV
ϕ_l	Potential at tip of Luggin capillary.	mV
ϕ_m	Potential at electrode surface.	mV
ϕ_s	Potential of the solution at the edge of the double-layer.	mV
ω	Angular velocity of rotating disk electrode	rad/s
ω	AC Frequency.	Hz

Subscripts

A	Appertaining to species A or to primary electrochemical reaction.
B	Appertaining to species A or to secondary consecutive electrochemical reaction.
H	Appertaining to secondary electrode process, hydrogen evolution.
s	Appertaining to an area close to the electrode surface.
b	Appertaining to the bulk electrolyte.

REFERENCES

1. Kirk, R.E. and Othmer, D.F., "Encyclopedia of Chemical Technology", (London, John Wiley & Sons, 1978–1984).

2. BASF, Ger. Patent No. DT 2617808 A1, (1977).

3. Noel, M., Anantharaman, P.N. and Udupa, H.V.K., J. Appl. Electrochem., 12(3), (1982), 291–298.

4. Pourassamy, A., Anantharaman, P.N., Subramanian, G.S. and Udupa, H.V.K., Proceedings of 13th Seminar on Electrochemistry, (Karaikudi, India; Central Electrochem. Res. Inst.; 1972), 34–36.

5. Anantharaman, P., Swaminathan, K., Subramanian, G. and Udupa, H.V.K., J. Appl. Electrochem., 2(3), (1972), 169–173.

6. Anantharaman, P., and Udupa, H.V.K., J. Electrochem. Soc. India, 27(4), (1978), 217–224.

7. Hirajima, T. and Nishiguchi, I., Japanese Patent No. JP 80154590, (1979), (C.A. 94:164822m).

8. Chiba, T., Okimoto, M., Nagai, H. and Takata, Y., Bull. Chem. Soc. Jpn., 56(3), (1983), 719–23.

9. Tsenyuga, V.S., Nadezhina, N.A., Ovchinnikov, P.N. and Timofeeva, E. Ya., Zh. Org. Khim., 14(2), (1978), 337–339; USSR Patents Nos. 644781, (1979) and 578302, (1977), (C.A. 90:168252r and 88:50469x).

10. Sone, T., Karikora, M., Shinkai, S. and Manabe, O., Nippon Kagaku Kaizhi, 2, (1980), 245–249.

11. Mitsui Toatsu Chemicals Inc. Japanese Patent No. JP 61/1009759, (1986), (C.A. 106:4647).

12. Gatterman, L., Berichte, 26, (1893), 1844–1856; Chem. Zeitung, 17, (1893), p210ff.

13. Haussermann, Chem. Zeitung, 17, (1893), pp129 and 209.

14. Noyes, A. and Clement, A., Berichte, 26, (1893), 990–992.

15. Haber, F., Zh. Elektrochem., 4, (1898), 506; Haber, F. and Schmidt, C., Zh. Physik. Chem., 32, (1900), pp193 and 271.

16. Bamberger, E., Berichte, 27, (1894), pp1347–1350 and 1548.

17. Heyrovsky, M. and Vavricka, S., J. Electroanal. Chem., 28, (1970), 409–420.

18. Harwood, W.H., Hurd, R.M. and Jordan, W.H., I.& E.C. Proc. Des. and Dev., 2(1), (1963), 72–77.

19. Marquez, J. and Pletcher, D., J. Appl. Electrochem., 10, (1980), 567–573.

20. Darchen, A. and Moinet, C., J. Electroanal. Chem., 68, (1976), p173ff.

21. Pezzatini, G. and Guidelli, R., J. Electroanal. Chem., 102, (1979), 205–219.

22. Fleischmann, M., Petrov, I.N. and Wynne-jones, W.F.K., Proc. of 1st Australian Conference on Electrochemistry, (London, Pergamon, 1965), 500–517.

23. Martinyuk, G. and Shlygin, A., Zh. Fiz. Khimii, 32, (1958), pp368 and 1907–1912.

25. Lund, H. in "Organic Electrochemistry", edited by Baizer, M., (New York, Marcel Dekker Inc., 1973), 315–345.

26. See for example: Popp, F. and Schultz, H., Chem. Rev., 62, (1962), p19ff; Wazwonek, S., Synthesis, 6, (1971), 285–302.

27. See for example: Zuman, P. and Meitas, L., "C.R.C. Handbook Series in Organic Electrochemistry", (Ohio, CRC Press, 1976); Bard, A.J. and Lund, H., "Encyclopedia of Electrochemistry of the Elements", Volume XIII, Chapter 2, (New York, Marcel Dekker, 1979).

28. Fichter, F., "Organische Elektrochemie", (Dresden and Leizig, T. Steinkopff, 1942), p144ff.

29. Dey, B.B., Govindachi, T. and Rajagopalan, S.C., J. Sci. Ind. Res. (India), 4, (1946), p574ff.

30. Wilson, C.L. and Udupa, H.V.K., J. Electrochem. Soc., 99, (1952), 289-294; Udupa, H.V.K. and Dey, B.B., Bull. India Sect. Electrochem. Soc., 5, (1956), 58-61; Krishnamurthy, G., Dey, B.B. and Udupa, H.V.K., J. Sci. Ind. Res. (India)., 15B, (1956), 47-48.

31. Subbiah, P., Subramanian, G.S. and Udupa, H.V.K., Electrochim. Acta, 11, (1966), 863-868.

32. Thirunavukkarasu, P., Subbiah, P., Subramanian, G.S. and Udupa, H.V.K., Proceedings of 13th Seminar on Electrochemistry, (Karaikudi, India; Central Electrochem. Res. Inst.; 1972), 52-56.

33. Subbiah, P., Subramanian, G.S. and Udupa, H.V.K., Bull. Acad. Pol. Sci.; Ser. Sci. Chem., 14(10), (1966), 767-771.

34. Udupa, H.V.K., AIChE Sympos. Ser., 75, (1979), p185ff.

35. Rance, H.C. and Coulson, J.M., Electrochim. Acta, 14, (1969), 283-292.

36. Dey, B.B., Maller, R. and Pai, B., J. Sci. Ind. Res., India, 7B, (1948), p113ff; Dey, B.B., Govindachari, T.R. and Rajagopalan, S., ibid., 4, (1946), p574ff.

37. References 12, 13 and 14 from Rance and Coulson[35]

38. Benkesser, R., Watanabe, H., Mels, S. and Sabol, M., J. Org. Chem., 35, (1970), 1210.

39. Gigi, S., Paucescu, V. and Kurth, S., Romanian Patent No. RO 72382, (1980), (C.A. 96:151408x).

40. Udupa, H.V.K., Udupa, K.S. and Jayaraman, K., Indian Patent No. 142241, (1977), (C.A. 92:84928u).

41. Gunawardena, N.E. and Pletcher, D., Acta Chem. Scan., B, 37, (1983), 549-553.

42. PPG Industries Inc., U.S. Patent No. US 4584070, (1986).

43. Pecheva, I., Merdzhanova, D., Polapchieva, M. and Levi, M., Tr. Nauch. Khim. Farm. Inst., 12, (1982), 75-82.

44. Marquez, J. and Pletcher, D., Electrochim. Acta, 26(12), (1983), 549-553.

45. BASF AG, Private Communication.

46. BASF AG, Ger. Patent No. DE 2262851, (1974).

47. Skulikidis, Th.N., Sarropoulos, K. and Chanos, S., Kolloid - Z., 193(1), (1963), 45-47.

48. Yukawa, Y., J. Chem. Soc. Japan; Pure Chem. Sect., 71, (1950) pp547 and 603-5.

49. Guegeun, M.J. and Tallec, A., C. R. Acad. Sci. Paris; Ser. C., 268(23), (1969), 2042-45.

50. Heller, H.E., Hughes, E.D. and Ingold, C.K., Nature (London), 168, (1951), p909ff; Hughes, E.D. and Ingold, C.K., Quart. Rev., 6, (1952), p34ff.

51. Oae, S. and Kitao, T., Yuki Gosei Kagaku Kyokai Shi., 19, (1961), p880ff; Kukhtenko, I.I., Zh. Org. Khim., 7, (1971), p330ff.

52. Sone, T., Tokuda, Y., Sakai, T., Shinkai, S. and Manabe, O., J. Chem. Soc., Perkins Trans. II, 2, (1981), 298-302; Sone, T., Hamamoto, K, Seiji, Y., Shinkai, S. and Manabe, O., ibid., 12, (1981), 1596-8.

53. Goodridge, F. and Wright, A. in "Comprehensive Treatise on Electrochemistry", (London, Plenum Press, 1983), Vol 6, Chap 6, 393-443.

54. For example Goodridge and Wright[53] references 4 and 58-67.

55. Braithwaite, D.G., U.S. Patents Nos. US 3007857, US 3256161, US 3287248 and US 3391067 (1966 - 1968).

56. CJB Developments Ltd., British Patent No. 1239983, (1972).

57. Goodridge, F., J. Chem. Tech. Biotechnol., 38, (1987), 127-142.

58. Hamilton, M.A., Ph.D. Thesis, University of Newcastle-upon-Tyne, (1979).

59. CJB Developments Ltd., German Patent No. DE 2026039, (1969).

60. Yoshizawa, S., Takehara, Z. and Ogumi, Z., As. Gar. Kog. Gij. Shor. Ken. Mok., 28, (1976), 123-34, (C.A. 87:134159p); Yoshizawa, S., Takehara, Z., Ogumi, Z. and Tsuji, T., Bull. Chem. Soc. Japan, 49(11), (1976), 2889-2891.

61. Yoshizawa, S., Takehara, Z. and Ogumi, Z., Bull. Chem. Soc. Japan, 49(12), (1976), 3372-3375.

62. Goodridge, F. and Hamilton, M.A., Electrochim. Acta, 25, (1980), 481-6.

63. Scott, K., Electrochim. Acta., 30(2), (1985), 235-244 and 245-251.

64. Harrison, J.A., Electrochim. Acta, 25, (1980), pp447,657,899,1147,1153 and 1165; ibid., 27, (1982) pp1113 and 1123; Harrison, J.A., 3rd Symp. Electrochem. Processes, edited by Bruckenstein, J., McIntyre, B., Miller, B. and Yeager, E., (New York, Electrochem. Soc. 1980).

65. Du Pont Co., Concord Plaza, Read Building, Wilmington, DE 19898 U.S.A.

66. Sybron Chemicals Inc., Birmingham Road, P.O. Box 66, Birmingham, New Jersey 08011, U.S.A.

67. Goodridge, F. and King, C.J.H. in "Techniques of Electroorganic Synthesis, Part I", edited by Weinberg, N.L., (London, John Wiley & Sons, 1974), page 35.

68. Harrison, J.A., Caldwell, D.L. and White, D.E., Electrochim. Acta 29, (1984) 203.

69. Bachurina, T.D. and Yankovskii, A.A., Fiz. Khim., 1, (1974), 69–72, (C.A. 84:97006b).

70. Nolen, T., J. Electrochem. Soc., 135(1), (1988), 29C–31C.

71. Vijayalakshamma, S.K. and Subrahmanya, R.S., J. Electroanal. Chem., 23, (1969), 99–114.

72. Malachesky,P.A., Marcoux, L.S. and Adams, R.N., J. Phys. Chem., 70, (1966), p4068ff.

73. Plimley, R.E. and Wright, A.R., Chem. Eng. Sci., 39(3), (1984), 395–405.

74. Mamoor, G.M., Ph.D. Thesis, University of Newcastle–upon–Tyne, (1983); Goodridge, F., Mamoor, G.M. and Plimley, R.E., IChemE Symp. Ser. No. 98, (1986), p61.

75. "Nova–PAK Column – Care and Use Manual", Waters Associates (Inst.) Ltd., 324 Chester Road, Hartford, Northwich, Cheshire, UK.

76. Levich, V.G., "Physico-chemical Hydrodynamics", (New York, Prentice-Hall, 1962); Riddiford, E.C., "Advances in Electrochemistry and Electrochemical Engineering", Vol 4, (New York, Interscience, 1966);Albery, W.J. and Hitchman, M.L., "Ring-Disk Electrodes", (Oxford, UK, Clarendon Press, 1971).

77. Bard, A.J. and Faulkner, L.R., "Electrochemical Methods", (New York, John Wiley & Sons, 1980).

78. Treybal, R.E., "Mass-Transfer Operations", (London, McGraw-Hill, 1980), Chap. 3.

79. Plimley, R.E. and Harrison, S., Private Communication.

80. Coeuret, F., Electrochim. Acta., 21, (1976), 185-193.

APPENDIX A.

Analysis Methods.

A1.0 Reaction Products.

During the reduction of nitrobenzene in methanol / sulphuric acid, the main products were initially assumed to be ortho-anisidine, para-anisidine and aniline. However, a consistent failure to account for all the current and nitrobenzene consumed during an experiment led us to question the validity of this assumption. As can be seen from the reaction scheme shown in figure 1.2, in chapter 1, side reactions are possible and many by-products could, therefore, be formed. To investigate this further, reaction samples were analysed by mass spectroscopy and results compared to pure samples of possible by-products. The mass spectroscopy was carried out in the chemistry department of Newcastle University. The mass spectrum showed a rather complex mixture of fragments, which were interpreted using the spectra of pure substances. The following compounds were confirmed to be present in the reaction mixture after a typical experiment:

Reactant:	Nitrobenzene.
Major Products:	Para-anisidine, Ortho-anisidine, Aniline, Para-aminophenol.
Minor Products:	Azoxybenzene, Hydrazobenzene, Para-methoxyhydrazobenzene, Azobenzene, Para-methoxyazobenzene.

Quantitative product analysis was initially carried out using gas chromatography techniques, which proved very unsatisfactory. Following the purchase of new equipment all the results presented in this thesis were determined using high performance liquid chromatography (HPLC), described below.

A2.0 HPLC Analysis.

Using the equipment and techniques described in this section, the major products could be routinely analysed. Due to the comparatively low concentrations and the difficulty in separation of the minor products, their quantitative analysis proved difficult and inaccurate. It was found, however, that in all experiments the formation of the major products accounted for between 70% and 90% of the nitrobenzene consumed. It was estimated that the minor products formed during an experiment accounted for not more than 10% of the nitrobenzene consumed. These by-products were never routinely determined.

A2.1 Equipment.

The HPLC system consisted of a Pye Unicam 4010 pump, 4020 variable wavelength UV detector and a Rheodyne 7125 rotary sample injection valve. The column was a Waters "Nova-PAK" C_{18} reverse phase column, which proved much superior, in both performance and reproducibility, to the Pye Unicam Spherisorb 5ODS column that was supplied with the system. This equipment is detailed below.

All solvents used were HPLC grade and supplied by Fisons plc, the water was glass double-distilled. All liquids were routinely filtered through 0.45 micron filters, before use.

A2.2 Mobile Phase

The mobile phase was a 40:60 mixture of methanol and water, buffered to a pH of 6.0 using phosphates. This composition was chosen to give the optimal elution time, minimum peak broadening and highest resolution of the product peaks.

Resolution between peaks improves with an increase in elution time, however it is at the great expense of increased peak broadening and

subsequent loss of accuracy. The 40:60 mixture was found to give the optimum peak shape and resolution for this analysis.

The buffering of the mixture improved the resolution between para-anisidine and aniline, as well as the reproducibility of the analysis, since the sample pH was slightly variable. Phosphate buffers were chosen to minimise damage to the pump and column that could occur with other buffering agents[75]. A mobile phase pH of 6.0 was achieved by making the mixture up with water which contained 39.36 mmol/litre KH_2PO_4 and 0.64 mmol/litre $Na_2HPO_4.2H_2O$.

The mobile phase mixtures, including the un-buffered washing solutions, were routinely filtered and degassed ultrasonically before use.

A2.3 Sample Pre-treatment.

It has been reported[49,58,62] that the rearrangement of the phenylhydroxylamine intermediate to aminophenol is slow. The presence of para-aminophenol as a product in a non-aqueous system suggests that this rearrangement is faster than the analogous rearrangement to anisidine. To avoid possible problems with unreacted intermediate, samples were routinely heated at 55°C for several hours before analysis. However, the sample life was limited, particularly at elevated temperatures, due to oxidation of the amines. Thus, if samples could not be analysed immediately after the heating period, they were refrigerated and analysed within 24 hours. The degeneration of samples was much reduced once they had been diluted and neutralised; samples could be kept refrigerated for several days without any noticeable deterioration.

Samples typically contained 41 g/l nitrobenzene, 2-10 g/l para-anisidine, 0.5-2 g/l ortho-anisidine, 1-10 g/l aniline, 0.5-2 g/l para-aminophenol and 10% H_2SO_4 by volume in methanol. After dilution by 100 times, the pH of a sample would usually be about 1.5. Not only is this value far too acidic for injection onto a silica based column[75], but the amines would be protonated and hence unretained by the column. Raising the pH above 5.34 (the pK_a of p-anisidine and the highest of all the amines in a sample) is necessary to avoid the latter problem, whilst the recommended

pH range for the longest column life is 3.5 to 6.5[75]. A pH of 6.0 was found to give the best separation and was inside this "safe" range.

Samples were, therefore, first diluted using mobile phase as diluent, and then shaken with $NaHCO_3$ to give a solution of pH = 6.0, which could then be injected onto the column. Slight inaccuracies in the neutralisation process were compensated for by the buffering effect of the mobile phase. Samples were typically diluted by 100 times to bring all the peaks, except nitrobenzene, onto a suitable scale. A further dilution of up to 50 times was required to analyse the nitrobenzene peak. 2–20 μl portions of the diluted and neutralised samples were injected onto the column using a sample loop or microsyringe.

A2.4 Conditions Of Operation.

The conditions under which the analyses were carried out are shown in the table below. The mobile phase flowrate was the fastest possible within the pressure limitations of the column[75]. The temperature of the column was kept constant throughout an analysis.

COLUMN:	3.9mm ID x 15 cm Reverse-phase Waters "Nova-PAK" C_{18}, >10,000 theoretical plates (as determined by Waters test method[75]).
DETECTION:	Pye-Unicam 4020 UV variable wavelength detector.
PUMP:	Pye-Unicam dual headed reciprocating HPLC 4010 pump, capable of 0.1–9.9 ml/min at pressures up to 350 bar.
INJECTION:	Rheodyne Type 7125 rotary sample injection valve with 20 μl sample injection loop or 2–20 μl microsyringe.
MOBILE PHASE:	60:40 water / methanol, buffered to pH=6.0. Buffer concentrations: 39.36 mmol/l $K_2H_2PO_4$ 0.64 mmol/l $Na_2HPO_4.2H_2O$
SAMPLES:	Diluted 1:50 – 1:1000 with mobile phase, neutralised to pH=6.0 using $NaHCO_3$. Internal standard (if used): ortho-nitroaniline.
CONDITIONS:	UV detection at 254 nm. 2–20 μl sample injected via loop or syringe.

Mobile phase flowrate: 1.3 ml/min.

Pressure at pump: 150–200 bar (200 maximum).

pH METER: Dow Corning pH/ion meter type 135, Dow Corning standard glass pH electrode, type 003 11 1011, Dow Corning Calomel reference electrode, type 003 11 60211.

CONDUCTIVITY METER: Phillips Laboratory Conductivity Meter, model PW 9505, and standard cell.

PEAK RETENTION TIMES:

Para–aminophenol.....	0.95	mins.
Para–anisidine.....	1.60	mins.
Aniline.....	1.95	mins.
Ortho–anisidine.....	2.80	mins.
Ortho–nitroaniline.....	3.90	mins.
Nitrobenzene.....	6.00	mins.

A2.5 Peak Identification.

The peaks were identified by comparison of retention times with pure samples of the expected compounds. In a typical experimental sample, several small peaks remained unidentified; these were most probably reactant impurities or the result of injection port contamination. The first compounds to elute (giving peaks at 0.75 – 0.85 mins retention time) corresponded to compounds unretained by the column. In standard "made–up" samples, these peaks were small and due to the slight solubility differences between the sample solvent and the mobile phase. Experimental samples, however, usually showed a rather complex series of initial peaks. Identification or quantitative analysis was impossible since at a retention time equivalent to the column hold–up there is almost no separation and all the peaks occurred together. The first peak that could be identified was p–aminophenol (0.95 mins). The retention times of all the identified peaks are shown above.

A2.6 Quantitative Analysis.

The peaks on the chromatogram are a measure of the UV absorbance, at 254 nm, of the various components which have been separated from the sample mixture by the column. Thus the area under each peak is proportional to the concentration of that component in the mixture. For sharp, symmetrical peaks it can easily be shown that the area under the peak is proportional to the peak height. Considering the shape of the product peaks and the relative difficulty of integrating accurately, it was considered sufficient to use peak height to calculate the product concentrations.

Since HPLC can only give proportions of compounds in a sample mixture, the method needs to be calibrated in order that quantitative results can be obtained. Initially an internal standard method was adopted, however the HPLC system proved so reproducible that in later experiments an external standard was used. The internal standard involved the addition of a known quantity of ortho-nitroaniline to a sample before analysis (the nitroaniline was chosen so as not to interfere with any of the product peaks). A comparison of the height of a product peak to the height of the standard peak gave that product concentration in the sample.

For the external standard method a mixture of known amounts of all the expected components was made up and prepared in exactly the same way as an experimental test sample. This standard mixture was then injected before and after each test sample. The composition of the test sample could hence be calculated by comparing the peak heights of each compound in the standard with those in the test sample.

A2.7 Accuracy of the HPLC Analysis Method.

The HPLC system described above was most accurate for sample concentrations of 10-100 mg/l. Since a typical reaction mixture contained 2-20 g/l of products and 41 g/l nitrobenzene, dilution of the samples by 50 up to 1000 times was necessary. Such large dilutions could introduce large errors into the analysis and although great care was taken, some spurious analysis results did occur. One consequence of this method was that the

analysis of nitrobenzene was always subject to a greater error. For this reason an accurate mass balance, over an experiment, was difficult to achieve. Although the analysis was accurate for simulated reaction mixtures, as shown by the tables below, some problems were encountered when a real reaction mixture was analysed.

The tables below shows the accuracy and reproducibility of the analysis method.

Internal Standard Method

	p-anisidine		o-anisidine		aniline		nitrobenzene	
	Expected	Actual	Exp.	Act.	Exp.	Act.	Exp.	Act.
1	7.89	7.43	2.76	2.71	6.18	6.71	17.8	15.7
2	93.0	95.8	11.6	12.9	23.6	22.9	102.9	114.2
3	43.6	46.2	8.20	8.62	10.4	11.1	54.1	50.4
Average Error	4.9%		5.6%		5.8%		10.2%	

External Standard Method

	p-anisidine		o-anisidine		aniline		p-aminophenol		nitrobenzene	
	Exp.	Act.	Exp.	Act.	Exp.	Act.	Exp.	Act	Exp.	Act.
1	36.6	37.8	15.8	14.9	15.1	14.5	19.0	18.7	70.1	64.5
2	34.5	30.0	23.3	24.1	52.0	49.4	19.4	18.3	128.2	147.4
3	2.32	2.54	0.22	0.24	0.32	0.35	0.33	0.34	32.8	34.8
4	10.14	10.82	8.40	8.51	4.21	4.49	7.21	6.82	54.6	49.5
Average Error	8.2%		4.6%		6.1%		4.0%		9.4%	

A3.0 Total Amine Analysis

The analysis technique described above was potentially very accurate, but throughout this work problems were encountered with the analysis of samples taken during experiments. It was never possible to account for all of the current passed during a run, nor could an accurate mass balance be

made. In an attempt to resolve this problem an alternative analysis technique, suggested by BASF[45], was tried. In this method the amount of amine groups were measured by potentiometric titration.

A3.1 Theory

Amines are weak bases and are protonated in acidic solutions. In this method the amines extracted from a sample were titrated against perchloric acid. The expected amines ie. anisidine, aniline and aminophenol all have similar pK_a values for the acid dissociation. Hence the end-point determined by titration was clearly defined and gave the total amount of anisidine, aniline and aminophenol in a sample.

A3.2 Method

A known amount of sample (2 – 5 g) was first diluted with 5 ml methanol, phenolphthaline indicator (10 g/l in methanol) added and the solution neutralised with aqueous 1 M NaOH. Excess NaOH (5 ml) was added to ensure an alkaline mixture. The solution was then extracted three times with 10 ml methylene chloride. To the organic extract, 50 ml acetonitrile was added and then titrated against 0.075 M perchloric acid solution made up in isopropanol. The titration was followed potentiographically using a glass pH electrode and a standard calomel reference electrode. The end-point of the titration appeared as a point of inflection on the curve of pH against volume of titer.

The proportion of amine compounds in a sample was then determined from the end-point according to the equation below:

$$w = \frac{V}{m} \cdot M \cdot c \cdot \frac{100}{1000}$$

Where: w = Total Amine content (mass %)
V = Volume of titrate at end point (ml)
m = Sample weight (g)
c = Perchloric acid concentration (= 0.075 mol/l)
M = Average molecular mass of amine mixture (g/mol)

Knowing the sample density allowed the concentration of amine

compounds in the reaction mixture to be determined. The average molecular weight was estimated by assuming that the HPLC analysis gave the correct ratio between the amine products.

A3.3 Apparatus

CHEMICALS: All chemicals were supplied by B.D.H. Ltd. and were "AnalaR" grade.

pH METER: Dow Corning pH/ion meter type 135, used in mV mode so that no pH calibration was required.
Dow Corning standard glass pH electrode, type 003 11 1011,
Dow Corning Calomel reference electrode, type 003 11 60211.

A3.4 Accuracy and Reproducibility

Standard solutions of aniline and a mixture of aniline, ortho- and para- anisidine were made up and analysed with the following results:

Test 1: 53.5 g/l aniline, 10% H_2SO_4 in methanol

Measured by analysis: 57.80 g/l 53.94 g/l 57.81 g/l 56.35 g/l 54.52 g/l

Maximum Error: 8.1 % **Average Error: 4.8 %**

Test 2: 26.8 g/l aniline, 4.6 g/l ortho- anisidine, 22.9 g/l para-anisidine, 10% H_2SO_4 in methanol - 54.3 g/l total amines

Measured by analysis: 55.45 g/l 55.10 g/l 55.75 g/l 56.7 g/l

Maximum Error: 4.4 % **Average Error: 2.7 %**

A4.0 Analysis of Experimental Reaction Mixtures

Throughout this work there were problems with the analysis of reaction products. In most experiments the quantitative analysis did not account for either the nitrobenzene converted or the total number of

coulombs passed. Improvements were made but some uncertainty remained as to why an accurate analysis technique worked well for standard test reaction mixtures, but gave apparently spurious results for experimental mixtures. This section discusses the problem and assesses the validity of the experimental results in this work that were determined by product analysis. The assumptions that were made have particular impact on the derivation of the kinetic constants for the reaction model and this is discussed below in section 4.1. The methods of analysis and their accuracy and reproducibility for experimental reaction mixtures are also discussed. The effect on the bench scale work is discussed in a separate section 4.2.

A4.1 Effect of Product Analysis Problems on H-Cell Work

The first possibility considered was passage of reaction products across the membrane. The electrode reaction in the anode compartment was a mixture of hydrogen evolution and oxidation of methanol to formaldehyde. Reaction of an amine with formaldehyde leads to Schiff's base formation, thus removing any analysable reaction product from the anolyte. To test the possibility of passage across the membrane (either Nafion or Ionac-3470) a third compartment was added to the H-Cell between the catholyte and anolyte chambers. Experiments with this cell proved that no reaction products passed through either Nafion or Ionac, but that Nafion did allow some nitrobenzene through. As a consequence all further experiments, both in the H-Cell and in the bench scale cell, were performed using Ionac-3470.

A4.1.1 Possible Reaction By-Products

The obvious by-product possible is hydrogen and this was the first considered. The model suggested that in the range of electrode potentials used, hydrogen evolution was negligible. An experiment was devised to show this and it is fully described in appendix D. The conclusion was that hydrogen evolution could account for, at most, 1.6% of the current passed at 1600 A/m^2. Consequently, hydrogen evolution could not possibly account for the current shortfalls encountered.

The mass spectroscopy study described in the first section of this appendix showed the large range of products obtained when nitrobenzene was reduced in acidic methanol. Due to the difficulty in quantitative analysis of di-aromatic compounds by HPLC methods the minor products were never quantitatively analysed. The assumption that together they accounted for 10% of the nitrobenzene converted was made after studying work done by BASF[45] and others on this reaction. Typically they found that around 10% of the current passed remained unaccounted for by the major products, sometimes even more. In the opinion of most workers who have studied the reduction of nitrobenzene a 10% shortfall in products was reasonable, unless complex and lengthy analysis procedures were used. These by-products result from rearrangement and coupling reactions of the intermediate phenylhydroxylamine and are thus mainly four electron reduction products. The consequence of ignoring these products was that the analysis results tended to overestimate the ratio of aniline to four electron products. The effect on the model is that the predicted aniline formation will also be overestimated. The purpose of the present work was to maximise production of p-anisidine ie four electron products, to this end the model will be slightly pessimistic.

A4.1.2 H-Cell Experiments

Typically, in H-Cell experiments, HPLC analysis accounted for around 75% of the total coulombs passed. Allowing a maximum of 10% for unanalysed by-products, that still leaves 15% unaccounted for. Experiments showed that even at the highest current densities used hydrogen evolution was negligible (at most 1-2%). The inescapable conclusion is that the HPLC analysis was at fault. Section A2.6 above clearly demonstrates the accuracy of the HPLC methods. Indeed for a wide range of different concentrations of standard solutions the analysis proved both accurate and highly reproducible. There is no doubt that the "missing" current must have been consumed in product formation, even the rather inaccurate nitrobenzene

analysis revealed this fact*. The question to be answered is what these products are and to postulate why they could not be detected.

A4.1.3 Total Amine Analysis

The total amine analysis was employed to confirm the HPLC analysis. Table A1.0 below shows the results of total amine analysis on the H-Cell preparative results. The theoretical total and the figure for current efficiency were calculated assuming that the ratio of four to six electron products was given by the HPLC analysis, since the total amine analysis makes no distinction between aniline and o- or p- anisidine or p-aminophenol.

The total amine analysis (TA) consistently revealed more reaction products than the HPLC analysis as is shown by the current efficiencies in table A1.0. The efficiencies based on the HPLC vary between 65.7% and 89.6% with an average of 74.6%, whilst those based on the TA analysis lie between 81.9% and 96.9% and an improved average of 86.9%. This is clear proof that the HPLC analysis for experimental samples is not capable of accounting fully for the products formed, however it still does not account for all of the coulombs passed in an experiment.

There are three possibilities to explain why these figures are not closer to 100%. Firstly, by-product formation could account for as much as 10% of the products formed, as discussed above in section A4.1.1. The by-products found by mass spectroscopy, namely azo- and azoxy- benzenes would <u>not</u> be detected using the total amine analysis method and thus would explain the shortfall. It seems strange, however, since these by-products are results of reactions by the intermediate phenylhydroxylamine, that their formation seems largely unaffected by current density whilst the four electron products depend strongly upon current density. This could be explained by the second possibility.

---

*With only 10% conversion of a 0.3 M solution of nitrobenzene, the samples from H-Cell experiments contained too high a concentration of nitrobenzene to be accurately analysed by HPLC.

Table A1.0 Reaction Product Analysis - comparison between HPLC and TA

Cathode Potential ϕ (mV vs SCE)	Current Density i (A/m^2)	Total Products (g/l)		Current Efficiency of Total Products by Analysis			
				HPLC alone	Total Amine Analysis results assuming:		
		by HPLC	by TA		Product Ratio by HPLC	TA does not detect p-aminophenol	Difference TA - HPLC is aniline
217	252	4.31	4.88	76.4%	86.3%	98.9%	93.5%
256	704	4.22	-	69.5%	-	-	-
258	756	4.34	4.89	77.9%	87.9%	99.8%	94.4%
262	504	4.27	4.85	75.2%	85.4%	97.7%	92.9%
268	895	4.23	4.98	74.8%	87.9%	100.5%	95.3%
274	252	4.65	4.91	80.2%	84.7%	98.3%	90.5%
276	508	4.21	4.42	78.0%	81.9%	93.9%	88.2%
279	239	3.97	4.77	68.5%	82.2%	93.1%	91.6%
279	478	4.48	4.97	75.4%	83.7%	95.6%	91.1%
279	894	3.97	-	69.4%	-	-	-
291	910	3.99	4.52	74.5%	84.4%	96.7%	91.3%
307	1190	4.11	5.04	73.6%	90.2%	101.3%	97.8%
311	1591	3.31	4.13	67.1%	83.9%	93.2%	91.1%
316	1190	4.02	4.75	73.6%	86.8%	98.2%	94.4%
320	1137	3.79	4.69	69.5%	86.0%	97.0%	94.5%
322	762	4.64	5.01	78.6%	84.9%	97.0%	91.2%
324	1567	3.85	-	73.2%	-	-	-
334	1445	3.74	4.61	70.3%	86.6%	96.5%	94.4%
338	1778	4.07	4.55	78.7%	88.0%	98.9%	93.4%
344	1442	3.82	4.78	73.6%	92.1%	103.2%	99.0%
348	1818	4.08	4.31	82.5%	87.1%	96.7%	90.7%
372	2032	3.21	4.49	65.7%	91.9%	101.8%	99.6%
373	2032	4.44	4.79	89.6%	96.9%	108.8%	99.1%
Average Current Efficiencies =				74.6%	86.9%	98.4%	93.7%

The total amine analysis method relied on the alkaline extraction of the amines using aqueous NaOH. It is known that para-aminophenol forms sodium phenylate under strongly alkaline conditions such as used during the analysis. Sodium phenylate is soluble in aqueous NaOH and thus there is a chance that the para-aminophenol would be left behind in the aqueous phase and not be detected by the TA analysis. Para-aminophenol typically accounted for some 10 to 15% of the current passed. Table A1.0 shows the total product current efficiencies if it is assumed that p-aminophenol is undetected by the TA analysis and that the HPLC gives the correct ratio of individual products. It can be seen that almost all of the current can be accounted for if this assumption is true (98.4%).

The current efficiencies worked out for the TA analysis were calculated assuming that the ratio of four electron products to six electron products was as determined by the HPLC. If in reality more aniline was formed than this ratio suggests and that the difference between the total products by HPLC analysis and by TA analysis was, in fact, due entirely to aniline formation then the TA current efficiencies are given would be as shown in the last column of table A1.0. Here the average total current efficiency would be 93.7%, a very reasonable figure considering experimental error and the by-products formed.

Without a detailed analytical study beyond the scope of this work, it is not possible to assess which of these possibilities is true. Probably all three occur to a certain extent; by-products are indeed produced, it is also likely that all the para-aminophenol was not detected and it is always possible that more aniline was formed than was assumed.

A4.1.4 HPLC Analysis

It is clear from the total amine analysis work that the HPLC underestimated the products in the reaction mixture samples. It is possible to imagine many reasons for this. Obviously it has something to do with the experimental reaction mixtures, since made up standard samples were never a problem. Some of the possibilities are discussed below.

One candidate was oxidation of the amines; every effort was made to analyse as soon as possible after an experiment and if not the samples were kept sealed under refrigeration. There was always a slight over-pressure in the experimental rig making it unlikely for oxidation to occur during a run. Furthermore, the oxidation products of amines are strongly coloured and it was easy to tell if a sample had been subject to air oxidation and it was discarded.

Problems related to the HPLC methods and the column are also possible. For instance, a by-product, present in only small amounts, could affect the UV absorption of the other products causing a decrease in peak height. Some of the products could also be retained on the column and thus reduce the amount detected. More likely, however, is inadequate neutralisation leading to the presence of protonated amines, which would be unretained by the column and appear as the solute peak at the start of a chromatogram. There was some evidence that this could, indeed, occur. Certainly the size and appearance of the initial solute peak on a chromatogram was different for an experimental sample and for a standard made-up sample. Even greater care was taken in the neutralisation, but no improvement was observed. A last possibility applicable more to the bench scale experiments is the formation of copper complexes with the amines. If copper ions are present in solution then they will tend to form complexes and the resulting polar species would be unretained on the HPLC column and thus coincide with the solute peak.

In the absence of more information and further work beyond the scope of this thesis, no firm conclusions can be reached as to the exact reason for the problems experienced with the HPLC methods used. In general, HPLC can be recommended as a potentially accurate and highly reproducible analysis method for these amines. The author, however, suggests that an independent secondary analysis method, preferably a "work-up" or titration method, is used as a backup in case of problems similar to those encountered during this work.

A4.1.5 Conclusions

From the foregoing it is clear that the analysis techniques used in this work were not entirely problem free!. For the purpose of the model kinetic constants determination, we were thus forced to assume that the HPLC analysis gave the correct ratio of four to six electron products and that all the current passed was used in the formation of ortho- or para-anisidine or para-aminophenol or aniline. The implications of these assumptions are that the model so derived is probably subject to an error up to 25%. It will fail to predict the formation of azo- and azoxy-compounds and will tend to overestimate the total current efficiency of the products formed. However, considering all the information available it seems reasonable to suggest that the model is capable, nevertheless, of predicting the ratio of four to six electron products within experimental error.

A4.2 Bench Scale Work

Whilst it was a little worrying, the failure to account for all of the current passed during an experiment was not so crucial for the bench scale work. The severe dissolution of the electrode during all the experiments with the three dimensional electrode configuration meant that no meaningful comparisons could be made between the different cell types. Indeed the large concentrations of copper ions in the reaction mixtures almost certainly gave rise to copper - amine complex formation. These compounds, as mentioned above, would be unretained by the HPLC column so bringing errors into the measurements. Further inaccuracies are introduced by the catalytic reduction to aniline. In was unknown how much of the aniline formed in a packed or fluidised bed experiment was due to electrochemical reduction at the electrode via phenylhydroxylamine and how much was due to the direct electro-catalytic reduction.

One interesting phenomena was noticed, however, at conversions above 30%. At these and higher conversions, more of the current passed could be accounted for; in other words the total current efficiency <u>increased</u> with conversion. A possible reason for this is that the copper complex formation reaches an equilibrium level dependant on the copper ion concentration, so

the greater the amine production is, the less complex there is relative to the total amine present in the reaction mixture.

A5.0 Atomic Absorption Analysis

It was discovered in the bench scale work on three dimensional electrodes that the copper electrode dissolved into the electrolyte during an experiment. In order to confirm and further investigate this phenomena atomic absorption (AA) analysis was used to quantitatively determine the amount of copper, and later nickel, in the reaction mixture. This technique is well known and is therefore only briefly described below.

A5.1 Quantitative Atomic Absorption

Atomic absorption is the process by which light energy is absorbed by a ground state atom forming an excited state atom. The energy is absorbed in unique quanta, characteristic of a particular atom. Thus atoms of different elements can be identified by the characteristic wavelength they absorb. By using a light source emitting the characteristic wavelengths of a particular atom, quantitative analysis is possible. The absorption by the atoms under study, measured analytically as absorbance, A, is proportional to the number of absorbing atoms and hence to the solution concentration.

The relationship between the measured absorption and the concentration of a particular atom species is linear, but only over a small range of concentrations. Concentrations outside this range are normally measured by dilution or by plotting a calibration curve.

A5.2 Apparatus

A Perkin Elmer Model 560 spectrophotometer was used for sample analysis. The sample solution is aspirated through a high temperature air–acetylene flame, where the solution is successively crystallised, the

crystals liquified, vaporised and atomised. Light from a hollow cathode lamp, specific for either copper or nickel, is passed through the flame, the metal atoms excited and the resulting absorbance detected relative to a blank sample.

A5.3 Method

Samples were first neutralised in the same way as for the HPLC analysis (section A2.3), and then suitably diluted. Typically dilution factors between 100 and 500 were required. In addition a blank sample containing approximately the same concentrations of the same organic materials present in a reaction mixture, but without the metal ions, was made up. The absorbance relative to this blank was measured for each sample. Standard solutions of copper and nickel were used to calibrate the measurements. In this way the concentrations of copper and nickel ions in the reaction mixtures were determined.

Appendix B.

Estimation of the Ohmic Drop Between the Tip of the Luggin Capillary and the Electrode Surface.

The electrode potential was always measured using a Luggin capillary probe, positioned either in front of or through the rear of the electrode. In the former case the tip of the probe was placed close to the electrode surface to minimise the potential drop due to the resistivity of the electrolyte. To avoid seriously affecting current distribution and mass transport, the distance between electrode surface and the Luggin tip was at least as great as the capillary diameter (about 1 mm). This criteria introduced a source of error into the measurement of electrode potentials, namely ohmic or IR drop. This is the potential drop across a volume of electrolyte due to its finite electrical conductivity. In this case the volume was a cylinder with a cross-sectional area the same as that of the electrode and a height the distance between the electrode and the tip of the probe.

Normally, even for electrolytes with very low conductivities, IR drop can be minimised by the use of small electrodes and low currents and can usually be neglected. However, the preparative work done using the glass "H" cell involved the use of a relatively large electrode (around 10 cm^2), and consequently also significant currents (up to 2 A), in order to achieve sufficient product formation over the required range of current densities. Under these conditions IR drop became large and had to be corrected for. The method of correction that was used is described below. IR drop was also corrected for during the polarisation studies at the rotating disk electrode using a high frequency impedance method that has been described elsewhere[64,68] and outlined in section 2.1.1.

B1.0 Theory of Ohmic Drop.

The potentiostat measures the potential difference between the Luggin and the electrode $\phi_m - \phi_l$, not the true electrode potential $\phi_m - \phi_s$ (see

figure B3 below). The subscripts m, 1 and s refer to the metal electrode, the Luggin tip position and the outer edge of the double layer respectively. The difference between ϕ_s and ϕ_1 is R x i, where i is the current density at the electrode and R is the resistance of a volume of electrolyte of unit cross sectional area and length 1. Thus a knowledge of 1 and the electrolyte conductivity would allow the determination of R and hence the true electrode potential. Accurate measurement of a distance inside the "H"-cell around 1 mm was, of course impossible. Instead the distance was indirectly determined using the "$(I_{10} - I_1)$" method, described below, before a run, the assumption being that electrode and Luggin remained in the same relative positions throughout an experiment.

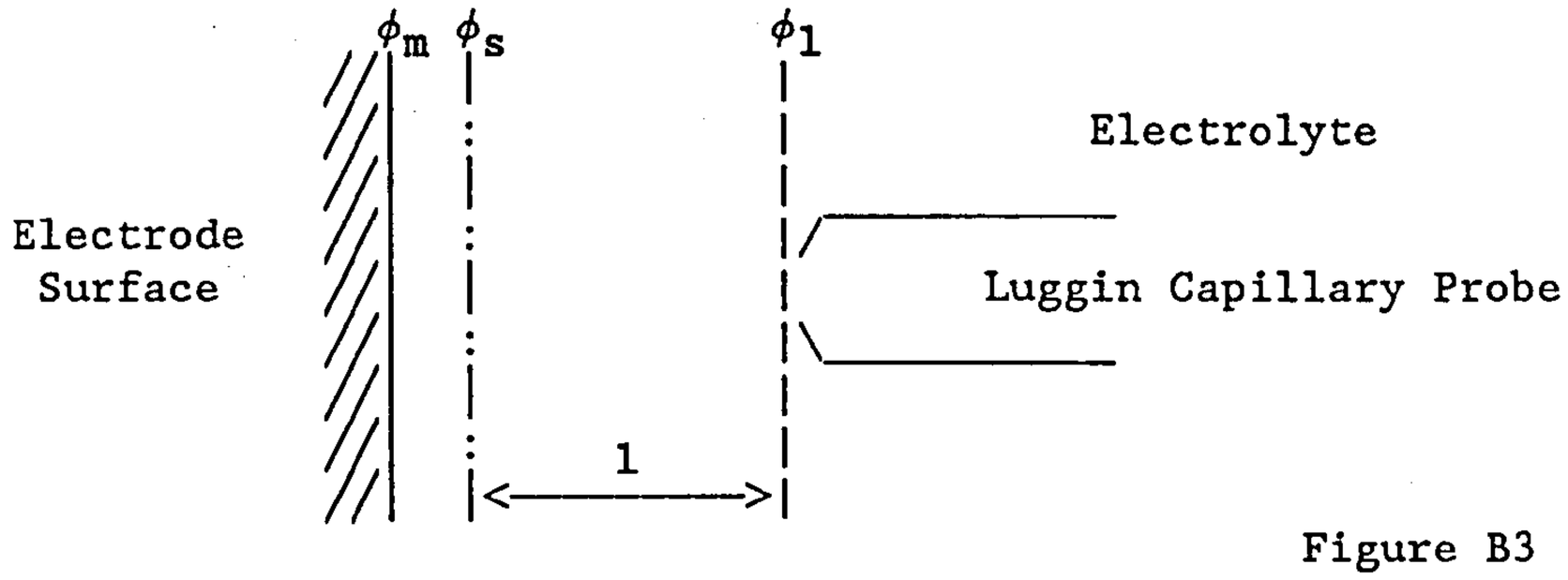

Figure B3

B2.0 Theory of "$(I_{10} - I_1)$" Ohmic Correction[79].

If E is the observed potential, ie. $\phi_m - \phi_1$, and ϕ is the true electrode potential, ie. $\phi_m - \phi_s$, then:

$$E = \phi + iR$$

The Tafel relationship between i and ϕ for a simple electrode reaction such as hydrogen evolution is:

$$i = k.e^{b.\phi}$$

substituting:

$$E = (2.303/b)\log i - (2.303/b) \log k + iR$$

considering conditions at the electrode for current densities i_{10} and i_1, where $i_{10} = 10i_1$:

$$E_{10} = (2.303/b)(\log i_{10} - \log k) + i_{10}R$$

$$E_1 = (2.303/b)(\log i_1 - \log k) + i_1R$$

subtracting, we have:

$$(E_{10} - E_1) = (2.303/b) + (i_{10} - i_1)R$$

Thus a plot of $(E_{10} - E_1)$ against $(i_{10} - i_1)$ gives a straight line with slope equal to R. The electrode area can be incorporated into k and hence $(i_{10} - i_1)$ may be replaced by $(I_{10} - I_1)$. This value can then be used to calculate the electrode potential from the observed potential and the current density thus:

$$\phi = E - iR$$

This method is only valid if there is a single electrode reaction occurring (ie. hydrogen evolution).

A knowledge of the electrolyte conductivity allows the characteristic dimension, 1, to be calculated.

B3.0 Estimation of Ohmic Correction During Experiments.

The method described above can only be used for a more complex system if certain assumptions are made. Firstly, the determination of the characteristic dimension, 1, is only valid if there is only one electrode process and if this can be approximated by the Tafel equation. For the methanol / 10% sulphuric acid system, it was assumed that the only cathode reaction was hydrogen evolution according to the Tafel approximation. It was shown that the gas evolution observed during an "acid-only" electrolysis was hydrogen and that the current / potential plot was indeed a characteristic straight line indicating a Tafel approximation was valid.

Thus the methanol / sulphuric acid (or "acid-only") electrolyte was used to determine the resistance, R_H, before each experiment. Then, taking great care not to change the cell set up or the Luggin position, nitrobenzene was added to the cell and an experiment started, the potential being continuously monitored during the experiment.

The true electrode potential, ϕ, could be calculated from the observed potential, E, and the current density, i,using the relationship derived above, namely:

$$\phi = E - iR_N$$

where resistance R_N is calculated from R_H using the conductivities of the "acid-only" and the "nitrobenzene" electrolytes:

$$R_N = \frac{R_H \times K_H}{K_N}$$

where K_H and K_N are the conductivities of the "acid-only" and the "nitrobenzene" electrolytes respectively.

This correction of observed potential to give the true electrode potential involves two crucial assumptions. Firstly, the dimension, l, must remain the same throughout the "acid-only" electrolysis and the nitrobenzene reduction; further, the conductivity of the electrolyte between the Luggin tip and the electrode surface must not change during the experiment.

B4.0 Alternative Methods of IR Correction for the H-Cell

Generally this method provided a reproducible and seemingly accurate value for the IR drop. For some experiments, particularly those using currents of above 1.5 A, the IR correction accounted for up to 50% of the measured electrode potential. Clearly with such a large correction the accuracy of its determination was crucial and it was felt that an alternative method was needed to corroborate the results.

The first approach was to find a method which could be used during a preparative experiment. Two possibilities were tried. The first used an interruption technique. The current flow to the electrode was instantaneously switched off and the potential fall off measured on a very short timescale (of the order of milliseconds). Theory dictates that the part of the potential due to IR drop will disappear instantaneously, whilst the true electrode potential will decay with time according to the capacitance of the double layer. This behaviour was observed but the results obtained for the IR drop were meaningless. It was thought that the switching of so large a current (1-2 A) caused instability in the measurement circuit and a common earth problem was also suspected. The method was abandoned.

A crude impedance method was also attempted, where a high frequency sinusoidal signal was superimposed upon the electrode potential during a potentiometric study. The phase change in the superimposed signal was measured and used to calculate the ohmic loss at various times throughout an experiment. Once again the results proved meaningless, this time electrical interference was blamed. In theory the technique should be reliable but time pressure forced the idea to be shelved.

B5.0 Discussion

Considering the alternatives tried above the ($I_{10} - I_1$) method was chosen as the method for IR correction for "H" - cell experiments. The possible errors were assessed in order to minimise them as far as was possible.

A condition of its use was that the reaction used to determine the correction must be a single electrode reaction obeying Tafel approximation, such as hydrogen evolution. By comparison with an aqueous sulphuric acid electrolyte, it was shown that for the methanol / acid electrolyte, although reduction of the methanol did occur, the dominating process was hydrogen evolution. Consequently, no difference was observed when the IR drop was determined using the methanol or the aqueous electrolytes.

Another possible source of error when using the ($I_{10} - I_1$) method was that conditions in that part of the electrolyte between the Luggin tip and the electrode surface differ from conditions in the bulk electrolyte. For instance, if there was a large concentration of ions close to the electrode surface the ohmic drop between the Luggin tip and the electrode would be lowered, ie. the local conductivity would increase. If the ion concentration changed with time, the IR drop would not be constant during an experiment.

A rather crude but effective method was devised to assess whether ion concentration was significant. Using the "H" cell, the IR drop was first determined in the usual way, then nitrobenzene was added to the electrolyte. Polarisation curves were measured under constant current conditions. For the first curve each point was determined by stepping the current from zero to the required value and immediately measuring the potential. The theory being that a significant concentration of ions would not have time to build up and affect the measured potential. The second curve was determined by slowly sweeping the current up and recording the potential. If ion formation was affecting the measurements then it was argued that at each current density the measured "apparent" electrode potentials would be significantly different for the two methods of determination. Figure B1 showed this was not the case.

A comparison between a steady state polarisation curve obtained using the equipment of Dr. J. Harrison with data obtained for the "H" cell using the ($I_{10} - I_1$) method is shown in figure B2. The average curves for the H-Cell are included for comparison. Note that the rate of mass transfer in the rotating disk cell was around 10 times that in the "H" cell. Also no significant preparative process occurred at the rotating disk, whereas the H-Cell results were averaged over a period when 10% conversion of nitrobenzene was taking place. Considering the large spread of polarisation results that was always obtained with the "H" cell and the similarity in the slopes of the linear portions of the polarisation curves, there seemed to be good agreement between the data.

On the basis of this indirect corroboration of the polarisation data obtained using the "H" Cell and in the absence of another method, it was concluded that, within acceptable experimental error, the ohmic correction of electrode potential in the "H" cell was accurate.

IR Correction Methods

Comparison of polarisation data obtained by steady state potential sweep and by potential step mesurements.

(55°C, copper electrode area = 12.6 cm^2, 0.3M nitrobenzene)

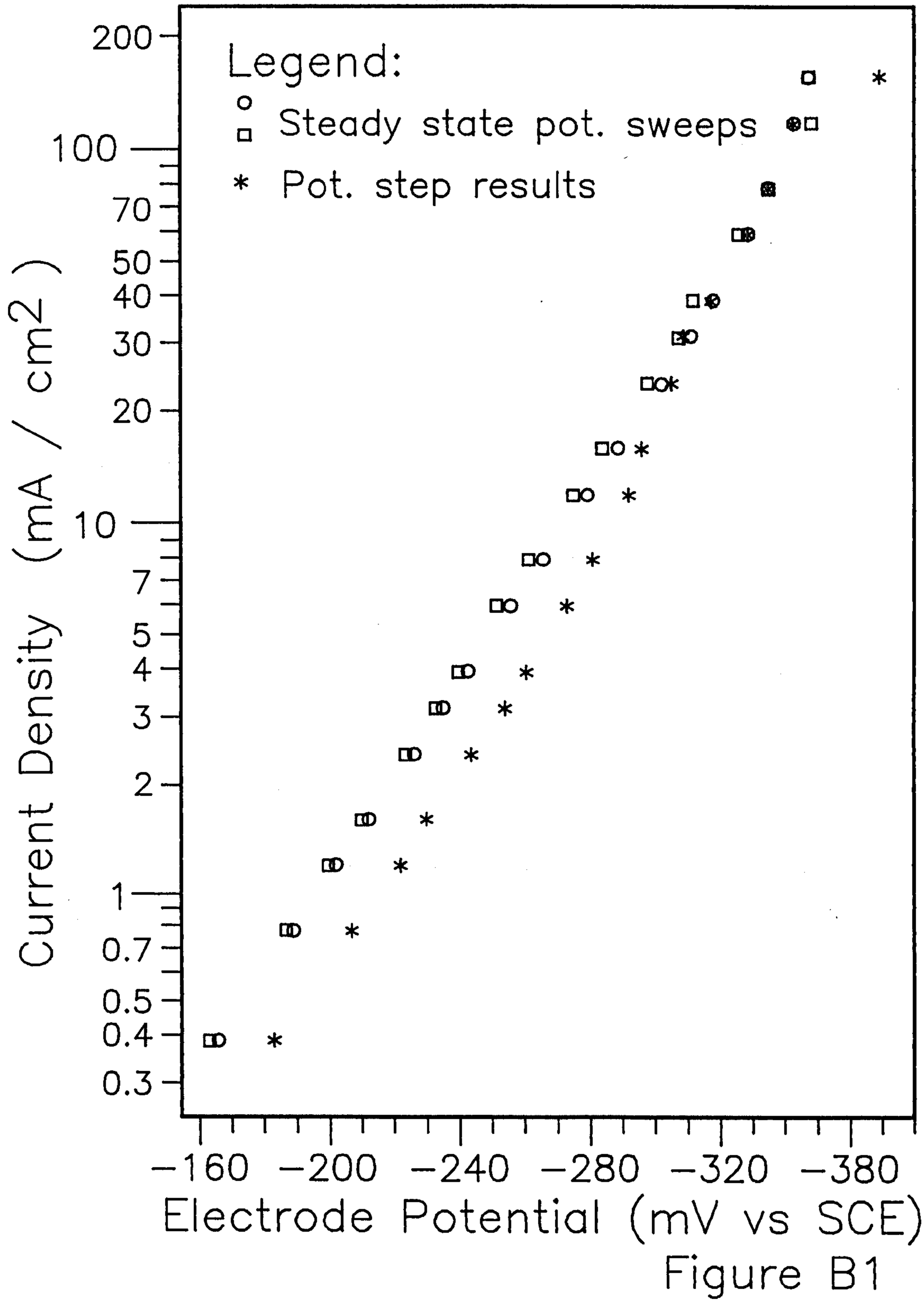

Figure B1

IR Correction Methods

Comparison between polarisation data for 0.3 M nitrobenzene at copper in rotating disk cell and H–Cell

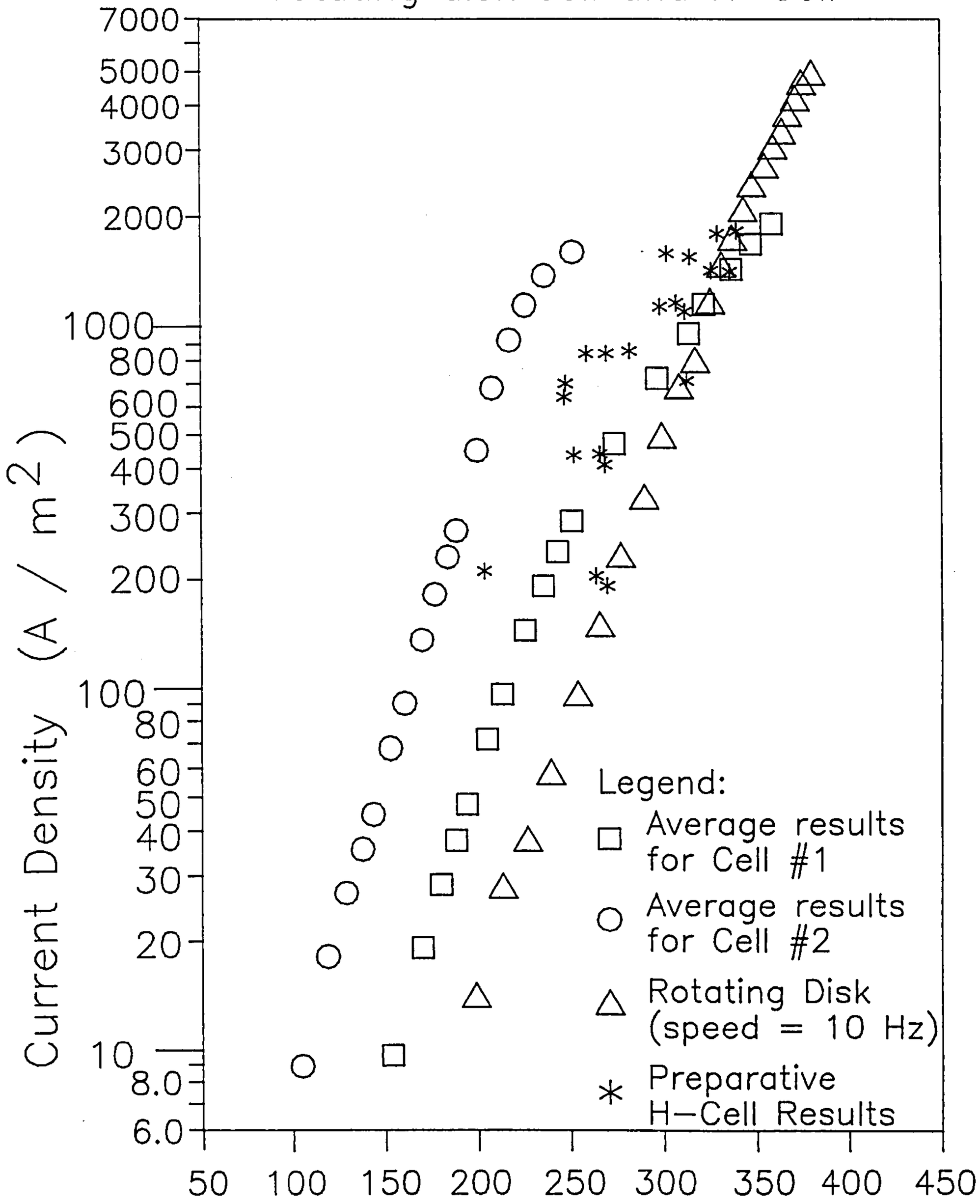

Figure B2

Appendix C.

The Derivation of the Kinetic Reaction Model

C1.0 Reaction Scheme

The reduction of nitrobenzene may be represented by the reaction scheme below. The nitrobenzene, "B", is transported to the electrode surface with flux N_A where it undergoes a four electron electrochemical reduction to phenylhydroxylamine, "B". The rate of this first electrochemical process is r_A. The intermediate may undergo further electrochemical reduction, this time a two electron process, to aniline, "D", which is then removed from the surface by mass transfer with a flux N_D. The rate of this secondary consecutive electrochemical reaction is r_{B2}. Alternatively, the intermediate may be removed from the electrode with flux N_B by mass transfer and be chemically rearranged in the bulk electrolyte to ortho- or para- anisidine or para- aminophenol, "C". The rate of the chemical step being r_{B1}. There is also a competing electrochemical process, namely hydrogen production, with a rate r_H.

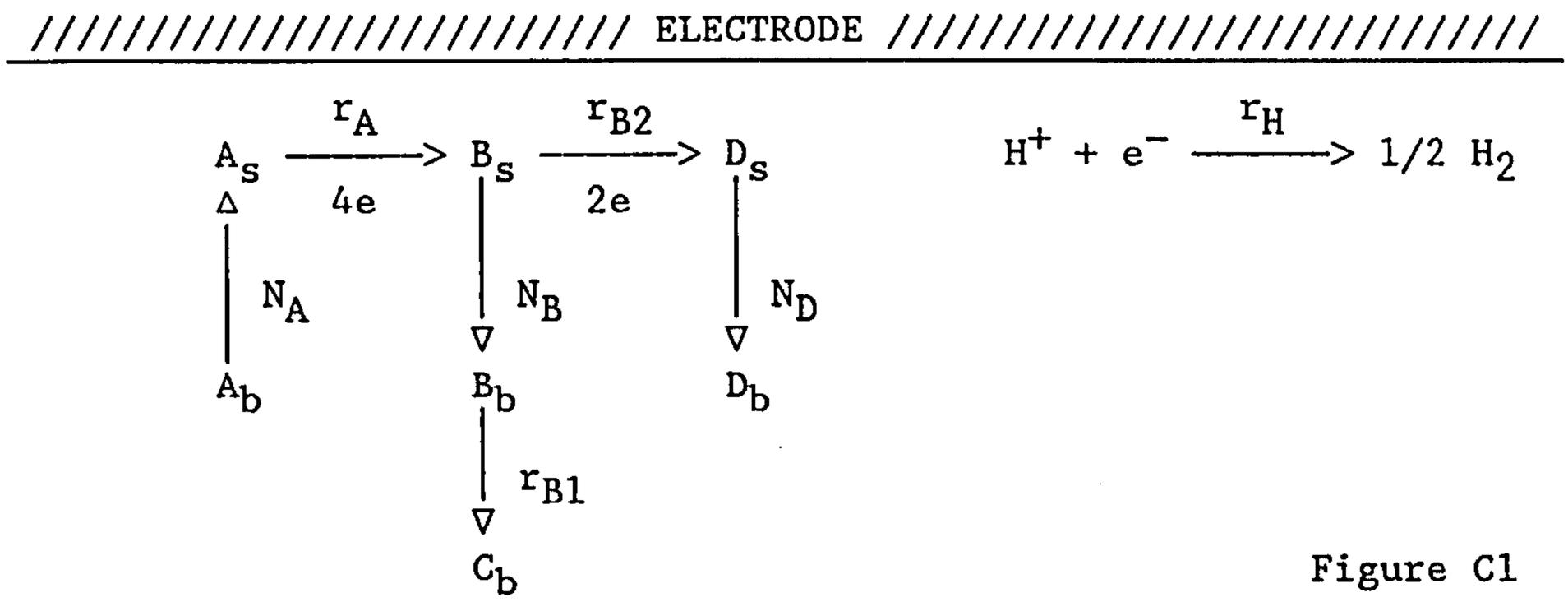

Figure C1

The subscripts b and s refer to the bulk electrolyte and to the region close to the electrode surface.

Before a model can be developed certain assumptions must be made. These are stated below, but are discussed in section 2.2.3.

C2.0 Assumptions

(i) All the individual electrochemical processes were assumed to be first order, irreversible and capable of being fully described by Tafel relationships.

(ii) Mass transport was assumed to be completely described by a single mass transfer coefficient, applicable for all species.

(iii) Steady state conditions were assumed for all processes.

(iv) No accumulation of reactants or reaction products was assumed to occur at the electrode surface

(v) The concentration of the intermediate, B, in the bulk electrolyte was assumed to be small compared to its concentration in the region close to the electrode surface.

(vi) The rate of chemical rearrangement was assumed to be small compared to the rate of mass transfer of the intermediate away from the electrode surface.

C3.0 Derivation

From assumptions (iii) and (iv) it follows that dA_s/dt, dB_s/dt, and dB_b/dt are negligible compared to the other processes, N_A for example. Thus:

$$N_A = r_A \tag{C1}$$

$$N_B = r_{B1} \tag{C2}$$

and $$r_A = r_{B1} + r_{B2} \tag{C3}$$

Now, noting assumption (ii):

$$N_A = k_L([A]_b - [A]_s) \qquad (C4)$$

where k_L is an individual mass transfer coefficient, the square brackets signify concentration of a species and the subscripts b and s to the bulk and surface respectively.

Furthermore, denoting the partial current density for the production of B by i_A, it follows that:

$$i_A = 4.F.r_A \qquad (C5)$$

In addition, from assumption (i):

$$i_A = k_A[A]_s e^{-b_A\phi} \qquad (C6)$$

From equation (C1) and (C5), equation (C4) becomes:

$$i_A / 4F = k_L([A]_b - [A]_s) \qquad (C7)$$

Eliminating $[A]_s$ from (C6) and (C7) leads to:

$$i_A / 4Fk_L = [A]_b - i_A / k_A e^{-b_A\phi}$$

$$\text{or} \qquad i_A = \frac{[A]_b}{\frac{1}{4Fk_L} + \frac{1}{k_A e^{-b_A\phi}}} \qquad (C8)$$

From equation (C2) and (C3)

$$r_A = N_B + r_{B2} \qquad (C9)$$

However, noting assumption (ii)

$$N_B = k_L([B]_b - [B]_s) \qquad (C10)$$

Assumption (v) states that $[B]_b$ can be ignored in comparison with $[B]_s$, hence equation (C10) becomes:

$$N_B = k_L[B]_s \qquad (C11)$$

Furthermore,

$$r_{B2} = i_B / 2F \qquad (C12)$$

where i_B is the partial current density associated with the $2e^-$ reduction of B to D.

From (C5), (C9), (C11) and (C12) it follows that:

$$i_A / 4F = k_L[B]_s + i_B / 2F \qquad (C13)$$

Following the first assumption and using a Tafel relationship for i_B, thus

$$i_B = k_B[B]_s e^{-b_B\phi} \qquad (C14)$$

and equation (C13) becomes:

$$i_A / 4F = k_L[B]_s + k_B[B]_s e^{-b_B\phi} / 2F$$

from which:

$$[B]_s = \frac{i_A}{4Fk_L + 2k_B e^{-b_B\phi}} \qquad (C15)$$

and therefore, from (C14):

$$i_B = i_A \left[\frac{k_B e^{-b_B\phi}}{4Fk_L + 2k_B e^{-b_B\phi}} \right] \qquad (C16)$$

Considering the hydrogen evolution, noting assumption (1):

$$i_H = k_H e^{-b_H\phi} \qquad (C17)$$

The total current,i, is simply:

$$i = i_A + i_B + i_H$$

and thus:

$$i = \left[\frac{[A]_b}{\frac{1}{4Fk_L} + \frac{1}{k_A e^{-b_A \phi}}} \right] \left[\frac{4Fk_L + 3k_b e^{-b_B \phi}}{4Fk_L + 2k_b e^{-b_B \phi}} \right] + k_H e^{-b_H \phi} \qquad \text{(C18)}$$

APPENDIX D

Estimation of Hydrogen Production During Experiments

In an attempt to explain the "lost" current during experiments, it was suggested that hydrogen evolution could be responsible. To investigate this an experiment was carried out in an H-Cell modified to allow measurement of any gas produced at the cathode. This appendix describes that experiment.

D1.0 Apparatus

A standard H-Cell, such as described in section 2.1.2, was modified by using a tight fitting greased lid for the catholyte compartment. The cathode was inserted through a septum and a collar screwed down to secure it. A gas collection port was provided in the lid, from which the gas was collected in a burette and its volume measured. The system was calibrated by using an aqueous H_2SO_4 electrolyte and passing a known constant current. Since the current efficiency is 100% for H_2 evolution, the number of coulombs required to collect a unit volume of gas can be determined. Stirring was by means of a magnetic follower.

D2.0 Conditions

Cell:		Modified H-Cell
Membrane:		Ionac - 3470
Electrodes -	cathode:	10 cm^2 copper plate
-	anode:	Graphite rod ($\approx$ 15 cm^2)
Electrolyte -	catholyte:	Methanol / 10% H_2SO_4 / 0.3 M nitrobenzene
-	anolyte:	Methanol / 10% H_2SO_4
Electrolyte agitation:		Catholyte stirring by magnetic stirrer and follower, anolyte by gas evolution.
Temperature:		55^oC
Type of Experiment:		Measurement of gas evolution.

Comments: Experiments were run at two different current densities under conditions of constant current. Potential was not recorded.

D3.0 Results

From the measurements of the volume of gas produced during the experiment and the calibration, the coulombs of gas produces was calculated. HPLC and TA analysis was used for the nitrobenzene reduction products and the current efficiencies for all products calculated:

Table D1.0 Hydrogen Evolution in H-Cell

Time (hrs)	Coulombs Passed	Current Density (mA/cm^2)	Current Efficiencies					
			p-anis.	o-anis.	p-a-p	Aniline	Total Organic	Hydrogen
0	0	158.2	0.0%	0.0%	0.0%	0.0%	0.0%	0.0%
1	6757	158.2	-	-	-	-	-	0.79%
2	12465	158.2	48.0%	8.4%	14.2%	15.1%	85.7%	1.6%
0	0	45.2	0.0%	0.0%	0.0%	0.0%	0.0%	0.0%
4.5	7956	45.2	55.0%	9.4%	16.5%	8.7%	89.6%	0.3%

D4.0 Conclusions

It is clear from the table above that hydrogen evolution is almost negligible even at the relatively high current density. The conclusion is that hydrogen evolution does occur to a small extent at current densities between 45 and 160 mA/cm^2 but that this is insignificant compared to the the other products formed. This is in agreement with the polarisation data, where, over the range of potentials used in the H-Cell, the hydrogen evolution current is negligible (Chapter 2.0).

Appendix E.

Methods of Determination of the Kinetic Constants

The determination of the kinetic constants (k_A, k_B, k_H, b_A, b_B and b_H) used in the reaction model from the experimental results required some algebraic manipulation of the model. This appendix details those manipulations and is the basis for the calculations in sections 2.3.1 and 2.3.3.

E1.0 Section 2.3.1 - Polarisation Studies - Determination of b_H, k_H and b_A

A) Hydrogen Evolution

Plotting the log. of current density against potential for the background, hydrogen evolution, reaction should give a straight line according to equation (C17):

$$i_H = k_H e^{-b_H \phi} \qquad \text{(E1)}$$

The slope is simply $-b_B$ and the intercept k_H.

B) Nitrobenzene Reduction

Consider the model behaviour when mass transport becomes negligible compared to the kinetic contribution, in other words when the reactions are under activation control at very low potentials:

At very low potentials,

$$\frac{1}{4Fk_L} \ll \frac{1}{k_A e^{-b_A \phi}} \quad \text{and} \quad 4Fk_L \ll k_b e^{-b_B \phi} \qquad \text{(E2)}$$

Noting that $i_H = 0$, equation (C18) then reduces to:

$$\frac{i}{[A]_b} = k_A e^{-b_A \phi}$$

and hence:

$$\log \left[\frac{i}{[A]_b} \right] = \log k_A - b_A \phi \qquad \text{(E3)}$$

From a plot of the left-hand side of this equation against electrode potential, b_A may be found from the slope of the straight line.

In order to use this relationship to calculate k_A, there must be significant product formation at the electrode (see section 2.3.1). At such low potentials and at a small rotating disk electrode, however, there is only a small current flowing and a negligible product formation. This approach was therefore unsuitable for the determination of k_A.

The assumption implicit in this simplification is that the rate of mass transfer is sufficiently high for the limits in (E2) to apply. In practice the speeds of disk rotation used were sufficient to make this assumption valid. For a rotation speed of 40 Hz, for example, the mass transfer coefficient was 8.8×10^{-5} m/s. Thus $4Fk_L = 34000$. From experimental data, at an electrode potential of −300 mV, $k_A e^{-b_A \phi} = 8.3 \times 10^{-6}$ and $k_A e^{-b_A \phi} = 2.0 \times 10^{-5}$. Clearly the assumption was valid.

E2.0 Section 2.3.3 – Preparative Study – Determination of k_A, b_B and k_B

Determination of the remaining constants requires the knowledge of the partial current densities or their ratio i_A/i_B at different potentials. This ratio can be calculated from the experimental preparative results by use of the following argument.

Referring to the model derivation in appendix C and figure C1, the rate of nitrobenzene conversion, r_A is given by:

r_A = Production rate of 4e products + Production rate of aniline

ie. $r_A = N_B + r_{B2}$

Noting from equation (C5), appendix C that $i_A = 4Fr_A$ it follows that:

i_A = 4F x production rate of all the products

Similarly from equation (C12), $i_B = 2Fr_{B2}$ and hence:

i_B = 2F x production rate of aniline

The discussion in appendix A highlighted the problems in product analysis encountered during the present work. The conclusion was reached that although the measured product concentrations were not equal to their true concentrations, there were proportional to them and so,

$i_A \propto$ 4F x measured production rate of all the products

and

$i_B \propto$ 2F x measured production rate of aniline

Thus:

$$\frac{i_A}{i_B} = \frac{\text{2 x measured production rate (total products)}}{\text{measured production rate (aniline)}} \qquad \text{(E4)}$$

Since hydrogen evolution was negligible the total current density, i, is given by:

$$i = i_A + i_B$$

and hence,

$$i_A = \frac{i}{\left\{\frac{i_B}{i_A} + 1\right\}} \quad \text{and} \quad i_B = \frac{i}{\left\{\frac{i_A}{i_B} + 1\right\}} \qquad \text{(E5)}$$

Having determined the ratio i_A / i_B at various electrode potentials, the equation (E6) derived below may be used to determine the kinetic constants for the secondary consecutive reaction, namely b_B and k_B.

Rearranging equation (C16):

$$\frac{i_A}{i_B} = \frac{4Fk_L + 2k_Be^{-b_B\phi}}{k_Be^{-b_B\phi}} = \frac{4Fk_L}{k_Be^{-b_B\phi}} + 2$$

Hence,

$$\frac{i_A}{i_B} - 2 = \frac{4Fk_L}{k_B} e^{b_B\phi} \qquad (E6)$$

and therefore,

$$\log\left[\frac{i_A}{i_B} - 2\right] = \log\left[\frac{4Fk_L}{k_B}\right] + b_B\phi \qquad (E7)$$

Thus plotting the LHS against electrode potential, ϕ, should give a straight line of slope b_B and intercept $4Fk_L / k_B$.

The remaining constant to be determined is k_A. For reasons explained in the discussion (Section 2.3.1), results from the preparative experiments must be used in determining k_A. Rearrangement of equation (C8) gives:

$$\text{or} \qquad Y = \frac{1}{\frac{1}{i_A} + \frac{1}{4.F.k_L.[A]_b}} = k_A.[A]_b.e^{-b_A\phi} \qquad (E8)$$

Noting i_A from equation (E5) above, Y can be calculated and plotted against $e^{-b_A\phi}$ to give a straight line through the origin with slope $k_A.[A]_b$.

Appendix F.

Mass Transport Considerations

F1.0 Mass Transport in the H-Cell

Early designs of the "H" cell incorporated a magnetic follower to ensure electrolyte agitation. This was found to be unsatisfactory because of both unreliability and a very low rate of mass transfer. Subsequently, and for all the preparative experiments used to determine the kinetic constants for the model, a propeller type stirrer was inserted through the top of the cell. This arrangement ensured a good rate of catholyte agitation and was very reproducible. To correlate the results obtained using the "H" cell, the mass transfer coefficient had to be determined. The method used is described in this appendix.

F1.1 Determination of the Mass Transfer Coefficient

The individual mass transfer coefficient for the transport to and from an electrode depends primarily on the cell design. It is a characteristic of a particular cell. Two similar "H" cells were used for the experiments and the coefficient was determined for each of them. The well known limiting current method was used, both for the nitrobenzene reduction and also using the well defined copper deposition reaction. The method is well known and has been extensively reported in the literature, the reader is referred to a standard text such as Bard and Faulkner[77] for a more detailed approach, than can be attempted here.

F1.2 Theory of the Limiting Current Method

Considering a simple electrode reaction, by a simple mass balance under steady state conditions it can be shown that the current, I, is given

by:

$$I = nFAk_L(C_b - C_s) \qquad (F2)$$

Under mass transfer limiting conditions, the rate of the electrochemical process is very fast compared to mass transport. Thus every molecule of the electroactive species that is transported to the electrode surface is immediately consumed by the electrochemical reaction. The surface concentration, C_s, becomes zero and the limiting current density, i_{lim}, is given by:

$$i_{lim} = nFk_L C_b \qquad (F1)$$

Thus by investigating the limiting current behaviour for a known reaction, the mass transfer coefficient may be determined.

F1.3 The Copper Deposition Reaction

The deposition of copper from aqueous acidic $CuSO_4$ solution was chosen as a model reaction for the determination of the mass transfer coefficients in the "H" cells. The main reasons were that the process was cathodic and that the same copper electrode which was used for the nitrobenzene reduction could be employed, making mass transport conditions the same for both cases. The copper deposition reaction is also a relatively fast process and was expected to produce well defined limiting current plateaus at potentials considerably less than the hydrogen overpotential.

F1.3.1 Method

Two different concentrations of $CuSO_4$ were used 0.1 and 0.2 mol/l. With the potentiostat working under potentiostatic conditions, the potential was slowly swept from -100 to -600 mV, whilst the current was recorded. When a current plateau was found, the stirring rate was increased from its usual level. Finding a new plateau at an increased current density confirmed that the plateau was due to mass transfer limitation. In this way

the limiting currents were determined for each "H" cell that was used and for each concentration of $CuSO_4$.

F1.3.2 Results

From the measured limiting currents, the mass transfer coefficient was determined according to equation (F1), noting that the deposition of copper is a two electron process:

	Cell No. 1		Cell No. 2	
$CuSO_4$ Concentration (mol / l)	0.1	0.2	0.1	0.2
Limiting Current, i_{lim} (mA / cm^2)	7.63	15.6	8.15	17.2
Mass Transfer Coefficient, k_L, (cm / s x 10^4)	3.96	4.04	4.22	4.46
	Average: 4.00		Average: 4.34	

There being only a small difference between the two cells the average value of 4.17 x 10^{-6} m /s was taken as the mass transfer coefficient for the "H" cells used. The aqueous $CuSO_4$ electrolytes used differed considerably to the 0.3M nitrobenzene in methanol / 10% sulphuric acid, which was used for the preparative experiments in the "H" cells. To take account of this the well known generalised correlation[78] between liquid phase mass transfer coefficients and physical properties of the solution was used to correct the measured value. The correlation states:

$$Sh = aRe^{b}Sc^{1/3}$$

Where Sh is the Sherwood no. = $k_L d_e/D$

Re is the Reynolds no. = $d_e U\rho/\mu$

Sc is the Schmidt no. = $\mu/\rho D$

The relevant data for the two electrolytes:

	$CuSO_4$ / H_2SO_4 / H_2O	$PhNO_2$ / H_2SO_4 / MeOH
	20°C	55°C
Density, (g/cm^3)	1.186	0.920
Viscosity, (cp)	1.1	1.27

Diffusivity, D (cm^2/s)	1.76×10^{-6}	1.10×10^{-5} (exp. value see sect. 2.3.1)

Using the above data, the value of 1.61×10^{-5} m /s was obtained for the mass transfer coefficient in the "H" cell under the conditions of the preparative experiments.

F1.4 Nitrobenzene Reduction

A limiting current plateau was never established when using the "H" cell equipment since it was "hidden" by hydrogen evolution, however it was possible to estimate a value from the polarisation curves by extrapolation. Considering the polarisation curves reported in section 2.3.3, it appeared that all the curves were approaching a limiting current plateau at around 300 mA / cm^2. It is clear from the model that any mass transfer limiting current would be associated with a transfer of six electrons. Noting this the value of the limiting current thus gave an estimated mass transfer coefficient of 1.55×10^{-5} m /s, by the analysis above.

A further estimate was obtained from the plot of the partial current densities determined from the "H" cell preparative work. Figure 2.25 in section 2.3.3 shows the two partial currents plotted against electrode potential. The partial current for the first electrochemical process, i_A, seemed to approach a limiting value of 200 mA/cm^2. Since this reaction is a four electron process, treatment of this current as mass transfer limited gave a value for the mass transfer coefficient of 1.60×10^{-5} m /s.

F1.5 Conclusions

The three estimates for the local mass transfer coefficient for the "H" cell agreed very well. An average of them was taken as the value used in the model for determining the kinetic constants. This average gave:

$$k_L = 1.60 \times 10^{-5} \text{ m /s}$$

F2.0 Mass Transport in Parallel Plate and Packed Bed Cell

The mass transfer coefficients for the parallel plate and packed bed cell designs were estimated by using the appropriate correlations. Inherent in these correlations are assumptions which limit the application and accuracy of the coefficients so calculated. As a first approximation the mass transfer in the fluidised bed cell was assumed to be equal to the packed-bed for the Reynolds numbers used.

F2.1 Parallel Plate Cell

The correlation used, from Mamoor et al.[74] was derived for fully developed flow in a rectangular duct similar to the parallel plate cell used. The correlation states:

$$Sh = 0.014.Re^{0.86}.Sc^{1/3}$$

Where the Sherwood, Reynolds and Schmidt numbers are as defined above (F1.3.2).

For the conditions used in an experiment, Sc = 12550

Re = 966 for 4.00 l/min (IPP-1&2)
1250 for 5.17 l/min (PP-1)
5216 for 21.6 l/min (PP-2)
4781 for 19.8 l/min (MPP-1)

Sh = $340910k_L$

noting that the equivalent diameter of a rectangular d_e is given by:

$$d_e = \frac{4 \times \text{Free Area for Flow}}{\text{Wetted Perimeter}} = \frac{4 \times \text{width} \times \text{depth}}{2 \times (\text{width} + \text{depth})}$$

From this data k_L was estimated to be:

$k_L = 3.52 \times 10^{-6}$	m/s	IPP-1, -2
$k_L = 4.40 \times 10^{-6}$	m/s	PP-1
$k_L = 1.50 \times 10^{-5}$	m/s	PP-2
$k_L = 1.40 \times 10^{-5}$	m/s	MPP-1

F2.2 Packed Bed Cell

Coeuret[80] gives a correlation for packed bed mass transport as:

$$Sh_p = 5.4.Re_p^{1/3}.Sc^{1/4}$$

Where the subscript, $_p$, refers to "particle" and thus: $Sh_p = k_L d_p/D$

$Re_p = d_p U\rho/\mu$

$Sc = \mu/\rho D$

For the conditions used, $Sc = 12550$

$Re_p = 28.32$ for 4.0 l/min (IPB-1)

67.25 for 9.50 l/min (PB-1 and PB-2)

70.85 for 11.0 l/min (MPB-1)

$Sh = 10000k_L$ (PP-1 and PP-2)

$= 9091k_L$ (MPB-1)

From this data k_L was estimated to be:

$k_L = 1.74 \times 10^{-4}$	m/s	IPB-1
$k_L = 2.32 \times 10^{-4}$	m/s	PB-1
$k_L = 2.32 \times 10^{-4}$	m/s	PB-2
$k_L = 2.60 \times 10^{-4}$	m/s	MPB-1

Using the same correlation for an idea of the mass transfer in the fluidised bed cell gives:

$k_L = 2.24 \times 10^{-4}$	m/s	FB-1
$k_L = 2.18 \times 10^{-4}$	m/s	FB-2
$k_L = 2.31 \times 10^{-4}$	m/s	MFB-1

APPENDIX G

Tabulated Results For Chapter Two

In this appendix the full experimental conditions for all the work behind chapter two are detailed together with any relevant comments. In addition all experimental data, except for polarisation curves, is tabulated. Where appropriate the table numbers refer directly to the figure number in chapter two. Thus table G2.8 refers to figure 2.8.

G1.0 Initial Polarisation Data (section 2.2.2)

Polarisation curve for reduction of nitrobenzene at a copper electrode at 55 ^{o}C (Figure 2.7).

Cell:		H-Cell (see section 2.1.2)
Membrane:		Nafion
Electrodes	- cathode:	1 cm^2 copper plate
	- anode:	Graphite rod ($\approx$ 15 cm^2)
Electrolyte	- catholyte:	Methanol / 10% H_2SO_4 / 0.3 M nitrobenzene
	- anolyte:	Methanol / 10% H_2SO_4
Electrolyte agitation:		Catholyte stirring by magnetic stirrer and follower, anolyte by gas evolution.
Temperature:		55^{o}C
Type of Experiment:		Steady state potential sweeps, with and without nitrobenzene. Results are averaged between data recorded as potentials are swept more cathodically and data recorded on the return sweep.
Comments:		Correction for IR drop not required since the small electrode area meant that currents were small and thus the correction also small.

G2.0 Polarisation Studies - determination of b_H and k_H (section 2.3.1)

The polarisation curve for a copper electrode in methanol / 10% H_2SO_4 at 55 ^oC (Figure 2.11).

Cell:	Rotating Disk Cell (J.A.H) (Section 2.1.1)
Membrane:	Porous Frit
Electrodes - cathode:	0.196 cm^2 copper disk
- anode:	Platinum Foil ($\approx$ 2 cm^2)
Electrolyte - catholyte:	Methanol / 10% H_2SO_4
- anolyte:	Methanol / 10% H_2SO_4
Electrolyte agitation:	Catholyte stirring by rotating disk assembly.
Temperature:	55^oC
Type of Experiment:	Steady state linear potential sweep with high frequency impedance measurement
Comments:	IR drop determined and corrected for at each potential.

Figure 2.11 gives slope and intercept and hence:

$$b_H = 0.359\ mV^{-1}$$

$$k_H = 1.01 \times 10^{-10}\ A/m^2 \text{ per kmol/l}$$

G2.1 Polarisation Studies - Determination of D and b_A (section 2.3.1)

Polarisation curves for the reduction of nitrobenzene at a copper electrode at 20 and 55 ^oC in methanol / H_2SO_4 (Figures 2.12, 2.13 and 2.14.

Cell:	Rotating Disk Cell (J.A.H) (Section 2.1.1)
Membrane:	Porous Frit
Electrodes - cathode:	0.196 cm^2 copper disk
- anode:	Platinum Foil ($\approx$ 2 cm^2)
Electrolyte - catholyte:	Methanol / 10% H_2SO_4 / 0.3 or 0.03 M nitrobenzene
- anolyte:	Methanol / 10% H_2SO_4
Electrolyte agitation:	Catholyte stirring by rotating disk assembly at two different rotation speeds 10 and 40 Hz.
Temperature:	20^oC and 55^oC

Type of Experiment: Steady state linear potential sweep with or without high frequency impedance measurement

Comments: IR drop determined and corrected for at each potential when impedance method used, otherwise IR drop was determined at the start and the same value used for all potentials.

Figures 2.12 and 2.13 give the mass transfer limiting currents, i_{lim}, for 20 and 55 ^{o}C and 0.03 M nitrobenzene concentration ($[A]_b$):

20 ^{o}C, 10z:	i_{lim} = 580 A/m^2	(Frequency response)
20 ^{o}C, 10z	i_{lim} = 630 A/m^2	(Linear potential sweep)
20 ^{o}C, 40z:	i_{lim} = 1185 A/m^2	(Frequency response)
20 ^{o}C, 40z:	i_{lim} = 1190 A/m^2	(Linear potential sweep)
55 ^{o}C, 10z:	i_{lim} = 880 A/m^2	(Frequency response)
55 ^{o}C, 40z:	i_{lim} = 1600 A/m^2	(Frequency response)

Equation (D5), appendix D gives $k_L = i_{lim} / 6.F.[A]_b$. Noting that $[A]_b$ = 0.03 $kmol/m^3$ and that k_L is given by equation (D2), also from appendix D, where ν = 0.019 cm^2/s at 20 ^{o}C and = 0.0138 cm^2/s at 55 ^{o}C; ω = 62.8 rad/s (10 Hz) or 251.3 rad/s (40 Hz):

$$k_L = 0.62 D^{2/3} \nu^{-1/6} \omega^{1/2}$$

From which the the diffusivity, D was calculated:

20 ^{o}C, 10z:	D = 7.01×10^{-6}	
20 ^{o}C, 40z:	D = 6.82×10^{-6}	Average: 6.9×10^{-6} cm^2/s
55 ^{o}C, 10z:	D = 1.14×10^{-5}	
55 ^{o}C, 40z:	D = 9.84×10^{-6}	Average: 1.1×10^{-5} cm^2/s

Table G2.15 Polarisation Curve for Nitrobenzene Reduction at Low Potentials

Determination of Kinetic Constant, b_A according to the method outlined in appendix E2.0.

Cathode Potential ϕ (mV vs SCE)	i / $[A]_b$ (A/m^2 per $kmol/m^3$) at nitrobenzene concentrations, $[A]_b$, of 0.03 and 0.3 $kmol/m^3$ and rotating disk speeds 10 and 40 Hz			
	0.03 M 10 Hz	0.03 M 40 Hz	0.3 M 10 Hz	0.3 M 40 Hz
200	24.70		4.67	1.50
215			9.33	3.00
220	43.30	4.33		
228			12.70	4.67
240	83.30	8.00	19.30	6.17
255			31.70	9.50
260	153.30	16.70		
266			48.30	
268				17.33
278			76.70	
280	286.70	36.00		
282				31.70
290			110.00	
294				58.30
300	500.00	75.00	163.30	

From figure 2.15 slope = 0.0348 mV^{-1} = b_A

G3.0 Preparative Study – Determination of k_A, b_B and k_B (section 2.3.3)

The effect of current density on the product formation during the reduction of nitrobenzene at a copper electrode in methanol/ H_2SO_4 at 55 ^oC and the effect on the electrode potential during a preparative process.

Cell:	H – Cell (Section 2.1.2)
Membrane:	Ionac – 3470
Electrodes – cathode:	10 – 10.4 cm^2 copper plate
– anode:	Graphite rod (≈ 15 cm^2)
Electrolyte – catholyte:	Methanol / 10% H_2SO_4 / 0.333 M nitrobenzene
– anolyte:	Methanol / 10% H_2SO_4
Electrolyte agitation:	Catholyte stirring by mechanical stirrer at constant rate. Anolyte by gas evolution.
Temperature:	55^oC

Type of Experiment: Bulk electrolysis by passage of 5000 coulombs at constant current density (< 10% $PhNO_2$ conversion). Electrode potential recorded continuously and time averaged.

Comments: IR drop determined from an initial background electrolysis using the ($I_{10} - I_1$) method (appendix B). Averaged potential corrected using this value

Table G2.22 (2.23) H-Cell Preparative Results

The effect of current density on the electrode potential and the formation of products in the reduction of nitrobenzene at a copper electrode in methanol / H_2SO_4.

Cathode Potential	Reaction Products (moles x 10^3)						Current Density
	4e			6e	Total	Total	
ϕ mV vs SCE	o-anisidine	p-anisidine	p-aminophenol	aniline	4e		i (A/ m^2)
217	1.46	6.22	1.76	0.3	9.44	9.74	252
256	1.24	5.73	1.47	0.39	8.44	8.83	704
258	1.37	6.3	1.64	0.54	9.31	9.85	756
262	1.4	6.27	1.72	0.24	9.39	9.63	504
268	1.27	5.76	1.71	0.65	8.74	9.39	895
274	1.5	6.67	1.93	0.2	10.1	10.3	252
276	1.48	6.65	1.7	0.19	9.83	10.02	508
279	1.19	5.86	1.53	0.2	8.58	8.78	239
279	1.32	6.56	1.68	0.14	9.56	9.7	478
279	1.09	4.94	1.39	1.08	7.42	8.5	894
291	1.13	5.58	1.65	0.89	8.36	9.25	910
307	1.19	5.49	1.48	0.94	8.16	9.1	1190
311	0.83	3.75	1.11	2.07	5.69	7.76	1591
316	1.23	5.68	1.54	0.74	8.45	9.19	1190
320	1.1	5.06	1.46	0.95	7.62	8.57	1137
322	1.38	6.77	1.7	0.23	9.85	10.08	762
324	0.95	4.16	1.22	2.17	6.33	8.5	1567
334	1.1	4.87	1.29	1.27	7.26	8.53	1445
338	1.14	5.37	1.4	1.57	7.91	9.48	1778
344	1.07	4.68	1.41	1.63	7.16	8.79	1442
348	0.99	4.56	1.13	2.76	6.68	9.44	1818
372	0.86	3.18	1.16	2.28	5.2	7.48	2032
373	1.08	5.16	1.44	2.71	7.68	10.39	2032

Table G2.26 (2.27) H-Cell Preparative Results

Calculation of the partial current densities, i_A and i_B, and hence the determination of the kinetic constants k_A, b_B and k_B.

Cathode Potential ϕ (mV vs SCE)	Current Density i (A/ m^2)	Partial Current Densities (A/m^2)		$\frac{i_A}{i_B} - 2$	% total current due to kinetic resist.	Y^*	$e^{-b_A\phi}$ *
		i_A	i_B				
217	252	248.18	3.82	62.93	88%	283	1815
256	704	688.79	15.21	43.28	66%	1040	6992
258	756	735.83	20.17	34.48	64%	1152	7492
262	504	497.80	6.20	78.25	76%	659	8604
268	895	865.06	29.94	26.89	58%	1503	10588
274	252	249.58	2.42	101.00	88%	284	13029
276	508	503.23	4.77	103.47	75%	668	13962
279	239	236.31	2.69	85.80	88%	267	15488
279	478	474.58	3.42	136.57	77%	619	15488
279	894	840.60	53.40	13.74	59%	1431	15488
291	910	868.23	41.77	18.79	57%	1513	23454
307	1190	1131.56	58.44	17.36	44%	2544	40785
311	1591	1403.77	187.23	5.50	31%		
316	1190	1143.94	46.06	22.84	44%		
320	1137	1077.29	59.71	16.04	47%		
322	762	753.40	8.60	85.65	63%		
324	1567	1389.62	177.38	5.83	32%		
334	1445	1344.88	100.12	11.43	34%		
338	1778	1642.03	135.97	10.08	19%		
344	1442	1319.64	122.36	8.79	35%		
348	1818	1586.13	231.87	4.84	22%		
372	2032	1763.27	268.73	4.56	13%		
373	2032	1797.57	234.43	5.67	12%		

* For the determination of k_A only data in which mass transfer was not the dominant process was used ie. data where kinetic resistance was relatively dominant.

$$Y = \frac{1}{\frac{1}{i_A} - \frac{1}{4.F.k_L.[A]_b}} \quad \text{(see appendix E3.0)}$$

From figure 2.26, noting $k_L = 1.6 \times 10^{-5}$,

slope and intercept give: $b_B = 0.0208\ mV^{-1}$

$k_B = 0.505\ A/m^2$ per $kmol/m^3$

Figure 2.27 gives a slope = 0.063 and hence,
noting $[A]_b$ = 0.330 kmol/m^3: k_A = 0.191 A/m^2 per kmol/m^3

G4.0 Reaction Model Results – Comparison With H-Cell (section 2.4)

Comparison between the model predictions for the H-Cell and the actual results under the same conditions.

The curves in figures 2.28 to 2.31 were all calculated for the case of the H-Cell conditions using the model (see appendix C3.0) with the following values:

$b_A = 0.0348\ mV^{-1}$ $k_A = 0.191\ A/m^2$ per kmol/m^3
$b_B = 0.0208\ mV^{-1}$ $k_B = 0.505\ A/m^2$ per kmol/m^3
$b_H = 0.0359\ mV^{-1}$ $k_B = 1.01 \times 10^{-10}\ A/m^2$

$k_L = 1.6 \times 10^{-5}$ m/s
$F = 9.645 \times 10^7$ Coulombs/ kequiv.
$[A]_b = 0.330$ kmol/m^3

G5.0 Reaction Model Results – Effect of Mass Transport (section 2.4)

The model predictions for the effect of the mass transfer coefficient on the polarisation data and the rate of product formation.

The curves in figures 2.32 to 2.34 were calculated using the kinetic constants listed above except that $[A]_b$ = 0.333 kmol/m^3.

APPENDIX H

Tabulated Results For Chapter Three

This appendix contains the experimental conditions and the analysis results for the bench scale experiments described in chapter three. All the work was carried out in the cell described in section 3.1, with the modifications indicated there for the three different cell configurations used. Samples were taken throughout experiments and the results are tabulated such that each period between samples is treated separately. The average of these results, providing no effects of nitrobenzene conversion are noted, is then taken. In the tables, current efficiency, selectivity, chemical yield, space time yield and energy consumption are used as defined below:

$$\text{Current Efficiency (CE)} = \frac{\text{Coulombs Passed to Produce a Particular Product}}{\text{Total Coulombs Passed}} \times 100\%$$

Note: Coulombs passed = moles x no. of electrons transferred x 96500

$$\text{Selectivity (SE)} = \frac{\text{Moles of a Particular Product}}{\text{Total Moles of Products Formed}} \times 100\%$$

$$\text{Chemical Yield } (Y_C) = \frac{\text{Moles of a Particular Product}}{\text{Moles of Nitrobenzene Converted}} \times 100\%$$

Space Time Yield (Y_{ST}) (kmol/ hr/ m^3) = Yield of product per unit time per unit cell volume

= $a.i.Q_E.CE$ where a = geometric electrode area per unit volume of cell, i = current density, Q_E = amount of product per unit charge and CE = current efficiency.

$$\text{Energy Consumption } (E_c) \text{ (kWh / kmol)} = \frac{\text{Cell Voltage x number of electrons transferred}}{0.036 \times \text{Current Efficiency}}$$

H3.2.1(I) Initial Bench Scale Work - Experiments IPP-1, -2 and IPB-1.

First experiments carried out on parallel plate and packed bed electrodes.

Membrane:		Nafion
Electrodes -	cathode:	225 cm^2 copper plate / feeder (+ 1.1 mm diam. copper particles for IPB-1 bed height = 30 cm)
-	anode:	Graphite plate (≈ 260 cm^2)
Specific Area:		IPP-1 and IPP-2: 0.333 cm^{-1}
		IPB-1: 32.7 cm^{-1}
Electrolyte-	catholyte:	Methanol / 10% H_2SO_4 / 0.333 M nitrobenzene
-	anolyte:	Methanol / 10% H_2SO_4
Electrolyte Volume		
-	catholyte:	12 litres
-	anolyte:	10 litres
Electrolyte Flowrate		
-	catholyte:	4.0 l/min IPP-1, IPP-2 and IPB-1.
-	anolyte:	2.0 l/min
Estimated Mass Transfer Coefficient: (see appendix F)		IPP-1 and IPP-2: 3.52×10^{-6} m/s
		IPB-1: 1.74×10^{-4} m/s
Temperature:		55°C
Geometric Current Density:		100 mA/cm^2 for IPP-1, IPP-2 and IPB-1
Comments:		At the time of experimentation, para-aminophenol was not routinely analysed for as it was thought to be only a very minor product. Subsequent work revealed significant amounts of p-aminophenol were formed during experiments. In order to be able to compare these initial results with succeeding ones, a p-aminophenol production was calculated assuming that the ratio of this product to the total four electron products was the same as for the later work.

Table H3.2.1(I)a Experiments IPP-1, IPP-2 and IPB-1 - Product Analysis Results

Samp. No.	Coulombs Passed between Samples	Moles Products					
		p-anisidine	o-anisidine	p-aminophenol (calc.)	aniline	Total 4e-	Total 6e-
Experiment IPP-1 ($i = 100.0$ mA/cm^2 $V = 8.55$ Volts)							
1	92511	0.0390	0.0060	0.0079	0.0220	0.0529	0.0220
2	85659	0.0560	0.0100	0.0116	0.0180	0.0776	0.0180
3	85658	0.0670	0.0130	0.0141	0.0230	0.0941	0.0230
4	85659	0.0770	0.0140	0.0160	0.0330	0.1070	0.0330
5	85658	0.0660	0.0090	0.0132	0.0350	0.0882	0.0350
6	39403	0.0110	0.0020	0.0023	0.0070	0.0153	0.0070
Experiment IPP-2 ($i = 100.0$ mA/cm^2 $V = 8.64$ Volts)							
1	87372	0.0310	0.0050	0.0063	0.0160	0.0423	0.0160
2	83945	0.0700	0.0140	0.0148	0.0160	0.0988	0.0160
3	83945	0.0660	0.0120	0.0137	0.0230	0.0917	0.0230
4	83946	0.0840	0.0170	0.0178	0.0350	0.1188	0.0350
5	85658	0.0750	0.0150	0.0158	0.0350	0.1058	0.0350
6	82232	0.0540	0.0130	0.0118	0.0440	0.0788	0.0440
Experiment IPB-1 ($i = 100.0$ mA/cm^2 $V = 5.06$ Volts)							
1	87372	0.0160	0.0040	0.0035	0.0640	0.0235	0.0640
2	85658	0.0330	0.0050	0.0067	0.0700	0.0447	0.0700
3	85659	0.0390	0.0060	0.0079	0.0770	0.0529	0.0770
4	87371	0.0500	0.0060	0.0099	0.0890	0.0659	0.0890
5	83946	0.0480	0.0090	0.0100	0.0710	0.0670	0.0710
6	95937	0.0590	0.0090	0.0120	0.0960	0.0800	0.0960

Table H3.2.1(I)b Experiments IPP-1, IPP-2 and IPB-1 - Current Efficiencies

Samp. No.	Current Efficiencies (%)					
	p-anisidine	o-anisidine	p-aminophenol (calculated)	aniline	Total 4e-	Total 6e-
Experiment IPP-1 ($i = 100.0$ mA/cm^2 $V = 8.55$ Volts)						
1	16.27	2.50	3.30	13.77	22.07	13.77
2	25.23	4.51	5.23	12.17	34.97	12.17
3	30.19	5.86	6.35	15.55	42.40	15.55
4	34.70	6.31	7.21	22.31	48.22	22.31
5	29.74	4.06	5.95	23.66	39.75	23.66
6	10.78	1.96	2.25	10.29	14.99	10.29
Average:	24.49	4.20	5.05	16.29	33.73	16.29
Experiment IPP-2 ($i = 100.0$ mA/cm^2 $V = 8.64$ Volts)						
1	13.70	2.21	2.78	10.60	18.69	10.60
2	32.19	6.44	6.81	11.04	45.43	11.04
3	30.35	5.52	6.30	15.86	42.17	15.86
4	38.62	7.82	8.18	24.14	54.63	24.14
5	33.80	6.76	7.12	23.66	47.68	23.66
6	25.35	6.10	5.54	30.98	36.99	30.98
Average:	29.00	5.81	6.12	19.38	40.93	19.38
Experiment IPB-1 ($i = 100.0$ mA/cm^2 $V = 5.06$ Volts)						
1	7.07	1.77	1.55	42.41	10.38	42.41
2	14.87	2.25	3.02	47.32	20.14	47.32
3	17.57	2.70	3.56	52.05	23.84	52.05
4	22.09	2.65	4.37	58.98	29.11	58.98
5	22.07	4.14	4.60	48.97	30.81	48.97
6	23.74	3.62	4.83	57.94	32.19	57.94
Average:	17.90	2.86	3.65	51.28	24.41	51.28

Table H3.2.1(I)c Experiments IPP-1, IPP-2 and IPB-1 - Average Selectivities, Chemical and Space-Time Yields and Energy Consumption

Exp. No.	p-anisidine	o-anisidine	p-aminophenol (calculated)	aniline	Total 4e-	Total 6e-
	Selectivity					
IPP-1	54.29%	9.31%	11.20%	25.20%	74.80%	25.20%
IPP-2	53.92%	10.59%	11.34%	24.15%	75.85%	24.15%
IPB-1	29.61%	4.84%	6.06%	59.48%	40.52%	59.48%
	Chemical Yield					
IPP-1	31.52%	5.40%	6.50%	14.01%	43.41%	14.01%
IPP-2	41.86%	8.05%	8.77%	17.95%	58.68%	17.95%
IPB-1	30.40%	4.97%	6.22%	56.49%	41.59%	56.49%
	Space-Time Yield (kmol / hr / m^3)					
IPP-1	0.076	0.013	0.016	0.034	0.105	0.034
IPP-2	0.090	0.018	0.019	0.040	0.127	0.040
IPB-1	5.460	0.871	1.115	10.43	7.445	10.43
	Energy Consumption (kWh / kmol)					
IPP-1	4583	27040	22210	9582	3327	9582
IPP-2	3711	19660	17730	8734	2649	8734
IPB-1	3732	21310	17920	1666	2678	1666

H3.2.1 Parallel Plate Cell - Experiments PP-1 and PP-2.

Experiments carried out with a parallel plate electrode configuration at various current densities.

Membrane:		Ionac - 3470
Electrodes -	cathode:	281 cm^2 copper plate
-	anode:	Graphite plate ($\approx$ 260 cm^2)
Specific Area:		PP-1 and PP-2: 0.333 cm^{-1}
Electrolyte-	catholyte:	Methanol / 10% H_2SO_4 / 0.333 M nitrobenzene
-	anolyte:	Methanol / 10% H_2SO_4
Electrolyte Volume		
-	catholyte:	12 litres
-	anolyte:	10 litres (PP-1), 12 litres (PP-2)
Electrolyte Flowrate		
-	catholyte:	5.17 l/min PP-1, 21.6 l/min PP-2.
-	anolyte:	4.0 l/min.
Estimated Mass Transfer		
Coefficient:		PP-1: 4.40 x 10^{-6} m/s
(see appendix F)		PP-2: 1.50 x 10^{-5} m/s
Temperature:		55°C
Geometric Current		
Density:		57.0 mA/cm^2 for PP-1-A and PP-2-A
		113.0 mA/cm^2 for PP-1-B and PP-2-B
		227.0 mA/cm^2 for PP-1-C and PP-2-C
Comments:		

Table H3.2.1a Experiment PP-1 and PP-2 – Product Analysis Results

Samp. No.	Coulombs Passed between Samples	Moles Products					
		p-anisidine	o-anisidine	p-aminophenol	aniline	Total 4e-	Total 6e-
PP-1-A (i = 57.0 mA/cm^2 V = 6.60 V)							
1	45296	0.0242	0.0044	0.0086	0.0289	0.0372	0.0289
2	45999	0.0333	0.0059	0.0102	0.0273	0.0494	0.0273
3	46101	0.0341	0.0061	0.0109	0.0256	0.0511	0.0256
4	92138	0.0761	0.0109	0.0185	0.0471	0.1055	0.0471
PP-1-B (i = 113.0 mA/cm^2 V = 11.28 V)							
1	46820	0.0246	0.0055	0.0057	0.0355	0.0358	0.0355
2	44346	0.0315	0.0064	0.005	0.0405	0.0429	0.0405
3	45924	0.0245	0.0069	0.0065	0.0323	0.0379	0.0323
4	92054	0.0594	0.0082	0.0159	0.0677	0.0835	0.0677
PP-1-C (i = 227.0 mA/cm^2 V = 19.78 V)							
1	91563	0.0461	0.0048	0.0112	0.1105	0.0621	0.1105
2	45788	0.0158	0.0034	0.0021	0.0513	0.0213	0.0513
3	45724	0.0141	0.004	0.0028	0.0455	0.0209	0.0455
4	46174	0.014	0.0041	0.0053	0.0456	0.0234	0.0456
PP-2-A (i = 57.0 mA/cm^2 V = 6.83 V)							
1	22929	0.0332	0.0055	0.0034	0.0014	0.0421	0.0014
2	22968	0.0304	0.0048	0.0052	0.002	0.0404	0.002
3	30546	0.0425	0.007	0.0037	0.0021	0.0532	0.0021
4	38318	0.0508	0.009	0.0082	0.0063	0.068	0.0063
PP-2-B (i = 113.0 mA/cm^2 V = 11.69 V)							
1	22860	0.033	0.0038	0.0024	0.0048	0.0392	0.0048
2	22821	0.0323	0.0026	0.0027	0.0036	0.0376	0.0036
3	23013	0.0339	0.0068	0.0033	0.0051	0.044	0.0051
4	47027	0.0532	0.0102	0.0077	0.016	0.0711	0.016
PP-2-C (i = 227.0 mA/cm^2 V = 20.48 V)							
1	43580	0.0484	0.0104	0.008	0.0109	0.0668	0.0109
2	22919	0.0262	0.0068	0.0044	0.0106	0.0374	0.0106
3	22817	0.0197	0.0074	0.002	0.0073	0.0291	0.0073
4	22882	0.0269	0.0065	0.002	0.0116	0.0354	0.0116

Table H3.2.1b Experiment PP-1 and PP-2 - Current Efficiencies

Samp. No.	Current Efficiencies (%)					
	p-anisidine	o-anisidine	p-aminophenol	aniline	Total 4e-	Total 6e-
PP-1-A (i = 57 mA/cm^2)						
1	20.62	3.75	7.33	36.94	31.70	36.94
2	27.94	4.95	8.56	34.36	41.45	34.36
3	28.55	5.11	9.13	32.15	42.79	32.15
4	31.88	4.57	7.75	29.60	44.20	29.60
Average:	27.25	4.59	8.19	33.26	40.03	33.26
PP-1-B (i = 113 mA/cm^2)						
1	20.28	4.53	4.70	43.90	29.51	43.90
2	27.42	5.57	4.35	52.88	37.34	52.88
3	20.59	5.80	5.46	40.72	31.86	40.72
4	24.91	3.44	6.67	42.58	35.01	42.58
Average:	23.30	4.84	5.30	45.02	33.43	45.02
PP-1-C (i = 227 mA/cm^2)						
1	19.43	2.02	4.72	69.87	26.18	69.87
2	13.32	2.87	1.77	64.87	17.96	64.87
3	11.90	3.38	2.36	57.62	17.64	57.62
4	11.70	3.43	4.43	57.18	19.56	57.18
Average:	14.09	2.92	3.32	62.39	20.34	62.39

Table H3.2.1b Continued – Current Efficiencies

Samp. No.	Current Efficiencies (%)					
	p-anisidine	o-anisidine	p-aminophenol	aniline	Total 4e-	Total 6e-
PP-2-A (i = 57 mA/cm^2)						
1	55.89	9.26	5.72	3.54	70.87	3.54
2	51.09	8.07	8.74	5.04	67.90	5.04
3	53.71	8.85	4.68	3.98	67.23	3.98
4	51.17	9.07	8.26	9.52	68.50	9.52
Average:	52.97	8.81	6.85	5.52	68.62	5.52
PP-2-B (i = 113 mA/cm^2)						
1	55.72	6.42	4.05	12.16	66.19	12.16
2	54.63	4.40	4.57	9.13	63.60	9.13
3	56.86	11.41	5.54	12.83	73.80	12.83
4	43.67	8.37	6.32	19.70	58.36	19.70
Average:	52.72	7.65	5.12	13.46	65.49	13.46
PP-2-C (i = 227 mA/cm^2)						
1	42.87	9.21	7.09	14.48	59.17	14.48
2	44.13	11.45	7.41	26.78	62.99	26.78
3	33.33	12.52	3.38	18.52	49.23	18.52
4	45.38	10.96	3.37	29.35	59.72	29.35
Average:	41.42	11.04	5.31	22.28	57.78	22.28

Table H3.2.1c Experiments PP-1 and PP-2 - Average Selectivities, Chemical and Space-Time Yields and Energy Consumption.

Exp. No.	p-anisidine	o-anisidine	p-aminophenol	aniline	Total 4e-	Total 6e-
	Selectivity					
PP-1-A	43.59%	7.36%	13.16%	35.89%	64.11%	35.89%
PP-1-B	36.61%	7.66%	8.44%	47.28%	52.72%	47.28%
PP-1-C	22.50%	4.86%	5.32%	67.32%	32.68%	67.32%
PP-2-A	73.31%	12.18%	9.45%	5.05%	94.95%	5.05%
PP-2-B	70.88%	10.13%	6.89%	12.10%	87.90%	12.10%
PP-2-C	57.06%	15.43%	7.30%	20.21%	79.79%	20.21%
	Chemical Yield					
PP-1-A	41.34%	6.97%	12.43%	33.64%	60.73%	33.64%
PP-1-B	35.29%	7.32%	8.02%	45.45%	50.63%	45.45%
PP-1-C	21.35%	4.43%	5.03%	63.01%	30.81%	63.01%
	Space-Time Yield (kmol / hr / m^3)					
PP-1-A	0.0482	0.0081	0.0145	0.0393	0.0709	0.0393
PP-1-B	0.0818	0.0170	0.0186	0.1053	0.1173	0.1053
PP-1-C	0.0993	0.0206	0.0234	0.2932	0.1434	0.2932
PP-2-A	0.0938	0.0156	0.0121	0.0065	0.1215	0.0065
PP-2-B	0.1850	0.0268	0.0180	0.0315	0.2298	0.0315
PP-2-C	0.2920	0.0778	0.0375	0.1047	0.4073	0.1047
	Energy Consumption (kWh / kmol)					
PP-1-A	2762	16200	9018	3329	1864	3329
PP-1-B	5467	27050	24302	4217	3779	4217
PP-1-C	16260	78620	78320	5322	11080	5322
PP-2-A	1435	8638	11840	23830	1106	23830
PP-2-B	2492	19170	26128	15610	2000	15610
PP-2-C	5577	20880	49380	16590	3973	16590

H3.2.4 Packed Bed Cell - Experiments PB-1 and PB-2.

Experiments carried out with a parallel plate electrode configuration at various current densities.

Membrane:		Ionac - 3470
Electrodes -	cathode:	259 cm^2 copper feeder + 1.1 mm diam. copper particles. Bed height = 35 cm
-	anode:	Graphite plate (≈ 260 cm^2)
Specific Area:		PB-1 and PB-2: 32.7 cm^{-1}
Electrolyte-	catholyte:	Methanol / 10% H_2SO_4 / 0.333 M nitrobenzene
-	anolyte:	Methanol / 10% H_2SO_4
Electrolyte Volume		
-	catholyte:	14 litres (PB-1), 12 litres (PB-2)
-	anolyte:	10 litres
Electrolyte Flowrate		
-	catholyte:	9.50 l/min PB-1 and PB-2.
-	anolyte:	4.0 l/min.
Estimated Mass Transfer Coefficient: (see appendix F)		PB-2 and PB-1: 2.32 x 10^{-4} m/s
Temperature:		55°C
Geometric Current Density:		62.0 mA/cm^2 for PB-1-A and PB-2-A 124.0 mA/cm^2 for PB-1-B and PB-2-B 247.0 mA/cm^2 for PB-1-C and PB-2-C
Comments:		Nitrobenzene concentrations in samples was not measured. Three different current densities were used in each experiment. For PB-1 the experiment was started at the lowest current density and after 4 hrs was increased to 124 mA/cm^2 for a further two hours and finally 1 hr at the highest current density. For PB-2, this order was reversed ie. the highest current density was first etc.

Table H3.2.4a Experiment PB-1 and PB-2 - Product Analysis Results

Samp. No.	Coulombs Passed between Samples	Moles Products					
		p-anisidine	o-anisidine	p-aminophenol	aniline	Total 4e-	Total 6e-
PB-1-A (i = 62.0 mA/cm^2 V = 5.38 V)							
1	45986	0.0087	0.0007	0.0069	0.019	0.0163	0.019
2	45909	0.0234	0.0057	0.0036	0.0258	0.0327	0.0258
3	51789	0.0211	0.0041	0.0153	0.0202	0.0405	0.0202
4	40222	0.0116	0.0024	0.0042	0.0256	0.0182	0.0256
5	45781	0.0076	0.0029	0.0077	0.0448	0.0182	0.0448
PB-1-B (i = 124.0 mA/cm^2 V = 8.50 V)							
1	47797	0.0251	0.0041	0.0034	0.0245	0.0326	0.0245
2	44077	0.0136	0.0035	0.0056	0.0196	0.0227	0.0196
3	45925	0.0283	0.0043	0.0041	0.0472	0.0367	0.0472
4	46065	0.0218	0.0059	0.0042	0.0385	0.0319	0.0385
PB-1-C (i = 247.0 mA/cm^2 V = 12.47 V)							
1	45852	0.0327	0.0088	0.0058	0.0507	0.0473	0.0507
2	45801	0.0218	0.0058	0.0049	0.0595	0.0325	0.0595
3	45878	0.0256	0.0058	0.0132	0.0595	0.0446	0.0595
4	45917	0.0136	0.0086	0.0075	0.0577	0.0297	0.0577
PB-2-A (i = 62.0 mA/cm^2 V = 5.30 V)							
1	45539	0.0059	0.0009	0.004	0.0635	0.0108	0.0635
2	53872	0.0047	0.0023	0.0041	0.0832	0.0111	0.0832
3	37129	0.0013	0.0022	0.0041	0.0632	0.0076	0.0632
4	91435	0.0258	0.0075	0.022	0.222	0.0553	0.222
PB-2-B (i = 124.0 mA/cm^2 V = 8.33 V)							
1	47592	0.0061	0.0021	0.0011	0.0688	0.0093	0.0688
2	45873	0.0096	0.0027	0.0061	0.0647	0.0184	0.0647
3	44758	0.0071	0.0009	0.0061	0.0482	0.0141	0.0482
4	45090	0.0054	0.0012	0.0053	0.0617	0.0119	0.0617
5	45808	0.0049	0.0018	0.0036	0.0871	0.0103	0.0871
PB-2-C (i = 247.0 mA/cm^2 V = 15.54 V)							
1	49704	0.0201	0.0042	0.0148	0.03	0.0391	0.03
2	42193	0.0273	0.0045	0.0076	0.0312	0.0394	0.0312
3	46174	0.0219	0.0048	0.0088	0.0326	0.0355	0.0326
4	46122	0.0211	0.0027	0.0072	0.0362	0.031	0.0362
5	45903	0.0228	0.004	0.0044	0.0441	0.0312	0.0441

Table H3.2.4b Experiment PB-1 and PB-2 - Current Efficiencies

Samp. No.	Current Efficiencies (%)					
	p-anisidine	o-anisidine	p-aminophenol	aniline	Total 4e-	Total 6e-
PB-1-A (i = 62.0 mA/cm^2 V = 5.38 V)						
1	7.30	0.59	5.79	23.92	13.68	23.92
2	19.67	4.79	3.03	32.54	27.49	32.54
3	15.73	3.06	11.40	22.58	30.19	22.58
4	11.13	2.30	4.03	36.85	17.47	36.85
5	6.41	2.45	6.49	56.66	15.35	56.66
Average:	12.05	2.64	6.15	34.51	20.83	34.51
PB-1-B (i = 124.0 mA/cm^2 V = 8.50 V)						
1	20.27	3.31	2.75	29.68	26.33	29.68
2	11.91	3.07	4.90	25.75	19.88	25.75
3	23.79	3.61	3.45	59.51	30.85	59.51
4	18.27	4.94	3.52	48.39	26.73	48.39
Average:	18.56	3.73	3.65	40.83	25.95	40.83
PB-1-C (i = 247.0 mA/cm^2 V = 12.47 V)						
1	27.53	7.41	4.88	64.02	39.82	64.02
2	18.37	4.89	4.13	75.22	27.39	75.22
3	21.54	4.88	11.11	75.09	37.52	75.09
4	11.43	7.23	6.30	72.76	24.97	72.76
Average:	19.72	6.10	6.61	71.77	32.43	71.77

Table H3.2.4b Continued - Current Efficiencies

Samp. No.	Current Efficiencies (%)					
	p-anisidine	o-anisidine	p-aminophenol	aniline	Total 4e-	Total 6e-
PB-2-A (i = 62.0 mA/cm^2 V = 5.30 V)						
1	5.00	0.76	3.39	80.74	9.15	80.74
2	3.37	1.65	2.94	89.42	7.95	89.42
3	1.35	2.29	4.26	98.56	7.90	98.56
4	10.89	3.17	9.29	140.58	23.35	140.58
Average:	5.15	1.97	4.97	102.32	12.09	102.32
PB-2-B (i = 124.0 mA/cm^2 V = 8.33 V)						
1	4.95	1.70	0.89	83.70	7.54	83.70
2	8.08	2.27	5.13	81.66	15.48	81.66
3	6.12	0.78	5.26	62.35	12.16	62.35
4	4.62	1.03	4.54	79.23	10.19	79.23
5	4.13	1.52	3.03	110.09	8.68	110.09
Average:	5.58	1.46	3.77	83.41	10.81	83.41
PB-2-C (i = 247.0 mA/cm^2 V = 15.54 V)						
1	15.61	3.26	11.49	34.95	30.36	34.95
2	24.98	4.12	6.95	42.81	36.04	42.81
3	18.31	4.01	7.36	40.88	29.68	40.88
4	17.66	2.26	6.03	45.44	25.94	45.44
5	19.17	3.36	3.70	55.63	26.24	55.63
Average:	19.14	3.40	7.11	43.94	29.65	43.94

Table H3.2.4c Experiments PB-1 and PB-2 - Average Selectivities, Space-Time Yields and Energy Consumption.

Exp. No.	p-anisidine	o-anisidine	p-aminophenol	aniline	Total 4e-	Total 6e-
	Selectivity					
PB-1-A	27.59%	5.71%	14.54%	52.15%	47.85%	52.15%
PB-1-B	35.20%	7.24%	7.51%	50.05%	49.95%	50.05%
PB-1-C	24.30%	7.67%	8.13%	59.90%	40.10%	59.90%
PB-2-A	6.02%	2.37%	5.86%	85.75%	14.25%	85.75%
PB-2-B	8.63%	2.17%	5.89%	83.31%	16.69%	83.31%
PB-2-C	32.32%	5.77%	12.33%	49.58%	50.42%	49.58%
	Space-Time Yield (kmol / hr / m^3)					
PB-1-A	2.2782	0.4986	1.1627	4.3503	3.9395	4.3503
PB-1-B	7.0182	1.4119	1.3818	10.294	9.8119	10.294
PB-1-C	14.853	4.5961	4.9760	36.043	24.426	36.043
PB-2-A	0.9743	0.3717	0.9397	12.898	2.2857	12.898
PB-2-B	2.1102	0.5518	1.4262	21.028	4.0882	21.028
PB-2-C	14.422	2.5633	5.3527?	22.067	22.338	22.067
	Energy Consumption (kWh / kmol)					
PB-1-A	5945	36830	11870	2898	3168	2898
PB-1-B	5432	26140	26970	3896	3733	3896
PB-1-C	7782	23650	24100	2908	4445	2908
PB-2-A	19560	39320	14390	901.6	5953	901.6
PB-2-B	17540	73090	38060	1720	9122	1720
PB-2-C	9238	53130	27730	6030	5906	6030

H3.2.4 Fluidised Bed Cell - Experiments FB-1 and FB-2.

Experiments carried out with a parallel plate electrode configuration at various current densities.

Membrane:		Ionac - 3470
Electrodes -	cathode:	258 cm^2 copper feeder + 1.1 mm diam. copper particles. Bed height = 40 cm
-	anode:	Graphite plate (≈ 260 cm^2)
Specific Area:		FB-1 and FB-2: 54.5 cm^{-1}
Electrolyte- catholyte:		Methanol / 10% H_2SO_4 / 0.333 M nitrobenzene
-	anolyte:	Methanol / 10% H_2SO_4
Electrolyte Volume		
- catholyte:		12 litres
-	anolyte:	10 litres
Electrolyte Flowrate		
- catholyte:		8.50 l/min PB-1, 7.90 l/min PB-2.
-	anolyte:	4.0 l/min.
Estimated Mass Transfer		
Coefficient:		FB-1: 2.24 x 10^{-4} m/s
(see appendix F)		FB-2: 2.18 x 10^{-4} m/s
Temperature:		55°C
Geometric Current		
Density:		62.0 mA/cm^2 for FB-1-A and FB-2-A
		124.0 mA/cm^2 for FB-1-B and FB-2-B
		247.0 mA/cm^2 for FB-1-C and FB-2-C
Comments:		Nitrobenzene concentrations in samples was not measured. Three different current densities were used in each experiment. For FB-1 the experiment was started at the lowest current density and after 4 hrs was increased to 124 mA/cm^2 for a further two hours and finally 1 hr at the highest current density. For FB-2, this order was reversed ie. the highest current density was first etc.

Table H3.2.4d Experiment FB-1 and FB-2 – Product Analysis Results

Samp. No.	Coulombs Passed between Samples	Moles Products					
		p-anisidine	o-anisidine	p-aminophenol	aniline	Total 4e-	Total 6e-
FB-1-A (i = 62.0 mA/cm^2 V = 8.03 V)							
1	91883	0.0191	0.0044	0.0092	0.0209	0.0327	0.0209
2	45372	0.0316	0.0057	0.0151	0.0159	0.0524	0.0159
3	46191	0.0314	0.0051	0.0075	0.0203	0.044	0.0203
4	46612	0.0233	0.0045	0.0021	0.0182	0.0299	0.0182
FB-1-B (i = 124.0 mA/cm^2 V = 12.54 V)							
1	92875	0.0645	0.0113	0.0231	0.0621	0.0989	0.0621
2	46347	0.0194	0.0019	0.0069	0.0143	0.0282	0.0143
3	46130	0.0485	0.0093	0.0069	0.0402	0.0647	0.0402
4	45488	0.0216	0.0026	0.0063	0.0231	0.0305	0.0231
FB-1-C (i = 247.0 mA/cm^2 V = 16.95 V)							
1	46392	0.0332	0.0053	0.0042	0.0462	0.0427	0.0462
2	46560	0.0369	0.0072	0.0224	0.0343	0.0665	0.0343
3	46675	0.0237	0.0033	0.0059	0.0501	0.0329	0.0501
4	46109	0.0301	0.004	0.0012	0.0508	0.0353	0.0508
FB-2-A (i = 62.0 mA/cm^2 V = 7.89 V)							
1	51686	0.0123	0.0012	0.007	0.0126	0.0205	0.0126
2	39762	0.0264	0.0028	0.008	0.0106	0.0372	0.0106
3	45322	0.0105	0.0042	0.0138	0.0303	0.0285	0.0303
4	46228	0.035	0.0068	0.0055	0.0346	0.0473	0.0346
5	46728	0.0122	0.0158	0.0261	0.1006	0.0541	0.1006
FB-2-B (i = 124.0 mA/cm^2 V = 11.38 V)							
1	48784	0.0364	0.0082	0.0077	0.0351	0.0523	0.0351
2	79778	0.025	0.003	0.0075	0.0247	0.0355	0.0247
3	11737	0.0177	0.0018	0.0042	0.0082	0.0237	0.0082
4	46335	0.0293	0.003	0.0073	0.0395	0.0396	0.0395
5	46617	0.0727	0.0138	0.016	0.0919	0.1025	0.0919
FB-2-C (i = 247.0 mA/cm^2 V = 15.46 V)							
1	46661	0.0313	0.0063	0.0155	0.0309	0.0531	0.0309
2	49512	0.0381	0.0063	0.0151	0.0369	0.0595	0.0369
3	41962	0.0734	0.00695	0.0186	0.0698	0.0990	0.0698
4	45737	0.0051	0.00695	0.0037	0.0218	0.0158	0.0218
5	46212	0.0547	0.0082	0.0124	0.0583	0.0753	0.0583

Table H3.2.4e Experiment FB-1 and FB-2 - Current Efficiencies

Samp. No.	Current Efficiencies (%)					
	p-anisidine	o-anisidine	p-aminophenol	aniline	Total 4e-	Total 6e-
FB-1-A (i = 62.0 mA/cm^2 V = 8.03 V)						
1	8.02	1.85	3.86	13.17	13.74	13.17
2	26.88	4.85	12.85	20.29	44.58	20.29
3	26.24	4.26	6.27	25.45	36.77	25.45
4	19.30	3.73	1.74	22.61	24.76	22.61
Average:	20.11	3.67	6.18	20.38	29.96	20.38
FB-1-B (i = 124.0 mA/cm^2 V = 12.54 V)						
1	26.81	4.70	9.60	38.71	41.10	38.71
2	16.16	1.58	5.75	17.86	23.49	17.86
3	40.58	7.78	5.77	50.46	54.14	50.46
4	18.33	2.21	5.35	29.40	25.88	29.40
Average:	25.47	4.07	6.62	34.11	36.15	34.11
FB-1-C (i = 247.0 mA/cm^2 V = 16.95 V)						
1	27.62	4.41	3.49	57.66	35.53	57.66
2	30.59	5.97	18.57	42.65	55.13	42.65
3	19.60	2.73	4.88	62.15	27.21	62.15
4	25.20	3.35	1.00	63.79	29.55	63.79
Average:	25.75	4.11	6.99	56.56	36.85	56.56

Table H3.2.4e Continued - Current Efficiencies

Samp. No.	Current Efficiencies (%)					
	p-anisidine	o-anisidine	p-aminophenol	aniline	Total 4e-	Total 6e-
FB-2-A (i = 62.0 mA/cm^2 V = 7.89 V)						
1	9.19	0.90	5.23	14.11	15.31	14.11
2	25.63	2.72	7.77	15.44	36.11	15.44
3	8.94	3.58	11.75	38.71	24.27	38.71
4	29.22	5.68	4.59	43.34	39.50	43.34
5	10.08	13.05	21.56	124.65	44.69	124.65
Average:	16.61	5.18	10.18	47.25	31.98	47.25
FB-2-B (i = 124.0 mA/cm^2 V = 11.38 V)						
1	28.80	6.49	6.09	41.66	41.38	41.66
2	12.10	1.45	3.63	17.93	17.18	17.93
3	58.21	5.92	13.81	40.45	77.94	40.45
4	24.41	2.50	6.08	49.36	32.99	49.36
5	60.20	11.43	13.25	114.14	84.87	114.14
Average:	36.74	5.56	8.57	52.71	50.87	52.71
FB-2-C (i = 247.0 mA/cm^2 V = 15.46 V)						
1	25.89	5.21	12.82	38.34	43.93	38.34
2	29.70	4.91	11.77	43.15	46.39	43.15
3	67.52	6.39	17.11	96.31	91.02	96.31
4	4.30	5.87	3.12	27.60	13.29	27.60
5	45.69	6.85	10.36	73.05	62.90	73.05
Average:	34.62	5.85	11.04	55.69	51.50	55.69

Table H3.2.4f Experiments FB-1 and FB-2 - Average Selectivities, Space-Time Yields and Energy Consumption.

Exp. No.	p-anisidine	o-anisidine	p-aminophenol	aniline	Total 4e-	Total 6e-
	Selectivity					
FB-1-A	44.79%	8.46%	13.83%	32.92%	67.08%	32.92%
FB-1-B	43.86%	6.30%	12.23%	38.41%	61.59%	38.41%
FB-1-C	34.37%	5.43%	8.86%	51.34%	48.66%	51.34%
FB-2-A	32.17%	7.03%	16.99%	43.81%	56.19%	43.81%
FB-2-B	42.62%	6.18%	10.38%	40.82%	59.18%	40.82%
FB-2-C	34.96%	8.56%	12.85%	43.62%	56.38%	43.62%
	Space-Time Yield (kmol / hr / m^3)					
FB-1-A	6.338	1.157	1.945	4.281	9.442	4.281
FB-1-B	16.05	2.563	4.170	14.33	22.79	14.33
FB-1-C	32.33	5.165	8.772	47.34	46.27	47.34
FB-2-A	5.235	1.634	3.208	9.927	10.08	9.927
FB-2-B	23.16	3.503	5.403	22.15	32.06	22.15
FB-2-C	43.47	7.340	13.86	46.61	64.66	46.61
	Energy Consumption (kWh / kmol)					
FB-1-A	5616	27890	23890	6984	3632	6984
FB-1-B	6214	49690	22240	7087	4320	7087
FB-1-C	7514	49880	72530	5124	5503	5124
FB-2-A	6893	35350	11730	5065	3189	5065
FB-2-B	4859	37920	19020	5065	3472	5065
FB-2-C	11730	29830	21920	5646	5031	5646

H3.3 Monel Electrode Results - Experiments MPP-1, MPB-1 and MFB-1.

Experiments carried out with a parallel plate, packed bed and fluidised bed electrode configurations at various current densities, but with Monel cathode or feeder and monel particles.

Membrane:		Ionac - 3470
Electrodes -	cathode:	278 cm^2 Monel plate (MPP-1), 150 cm^2 Monel feeder (MPB-1), 225 cm^2 Monel feeder (MFB-1) + 1.0 mm diam.Monel particles. Bed height = 20 cm (MPB-1), 30 cm (MFB-1)
-	anode:	Graphite plate ($\approx$ 260 cm^2)
Specific Area:		MPP-1: 0.330 cm^{-1}, MPB-1: 32.7 cm^{-1} and MFB-1: 54.5 cm^{-1}.
Electrolyte-	catholyte:	Methanol / 10% H_2SO_4 / 0.333 M nitrobenzene
-	anolyte:	Methanol / 10% H_2SO_4
Electrolyte Volume		
-	catholyte:	6 litres
-	anolyte:	10 litres
Electrolyte Flowrate		
-	catholyte:	19.8 l/min MPP-1
		11.0 l/min MPB-1.
		7.70 l/min MFB-1.
-	anolyte:	4.0 l/min.
Estimated Mass Transfer		
Coefficient:		MPP-1: 1.40×10^{-5} m/s
(see appendix F)		MPB-1: 2.60×10^{-4} m/s
		MFB-1: 2.31×10^{-4} m/s
Temperature:		55°C
Geometric Current		
Density:		108.0 mA/cm^2 for MPP-1
		133.0 mA/cm^2 for MPB-1
		107.0 mA/cm^2 for MFB-1
Comments:		Experiments were run to high conversions (-> 70%). For comparison, results were averaged over the first 40% conversion where no great effect of conversion was observed in the results.

Table H3.3a Experiment MPP-1, MPB-1 and MFB-1 - Product Analysis Results

Samp. No.	Coulombs Passed between Samples	Moles Products					
		p-anisidine	o-anisidine	p-aminophenol	aniline	Total 4e-	Total 6e-
MPP-1 (i = 108.0 mA/cm^2 V = 12.0 V)							
1	108000	0.168	0.03	0.048	0.008	0.246	0.008
2	108000	0.143	0.024	0.042	0.032	0.209	0.032
3	115000	0.184	0.031	0.053	0.055	0.268	0.055
4	99000	0.12	0.02	0.022	0.06	0.162	0.06
5	107000	0.086	0.016	0.027	0.083	0.129	0.083
6	109000	0.093	0.015	0.029	0.094	0.137	0.094
MPB-1 (i = 133.0 mA/cm^2 V = 7.90 V)							
1	72000	0.101	0.017	0.033	0.012	0.151	0.012
2	72000	0.091	0.016	0.025	0.016	0.132	0.016
3	72000	0.108	0.018	0.033	0.015	0.159	0.015
4	72000	0.114	0.02	0.032	0.023	0.166	0.023
5	72000	0.063	0.012	0.022	0.02	0.097	0.02
6	73000	0.078	0.011	0.019	0.023	0.108	0.023
7	71000	0.115	0.022	0.029	0.043	0.166	0.043
MFB-1 (i = 107.0 mA/cm^2 V = 13.00 V)							
1	88600	0.068	0.011	0.031	0.059	0.11	0.059
2	88400	0.041	0.0006	0.016	0.077	0.058	0.077
3	87000	0.038	0.0006	0.015	0.083	0.054	0.083
4	87000	0.04	0.0007	0.012	0.068	0.053	0.068
5	89000	0.035	0.005	0.007	0.064	0.047	0.064
6	89000	0.034	0.008	0.024	0.074	0.066	0.074
7	88000	0.039	0.008	0.005	0.065	0.052	0.065
8	87000	0.045	0.005	0.017	0.089	0.067	0.089

Table H3.3b Experiment MPP-1, MPB-1 and MFB-1 - Current Efficiencies

Samp. No.	Current Efficiencies (%)					
	p-anisidine	o-anisidine	p-aminophenol	aniline	Total 4e-	Total 6e-
MPP-1 (i = 108.0 mA/cm^2 V = 12.0 V)						
1	60.04	10.72	17.16	2.86	87.92	2.86
2	51.11	8.58	15.01	11.44	74.70	11.44
3	61.76	10.41	17.79	18.46	89.95	18.46
4	46.79	7.80	8.58	23.39	63.16	23.39
5	31.02	5.77	9.74	29.94	46.54	29.94
6	32.93	5.31	10.27	33.29	48.52	33.29
Average:	54.93	9.38	14.63	14.04	78.93	14.04
(Calculated from first 4 results before conversion became significant)						
MPB-1 (i = 133.0 mA/cm^2 V = 7.90 V)						
1	54.15	9.11	17.69	9.65	80.95	9.65
2	48.79	8.58	13.40	12.87	70.77	12.87
3	57.90	9.65	17.69	12.06	85.24	12.06
4	61.12	10.72	17.16	18.50	88.99	18.50
5	33.78	6.43	11.79	16.08	52.00	16.08
6	41.24	5.82	10.05	18.24	57.11	18.24
7	62.52	11.96	15.77	35.07	90.25	35.07
Average:	49.49	8.39	14.63	14.57	72.51	14.57
(Calculated from first 6 results before conversion became significant)						
MFB-1 (i = 107.0 mA/cm^2 V = 13.00 V)						
1	29.63	4.79	13.51	38.56	47.92	38.56
2	17.90	0.26	6.99	50.43	25.15	50.43
3	16.86	0.27	6.66	55.24	23.78	55.24
4	17.75	0.31	5.32	45.26	23.38	45.26
5	15.18	2.17	3.04	41.64	20.38	41.64
6	14.75	3.47	10.41	48.14	28.62	48.14
7	17.11	3.51	2.19	42.77	22.81	42.77
8	19.97	2.22	7.54	59.23	29.73	59.23
Average:	19.46	1.56	7.10	46.22	28.12	46.22
(Calculated from first 5 results before conversion became significant)						

Table H3.3e Experiments MPP-1, MPB-1 and MFB-1 - Average Selectivities, Chemical and Space-Time Yields and Energy Consumption.

Exp. No.	p-anisidine	o-anisidine	p-aminophenol	aniline	Total 4e-	Total 6e-
	Selectivity					
MPP-1	52.89%	9.07%	14.66%	23.39%	76.61%	23.39%
MPB-1	59.18%	10.19%	17.17%	13.46%	86.54%	13.46%
MFB-1	31.21%	3.53%	11.22%	54.04%	45.96%	54.04%
	Chemical Yield					
MPP-1	57.72%	9.92%	15.54%	28.16%	83.18%	28.16%
MPB-1	64.04%	11.08	18.53%	14.38%	93.65%	14.38%
MFB-1	29.33%	3.47%	11.80%	53.56%	44.61%	53.56%
	Space-Time Yield (kmol / hr / m^3)					
MPP-1	0.1586	0.0272	0.0439	0.0445	0.2296	0.0445
MPB-1	20.83	3.609	6.000	4.731	30.44	4.731
MFB-1	10.14	1.156	3.783	17.28	15.08	17.28
	Energy Consumption (kWh / kmol)					
MPP-1	3031	17680	11060	19920	2085	19920
MPB-1	1786	10460	6191	8724	1220	8724
MFB-1	8080	225460	28330	4632	5542	4632

APPENDIX I

Copper and Monel Particle Dissolution

Two experiments were carried out to establish a link between the dissolution of the electrode during experiments and increased aniline formation. Copper and Monel Particles were stirred vigorously in separate mixtures of methanol, H_2SO_4 and 0.3 M nitrobenzene at 55 ^oC for several hours (volume - 200 ml (copper) and 132 ml (Monel)). Samples were taken and analysed for metal ion concentration and any organic products.

In both cases aniline was formed (confirmed by mass spectroscopy) and quantitatively analysed by HPLC. The results are tabulated below, the number of coulombs that would have to have been passed had aniline been formed at an electrode is also included:

Table I1.0 Copper and Monel Particle Dissolution Experiments

Time (hrs)	Copper Particles			Monel Particles			
	Cu^{2+} Conc. (mg/l)	Aniline Conc. (g/l)	Equiv. Coulombs	Cu^{2+} Conc. (mg/l)	Ni^{2+} Conc. (mg/l)	Aniline Conc. (g/l)	Equiv. Coulombs
0	21.4	0.0	0	24.6	10.4	0.0	0
1	1241	0.44	639				
2	1802	0.86	1151				
3	1300	1.98	2493				
4	2293	2.11	2667	2080	1130	0.42	342

The results clearly demonstrate the formation of aniline by reduction of nitrobenzene, no other products were identified. Moreover, for the copper experiment, the aniline formed correlates to the copper ion concentration, although somewhat less was formed in the last hour. The other experiment demonstrates that whilst Monel particles are also subject to dissolution, much less aniline is formed.

The conclusion is that either copper ions catalyse the direct reduction of nitrobenzene to aniline, or that the aniline is formed as a cathodic process coupled with the anodic dissolution of the copper. It is be supposed that this same process occurs inside the packed and fluidised bed electrode during experiments.

Table H3.2.4b Continued - Current Efficiencies

Samp. No.	Current Efficiencies (%)					
	p-anisidine	o-anisidine	p-aminophenol	aniline	Total 4e-	Total 6e-
PB-2-A (i = 62.0 mA/cm^2 V = 5.30 V)						
1	5.00	0.76	3.39	80.74	9.15	80.74
2	3.37	1.65	2.94	89.42	7.95	89.42
3	1.35	2.29	4.26	98.56	7.90	98.56
4	10.89	3.17	9.29	140.58	23.35	140.58
Average:	5.15	1.97	4.97	102.32	12.09	102.32
PB-2-B (i = 124.0 mA/cm^2 V = 8.33 V)						
1	4.95	1.70	0.89	83.70	7.54	83.70
2	8.08	2.27	5.13	81.66	15.48	81.66
3	6.12	0.78	5.26	62.35	12.16	62.35
4	4.62	1.03	4.54	79.23	10.19	79.23
5	4.13	1.52	3.03	110.09	8.68	110.09
Average:	5.58	1.46	3.77	83.41	10.81	83.41
PB-2-C (i = 247.0 mA/cm^2 V = 15.54 V)						
1	15.61	3.26	11.49	34.95	30.36	34.95
2	24.98	4.12	6.95	42.81	36.04	42.81
3	18.31	4.01	7.36	40.88	29.68	40.88
4	17.66	2.26	6.03	45.44	25.94	45.44
5	19.17	3.36	3.70	55.63	26.24	55.63
Average:	19.14	3.40	7.11	43.94	29.65	43.94